PUBLISHED BY THE ACADEMY OF SCIENCES OF ALBANIA

JNTS

JOURNAL OF NATURAL AND TECHNICAL SCIENCES

2018 (2)
XXIII (47)

ACKNOWLEDGEMENT
TO REVIEWERS AND EDITORS

The Editor-in-Chief is very thankful to his Editorial Board team for their continued support and diligent, hard work. But I am especially thankful to our large groups of very faithful and excellent reviewers without whom we wouldn't have a journal of quality. Every paper is reviewed by a minimum of two reviewers and I expect authors of accepted papers to reciprocate by writing really good reviewed version of their manuscripts as well. Reviewing papers is one of the best ways to stay on top of developments in your area of research and it is a necessary component of your career path in Academia. Reviewing is a hard and time demanding process.

Most of the time, for better or worse, we respect the final decisions of the reviewers. In the case of very conflicting reviews, we call for a third reviewer which, of course, prolongs the review process.

Thank you for the time spent and constructive comments on manuscripts to the following reviewers' team:

Abedin Xhomo
Alaudin Kodra
Alda Kika
Alfred Frashëri
Angelo Desantis
Arjan Harxhi
Asti Papa
Blerina Kolgjini
Donika Prifti
Dorian Minarolli
Enea Mustafaraj
Flora Qarri
Frederik Dara
Gafurr Muka
Genc Sulcebe
Gjergji Foto
Ibrahim Milushi
Ilda Kazani
Ilia Mikerezi
Illir Alliu
Indrit Baholli
Indrit Inesi
Irakli Prifti
Isak Shabani
Jul Bushati
Klodian Zaimi
Kostandin Dollani
Luljeta Bozo
Lulzim Hanelli
Matilda Mema
Mentor Lame
Nevton Kodhelaj
Niko Pano
Pëllumb Berberi
Pëllumb Sadushi
Rigena Sema

With Best Regards from the Editor, the whole Editorial Board and myself,
Yours sincerely,

Salvatore Bushati
Editor-in-Chief

GREEN'S RELATION B IN RINGS AND IN THEIR MULTIPLICATIVE SEMIGROUPS

Florion ÇELA and Petraq PETRO
Department of Mathematics, Faculty of Natural Sciences,
University of Tirana, Albania

ABSTRACT

Green's relations in semigroups are successful tools for studying properties of semigroups. These relations areintroduced and studied also in rings. Gradually they have been transformed into tools not only for studying rings, but also to point out the connection between rings and their multiplicative semigroups. Firstly, in this paper we give solution to an open problem that has to do with equivalence classes of Green's relation $\mathcal{B}$ in rings. Further we find some conditions that show when the Green's relation $\mathcal{B}$ in ring is equal to Green's relation $\mathcal{B}$ $(\cdot)$ in the multiplicative semigroup of this ring. Lastly, we point out the rings in which the Green's relations $\mathcal{B}$ and $\mathcal{B}(\cdot)$ coincide. These rings are very close to regular rings, but we show by giving a counterexample, that they differ from each other.
Keywords: semigroups, rings, regular rings, Green's relations, bi-ideals.

1. INTRODUCTION

In this paper by a ring we mean an associative ring, which does not necessary have an identity element. The relations $\mathcal{L}, \mathcal{R}, \mathcal{H}$ and $\mathcal{D}$ are first introduced and studied by Petro (1981; 2002; 2014) and further by Sema (2014). These relations are called Green's relations in rings because they mimic the Green's relations $\mathcal{L}, \mathcal{R}, \mathcal{H}$ and $\mathcal{D}$ in semigroups, which are first introduced and studied by Green (1951). In a similar way like Green's relations in rings, in (Sema 2014) was introduced and studied another relation which is denoted by $\mathcal{B}$ and called Green's relation $\mathcal{B}$. In fact, the Green's relation $\mathcal{B}$ in rings mimics the relation $\mathcal{B}$ in semigroups which was first introduced and studied by Kupp (1969) which we will call it Green's relation $\mathcal{B}$ in semigroup. First, we aim to give solution to an open problem raised in

(Sema, 2014). For this, we study the Green's relation $\mathcal{B}$ in a ring $(A,+,\cdot)$ and the Green's relation $\mathcal{B}$ $(\cdot)$ in the multiplicative semigroup $(A,\ \cdot)$ of this ring, also. Further, we find some sufficient conditions and also a necessary and sufficient condition that show when the Green' s relation $\mathcal{B}$ ina ring $(A,+,\cdot)$ coincide to Green's relation $\mathcal{B}$ $(\cdot)$ in the multiplicative semigroup $(A,\ \cdot)$ of this ring. Hence, we find some conclusions when the relation $\mathcal{B}$ coincides with the relation $\mathcal{B}$ $(\cdot)$ and when they differ from each other. Lastly, after pointing out that in the class of regular rings the relation $\mathcal{B}$ coincide with the relation $\mathcal{B}$ $(\cdot)$ we will show that the class of rings in which the relation $\mathcal{B}$ and $\mathcal{B}$ $(\cdot)$ coincide and which we also don't have equivalence classes with more than one element, respect to $\mathcal{B}$ relation coincide with the class of regular rings. By a counter example we show that, even though the class of the rings in which the $\mathcal{B}$=$\mathcal{B}$ $(\cdot)$ is very close to regular rings, they differ from each other. In the end, we raise an open problem that has to do with a characterization of the class of regular rings by the equivalence classes of the Green's relation $\mathcal{B}$.

2. PRELIMINARIES

We give some notions and present some auxiliary result that will be used throughout the paper.

For all unexplained concepts and propositions the reader may refer to (Steinfeld, 1978) and (Howie, 1995).

Let $(A,+,.)$ be a ring and B,C two subsets of A. We write:

$$B+C=\{b+c\in A\,|\,b\in B,c\in C\},$$

$$BC=\{\sum_{i=1}^{n}b_ic_i\in A\,|\,b_i\in B,c\in C\}.$$

For simplicity we will write $b+C$, bC, Bc instead of $\{b\}+C$, $\{b\}C$ and $B\{c\}$.

A subring B of a ring $(A,+,\cdot)$ is called left (right) bi-ideal $B(R,L)$ if the following inclusion is satisfied $BAB\subseteq B$ $(RA\subseteq R, LA\subseteq L)$ (Steinfeld, 1978). Green's relations $\mathcal{B},\mathcal{R},\mathcal{L}$ in a ring A are defined as below(Petro 1981; 2002):

$$\forall(a,b)\in A^2, a\mathcal{R}b\Leftrightarrow(a)_r=(b)_r,$$

$$\forall(a,b)\in A^2, a\mathcal{L}b\Leftrightarrow(a)_l=(b)_l,$$

$$\forall(a,c)\in A^2, a\mathcal{B}b\Leftrightarrow(a)_b=(c)_b,$$

where $(a)_r, (b)_r$, $((a)_l, (b)_l, (a)_b, (c)_b)$ are respectively principle right ideals, principal left ideals, principal bi-idealswhich are generated by the elements a, b, c.

It is not difficult to prove that for each element*a* of a ring, the following equalities are satisfied:

$$(a)_r = \mathbb{Z}a + Aa, \quad (1.1)$$
$$(a)_r = \mathbb{Z}a + aA, \quad (1.2)$$
$$(a)_r = \mathbb{Z}a + \mathbb{Z}a^2 + aAa. \quad (1.3)$$

The relations $\mathcal{R}, \mathcal{L}$ and $\mathcal{B}$ in the ring $(A, +, \cdot)$ are equivalence relations in its support. The equivalence classes for an element $a \in A$ *mod*$\mathcal{R}$, *mod*$\mathcal{L}$, *mod*$\mathcal{B}$ are denoted respectively $\mathcal{R}_a, \mathcal{L}_a, \mathcal{B}_a$.

The subsemigroup *B* of a semigroup (*S*,.)*B* is called bi-ideal of this semigroup (*S*,.) if *BSB*⊆*B.*

Definition 2.1. (Kapp, 1969) *Let* $(S, \cdot)$ *be a semigroup. For each two elements* a, b *of* S *we write* $a\mathcal{B}c$ *if* $a = c$ *or there exist elements* u, v *of* S *such that:*

$$a = buc\,,\ c = ava\,.$$

Proposition 2.2. (Mielke, 1969) *Let* $(S, \cdot)$ *be a semigroup. Then*

$$\forall (a,b) \in S^2,\ a\mathcal{B}c \Leftrightarrow (a)_b = (c)_b\,,$$

where $(a)_b$ *and* $(c)_b$ *are principle bi-ideals* (*the intersection of all bi-ideals that contain respectively elements* a *and* c) *generated by elements* a, c *of* S.

It is clear thatthe relation $\mathcal{B}$ in a semigroup $(S, \cdot)$ is an equivalence relation on S which we will call it Green's relation $\mathcal{B}$.

If in the above definitions of the Green's relations $\mathcal{R}, \mathcal{L}$ and $\mathcal{B}$ in a ring $(A, +, \cdot)$ we replace the ring $(A, +, \cdot)$ with the semigroup $(S, \cdot)$, by using the **Proposition 2.2** and by regarding the principal right ideals, principal left ideals and principal bi-ideals of the ring (*A*,+,.) respectively as principal right ideals, principal left ideals and principal bi-ideals of the semigroup (*S*,.), then we have the respective Green's relation's in the semigroup $(S, \cdot)$. Throughout this paper, Green's relationsin the multiplicative semigroup $(A, \cdot)$ of the ring $(A, +, .)$ are denoted $\mathcal{R}(.), \mathcal{L}(.), \mathcal{B}(.)$ in order to distinguish them from

Green's relations $\mathcal{R},\mathcal{L},\mathcal{B}$ in the ring $(A,+,.)$. For the same purpose the equivalence classes of an element a withrespect to Green' s relations in the multiplicative semigroup of the ring $(A,+,.)$ are denoted $R_a(.), L_a(.), B_a(.)$.

Regarding $\mathcal{B}$-classes of the ring $(A,+,.)$ and $\mathcal{B}(.)$-classes of the multiplicative semigroup $(A,\cdot)$ of this ring in (Sema, 2014) is raised the following problem:

Problem 2.3. *In a ring* $(A,+,.)$ *for an element* $a \in A$ *is it true that* $\mathcal{B}_a$ *is a union of* $\mathcal{B}_a(.)$ *classes of the multiplicative semigroup* $(A,.)$ *of the ring* $(A,+,.)$ *which have only one element or satisfy the equality* $B_a = B_a(.)$ *?*

Proposition 2.4. (Howie, 1995) *Let* S *be a cancellable semigroup* (*that is a semigroup in which for all* a,b,c):

$$(ca = ca) \Rightarrow (a = b),$$
$$(ac = bc) \Rightarrow (a = b),$$

and suppose that S *has not an identity , then:*

$$\mathcal{R} = \mathcal{L} = 1_S,$$

where $\mathcal{R},\mathcal{L}$ *are Green's relations in semigroup* S *and* 1_S *is the identic relacion in* S.

3. MAIN RESULT

If the ring $(A,+,.)$ has an identity then from equality (1.3) is evident $\mathcal{B}(.) \subseteq \mathcal{B}$. In general, by using equality (1.3) we get that $\mathcal{B}_a(.) \subseteq \mathcal{B}_a$ and consequently $B(.) \subseteq B$. By an example (Sema, 2014) is shown that these inclusion is strict. We give a positive answer to **Problem 2.3** by the following theorem.

Theorem 3.1.*Let* $(A,+,.)$ *be a ring and* a *any element of* A. *Then* $\mathcal{B}$*-classes* $\mathcal{B}_a$ *is either a union of the* $\mathcal{B}(.)-$*classes of the multiplicative semigroup* $(A,.)$ *of the ring* $(A,+,.)$, *which must have a single element or* $B_a = B_a(.)$,

Proof. Let us consider the two following cases:

Case 1. Each class $B_x(.)$ that is included in $\mathcal{B}_a$ has only one element. Thus we have

$$B_a = \cup_{x \in \mathcal{B}_a} B_x(.).$$

Case 2. There exists a class $B_x(.)$, $x \in B_a$, such that has at least two elements. Let y be an element of A different from x such that $y \in \mathcal{B}_x(.)$. From **Definition 2.1** there exist elements u, v of A such that:

$y = xux,\ x = yvy.$

Let b be an arbitrary element of the class $\mathcal{B}_a$. Then there exists integers k_1, k_2, k_3, k_4 and elements u_1, u_2 of A such that:

$$x = k_1 b + k_2 b^2 + b u_1 b,$$

$$b = k_3 x + k_4 x^2 + x u_2 x.$$

By using appropriate replacements we get that:

$$y = xax = (k_1 b + k_2 b^2 + b u_1 b) u (k_1 b + k_2 b^2 + b u_1 b)$$

$$= b(k_1^2 u + k_1 k_2 ub + k_1 b u_1 + k_2 ub^2 + k_2^2 bub + k_2 b u_1 + k_1 ub + k_2 u_1 b^2 + u_1 bub u_1) b$$

$$b = k_3 x + k_4 x^2 + x u_2 x = k_3 yvy + k_4 yuy^2 uy + yuyu_2 yuy$$

$$= y(k_3 v + k_3 k_4 uy^2 uy + k_3 uyu_2 yu) y,$$

which show that $b \mathcal{B}(.) y$.

Now we have:

$$\mathcal{B}_a \subseteq \mathcal{B}_y(.) = \mathcal{B}_x(.) \subseteq \mathcal{B}_x = \mathcal{B}_a.$$

Thus, $\mathcal{B}_a = \mathcal{B}_x(.)$ and consequently $a \in \mathcal{B}_x(.)$. Hence are true the following equalities:

$$\mathcal{B}_a = \mathcal{B}_x,\ \mathcal{B}_a(.) = \mathcal{B}_x(.),$$

from which we have that $\mathcal{B}_a = \mathcal{B}_a(.)$ ■

Proposition 3.2.*Let* $(A, +, .)$ *be a ring whichhas at least two elements but it does not have an identity element and divisors of zero. Then the only* $\mathcal{B}$*-classes in the ring* $(A, +, .)$ *that coincide with the repective* $\mathcal{B}(.)$*-classes in the multiplicative semigroup* $(A, .)$ *of this ring are those which have only one element.*

Proof. By using the fact $(A, +, .)$ has no divisor of zero the set $A^* \{0\}$ is closed under the multiplication of the ring and it forms a semigroup. It is clear that $(A^*, .)$ has no identity element and it is a cancellative semigroup. According to **Proposition 2.4** we have that for each $a \neq 0$ of A, the class $B_a(.)$ of the element a respect to the relation $B(.)$ in the multiplicative

semigroup $(A,.)$ of the ring $(A,+,.)$ has only one element, since we have that $B_a(\cdot) \subseteq R(\cdot)$. Now it is obvious that the equality $B_a = B_a(\cdot)$ is true if and only if $\mathcal{B}_a$ has only one element. ■

From the above proposition and from theorem 3.2 we have the following corollary which in a special case is a necessary and sufficient condition that the Green's relation $\mathcal{B}$ in a ring coincide with the Green's relation $\mathcal{B}(.)$ in the multiplicative semigroup ne $(A,.)$ of this ring .

Corollary 3.3. *Let* $(A,+,.)$ *be a ring diffierent from the zero ring,which has neither identity element nor divisors of zero. Then the Green's relation* $\mathcal{B}$ *coincide with the Green's relation* $\mathcal{B}(.)$ *in its multiplicative semigroup* $(A,.)$ *if and only if* $\mathcal{B} = 1_A$, *where* 1_A *is the identic relation in* A.

Theorem 3.4.*Let* A *be a ring. Then it is true the following implication*

$$(\exists n \in \mathbb{N} - \{1,2,3,4\}, a^n \in \mathcal{B}_a) \Rightarrow \mathcal{B}_a = \mathcal{B}_a(.).$$

Proof. Suppose that for $a \in A$ it exists a natural number $n \geq 5$ such that $a^n \in B_a$. Let x be an arbitrary element of $\mathcal{B}-$class $B_a = B_{a^n}$. Then, by using equality (1.3) there exist integer k_1, k_2, k_3, k_4 and elements u_1, u_2 of A such that:

$$a = k_1 x + k_2 x^2 + x u_1 x,$$
$$x = k_3 a^n + k_4 a^{2n} + a^n u_2 a^n .$$

Hence

$$x = a(k_3 a^{n-2} + k_4 a^{2n-2} + a^{n-1} u_2 a^{n-1})a,$$
$$a^n = a a^{n-2} a = (k_1 x + k_2 x^2 x u_1 x) a^{n-2} (k_1 x + k_2 x^2 + xux)$$
$$= x(k_1 a + k_2 xa + a_1 xa) a^{n-4} (k_1 a + k_2 ax + axa_1)x,$$

Which show that $x\mathcal{B}(.)a^n$, and consequently $x \in \mathcal{B}_{a^n} = \mathcal{B}_a$.

So we have that $B_a \subseteq B_a(.)$. Since we have $\mathcal{B}_a(.) \subseteq \mathcal{B}_a$, we get the equality $\mathcal{B} = \mathcal{B}(.)$ ■

From the above theorem we get the following corollary which shows a necessary and suffiecient conditon that the Green's relation $\mathcal{B}$ in a ring $(A,+,.)$ doesn't coincide with the Green's relation $\mathcal{B}(.)$ in the multiplicative semigroup $(A,.)$ of this ring.

Corollary 3.5. Let $(A,+,.)$ *be a ring such that*

$$\exists a \in A, \forall n \in \mathbb{N} - \{1,2,3,4\},\ a^n \notin \mathcal{B}_a,$$

then $\mathcal{B} \neq \mathcal{B}(.)$.

Theorem 3.6. *Let* A *be a ring and* a *an arbitrary element of A such that* B_a *has at least two elements. Then* $B_a = B_a(.)$ *if and only if when* a *is a regular element.*

Proof. Suppose that $B = B_a(.)$. Let b be an arbitrary element of A different from a such that $b \in B_a = B_a(.)$.

So, there exist element u_1, u_2 of A such that:

$$a = bu_1b,\ b = au_2a.$$

Hence we get the following equalities:

$$a = (au_2a)u_1(au_2a) = a(u_2au_1au_2)a,$$

which show that a is a regular element.

Conversly, wesuppose that $a \in A$is a regular element. Thus it exists an element $v_1 \in A$such that $a = av_1a.$

Let b be an arbitrary element of B_a. Then there exist integers z_1, z_2, z_3, z_4 and elements v_2, v_3 of A such that:

$$b = z_3av_1a + z_4av_1a^2 + av_1av_3a = a(z_3v_1 + z_4v_1a + v_1av_3)a,$$

$$b = av_4a = av_1av_4a = (z_1b + z_2b^2 + bv_2b)v_1av_4(z_1b + z_2b^2 + bv_2b)$$

$$= b(z_1v_1a + z_2bv_1a + v_2bv_1a)(z_1v_4 + z_2v_4b + v_4bv_2)b = bv_5b,$$

where $v_5 = (z_1v_1a + z_2bv_1a)(z_1v_4 + z_2v_4b + v_4bv_2).,$

$a = zbv_5b + z_2bv_5b^2 + bv_5bv_2b = b(zv_5 + z_2v_5b + v_5bv_2),$ which show that $a\mathcal{B}(.)b$, and consecuently $B_a \subseteq B_a(.)b$. By using the inclusion $B_a(.) \subseteq B_a$ it follows that $\mathcal{B}_a = \mathcal{B}_a(.)$.

From the above theorem we obtain the following corollary, which show when the relation $\mathcal{B}$ in a ring $(A,+,.)$ coincides with the relation $\mathcal{B}(\cdot)$ in the multiplicative semigroup of this ring.

Corollary 3.7.*Let* $(A,+,.)$ *be a ring. Then the Green's relation* $\mathcal{B}$ *is equally with the Green's relation* $\mathcal{B}(.)$ *in the multiplicative semigroup* $(A,.)$ *of (A,+,.) if and only if*

$\forall a \in A, |\mathcal{B}_a| > 1 \Rightarrow a$ is a regular element. (*)

Proof. Suppose that in the ring $(A,+,.)$ we have that $\mathcal{B} = \mathcal{B}(.)$. On the view of **Propositon 3.6** and by using the fact that for an element a of A, B_a has more than one element, it follows that a is a regular element.

Conversely, we suppose that in the ring $(A,+,.)$ is satisfied the implication (*). Let a be an arbitrary element of the ring. If $|B_a| = 1$,then since $B_a(.) \subseteq B_a$, it follows that $|B_a(.)| = 1$ and consencantly $B_a(.) = B_a$. If $|B_a| > 1$, by of (*) it follows that a is a regular element, thus $B_a = B_a(.)$. So for each element $a \in A$ it follows that the relations $\mathcal{B}$ and $\mathcal{B}(.)$ has the same equivalent classes $\mathcal{B}_a$ and $\mathcal{B}_a(.)$, and therefore they concide.

Let $(A,+,.)$ be a regular ring. Then the Green's relation $\mathcal{B}$ in the ring $(A,+,.)$ is equal the Green's relation $\mathcal{B}(.)$ in the multiplicative semigroup. Realy, it is not difficult to prove that the bi-ideal generated by an arbitrary element a in the semigroup $(A,.)$ is the following set

$$\{a, a^2\} \cup aAa .$$

Since $(A,+,.)$ is a regular ring it follows that for each element $a \in A$ it exists an element $u \in A$ such that $a = aua$. and concencantely, we have:

$$\{a, a^2\} \cup aAa = aAa,$$

$$\mathbb{Z}a + \mathbb{Z}a^2 + aAa = aAa .$$

In view of the above equalities and equaltiy (3.1) it is clear that for any two elements a, c of A it follows that

$$a\mathcal{B}(.)c \Leftrightarrow a\mathcal{B}c .$$

Corollary 3.7 shows that if in a ring A the relations $\mathcal{B}$ and $\mathcal{B}(.)$ coincide and also if for any element $a \in A$, B_a has at least two elements, then $(A,+,.)$ is a regular ring.It is natural to ask that if the relations $\mathcal{B}$ and $\mathcal{B}(.)$ coincide is it true that the ring $(A,+,.)$ is a regular ring? The answer to this question is negative. For this we have the following counterexample:

Counterexample 3.8. In the ring $(\mathbb{Z}_4,+,.)$ is true that $\mathcal{B} = \mathcal{B}(.)$ because the following equalities are satisfied:

$$B_0 = B_0(.) = \{\bar{0}\},$$

$$B_1 = B_1(.) = \{\bar{1}, \bar{3}\},$$

$$B_2 = B_2(.) = \{\bar{2}\}.$$

But $(\mathbb{Z}_4, +, .)$ is not a regular ring since $\bar{2} \neq \bar{2}\bar{0}\bar{2}$, $\bar{2} \neq \bar{2}\bar{1}\bar{2}$, $\bar{2} \neq \bar{2}\bar{2}\bar{2}$, $\bar{2} \neq \bar{2}\bar{3}\bar{2}$. In this counterexample, the regularness of $\mathbb{Z}_4$ it is tru by the fact that there exists an equivalence class B_a which has only one elemente. Maybe the absence of such classes lead's to regularness of the ring. So we raise the following open problem.

Problem 3.9. *Is it true that a ring* $(A, +, .)$ *is regular if and only if for any element* $a \in A$ *its equivalence class* $\mathcal{B}_a$ *has at least two elements?*

A positive answer to the above question gives a characterization for the class of regular rings.

REFERENCES

Green JA. 1951. On the structure of semigroups. *Annals of Mathematics*. **54(1),** 163-172, USA.

Howie JM. 1995. Fundamentals of semigroup theory. Oxford *University Press*, USA.

Kapp KM. 1969. On bi-ideals and quasi-ideals in semigroups. *Publicationes Mathematica e Debrecen*, **16**, 179-185, Hungary.

Mielk BW. 1969. Anote on bi-ideals and quasi-ideals in semigroups. *Publicationes Mathematicae Debrecen*, **17**, 76-75, Hungary.

Petro P.1981. Two Green's type theorems for rings. *Buletini i Shkencave Natyrore*, **No.2**, 17-22, Albania.

Petro P. 2002. Green's relations and minimal quasi-ideals in rings. *Communication in Algebra*, **30(10),** 4677-4686, USA.

Sema R, Petro P.2014. Some results of Green's relation $\mathcal{L}$ and $\mathcal{R}$ in rings. *Journal of Natural and Technical Sciences* (JNTS) **36(1)**, 3-11. Academy of Sciences of Albania, Albania.

Sema R. 2014. Green's relations and generalisations of ideals in rings and their generalizations, *Ph.D thesis*, Albania.

Steinfeld O. 1978. Quasi-ideals in rings and semigroups. *Disqusitiones Mathematicae Hungaricae* **10**, Ahademiae Kiodo, Budapest, Hungary.

Lattice QCD with QCDLAB

Artan BORIÇI
University of Tirana
Department of Physics, Faculty of Natural Sciences
King Zog I Boulevard, Tirana, Albania
borici@fshn.edu.al

ABSTRACT

QCDLAB is a set of programs, written in GNU Octave, for lattice QCD compu-tations. Version 2.0 includes the generation of configurations for the SU(3) theory, computation of rectangle Wilson loops as well as the low lying meson spectrum. In this paper, we give a brief tutorial on lattice QCD computations using QCDLAB.

1. INTRODUCTION

Quantum Chromodynamics (QCD) is the theory of strong interactions. QCD has an ultraviolet fixed point at vanishing coupling constant, a property which was first demonstrated in the perturbative formulation by Gross and Wilczek [Gross,Wilczek,1973] as well as by Politzer [Politzer, 1973]. A year later, Wilson was able to formulate QCD non-perturbatively [Wilson, 1974]. He showed, that in the strong coupling regime, QCD is confining, meaning that the potential between two static charges grows linearly with the separation of charges. Later that year, Kogut and Sussking extended the non-perturbative formulation in the Hamiltonian formalism [Kogut, Susskind,1975]. It was immediately clear that a direct evaluation of QCD path integral was only possible using Monte Carlo simulations. Creutz was the first to show numerically that the weak and strong regimes are in the same phase in four dimensions [Creutz 1979]. Since then, lattice QCD has grown into a separate numerical discipline and has delivered results of growing accuracy. This development was possible from the exponential increase of computing power and more efficient algorithms.

In this paper we deal with the basic technology at the bottom of any contemporary lattice computation without going into the details that make lattice QCD confront experiment as well as predict physics beyond the Standard Model. Lattice QCD is a collaborative project, and as such, may not be brought into one review paper without missing a single contribution. Here

we profit from the QCDLAB programs which is a small set of short programs that allows one to ilustrate the basic properties of QCD without getting bogged down into the details of advanced computing technology and associated software and algorithms. In contrast to other sotware, QCDLAB maps linear operators of QCD to linear operators of the GNU Octave language [GNU Octave, 2018]. Although GNU Octave is an interpreted language, linear operators are precompiled. This property enables very efficient coding as well as minimal run times.

However, GNU Octave is a one-threaded software and runs in one computing core only. Therefore, QCDLAB usage is limited to moderate lattices. It is possible however to include multi-threaded C++ libraries such that the programs run in multiple cores. Writ-ing dedicated libraries of this sort will drive the QCDLAB project out of the original aim of keeping the programing effort small. Nonetheless, Octave is a language in development and is likely to include in the future multi-threaded linear algebra libraries.

In summary, QCDLAB serves three purposes: teaching, learning as well as algorithm prototyping. The latter helps developing a complex software by testing the basic idea of a new algorithm on GNU Octave using QCDLAB codes. QCDLAB programs, version 2.0, as well as this document are available at:

`https://sites.google.com/site/artanborici/qcdlab`

It is licensed under the GNU General Public License v3. The present document serves as a user guide of QCDLAB as well as an illustration of basic calculations in lattice QCD.

2. QCD DATA

The space-time world in lattice QCD is taken to be a four dimesnional regular lattice. At each lattice site go out four directed links, as ilustrated below in the case of two dimensions. The lattice sites are numberd in a lexicographical order.

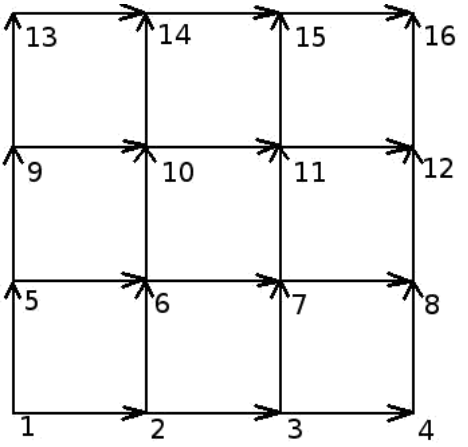

The basic degree of freedom on the lattice is the gauge field. Lattice gauge fields are SU(3) group elements in the fundamental representation, i.e. 3 3 complex unitary matrices with determinant one. We associate one such element to each directed link on the lattice. If i and $i+\hat{\mu}$ label two neighboring lattice sites along the direction $\mu \in \{1,2,3,4\}$ the associated link is denoted by $U_{\mu,i}$ as in the figure.

2.1. Lattice configurations

The collection of all lattice links is a lattice configuration. The basic linear operator in lattice QCD is the matrix of such a configuration along the direction μ:

$$U_\mu = \begin{pmatrix} U_{\mu,1} & & & \\ & U_{\mu,2} & & \\ & & \ddots & \\ & & & U_{\mu,N} \end{pmatrix}$$

where N is the total number of lattice sites and the ordering is lexicographical. If N_1,N_2,N_3 and N_4 are the number of sites along each direction, the total number of sites is $N = N_1N_2N_3N_4$. Note that U_μ is a block diagonal matrix with blocks of 3 x 3 size.

QCDLAB follows the same data structure. For example, a random gauge field, which is appropriate for QCD at strong copuling can be generated by the following routine:

```
function U=RandomGaugeField(N);
%
U1=[ ]; U2=[ ]; U3=[ ]; U4=[ ];
for k=1:N;
[u1,R]=qr(rand(3)+sqrt(-1).*rand(3));u1(:,3)=u1(:,3)/det(u1);
[u2,R]=qr(rand(3)+sqrt(-1).*rand(3));u2(:,3)=u2(:,3)/det(u2);
[u3,R]=qr(rand(3)+sqrt(-1).*rand(3));
u3(:,3)=u3(:,3)/det(u3); [u4,R]=qr(rand(3)+sqrt(-1).*rand(3));
u4(:,3)=u4(:,3)/det(u4); U1=[U1,u1];
U2=[U2,u2];
U3=[U3,u3];
U4=[U4,u4];
end
% form sparse matrices
[I,J]=find(kron(speye(N),ones(3)));
u1=sparse(I,J,U1,3.*N,3.*N);
u2=sparse(I,J,U2,3.*N,3.*N);
u3=sparse(I,J,U3,3.*N,3.*N);
u4=sparse(I,J,U4,3.*N,3.*N);
U=[u1,u2,u3,u4];
```

Note the sequential loop creating the gauge fields one by one. It is the only instance where QCDLAB uses such a loop in connection to degrees of freedom. This routine is called only once, usually at the begining of the simulation code. The user can avoid its call by simply starting with identity matrices and create random gauge fields using the simulation routine. This is controlled by the `GaugeField` function. Note also that the set of four gauge fields is stored in a single matrix `U=[u1,u2,u3,u4]`.

2.2. Shift operators

An important operator on the lattice is the permutation operator that shifts lattice sites along the positive direction m:

$$T_\mu = \begin{pmatrix} & 1 & & \\ & & 1 & \\ & & & \ddots \\ 1 & & & \end{pmatrix}$$

In total we have four such operators, one for each direction. In four dimensions these are built using Kronecker products with identity matrices I_{N1}, I_{N2}, I_{N3}, I_{N4}:

$$E_1 = I_4 \otimes I_3 \otimes I_2 \otimes T_1 \otimes I_3$$
$$E_2 = I_4 \otimes I_3 \otimes T_2 \otimes I_1 \otimes I_3$$
$$E_3 = I_4 \otimes T_3 \otimes I_2 \otimes I_1 \otimes I_3$$
$$E_4 = T_4 \otimes I_3 \otimes I_2 \otimes I_1 \otimes I_3$$

Note that the extra Kronecker product with the identity 3 3 matrix is neccessary in order to accomodate the space of gauge fields. The following routine creates the required operators:

```
function E=ShiftOperators(N1,N2,N3,N4);
% Shift operators

p1=[N1,1:N1-1]; p2=[N2,1:N2-1]; p3=[N3,1:N3-1]; p4=[N4,1:N4-1];
I1=speye(N1); I2=speye(N2); I3=speye(N3); I4=speye(N4);
T1=I1(:,p1); T2=I2(:,p2); T3=I3(:,p3); T4=I4(:,p4);
e1=kron(I4,kron(I3,kron(I2,kron(T1,speye(3)))));
e2=kron(I4,kron(I3,kron(T2,kron(I1,speye(3)))));
e3=kron(I4,kron(T3,kron(I2,kron(I1,speye(3)))));
e4=kron(T4,kron(I3,kron(I2,kron(I1,speye(3)))));
E=[e1,e2,e3,e4];
```

Like in the case of gauge fields the set of four shift operators is stored in a single matrix `E=[e1,e2,e3,e4]`.

2.3. Wilson action

With the above operators we can write down the action of the SU(3) lattice theory as proposed by Wilson:

$$S_{gauge}(U) = -\frac{1}{g^2}\sum_{\mu\nu} tr(U_\mu E_\mu)(U_\nu E_\nu)(U_\mu E_\mu)^*(U_\nu E_\nu)^*$$

where the star symbolises the matrix Hermitian conjugation, the trace is taken in the 3N dimensional space and g is the bare coupling constant of the theory. In lattice gauge theory it is standart to use the inverse coupling constant:

$$\beta = \frac{6}{g^2}$$

An important observable in QCD is the Wilson loop. The elementary Wilson loop, called plaquette, is the colorless product of gauge fields around an elementary suqare:

$$P_{\mu\nu,1} = \frac{1}{3}\mathrm{Re}\,tr_C U_{\mu,i} U_{\nu,i+\mu} U^*_{\mu,i+\nu} U^*_{\nu,i}$$

where the trace in performed in the color space.

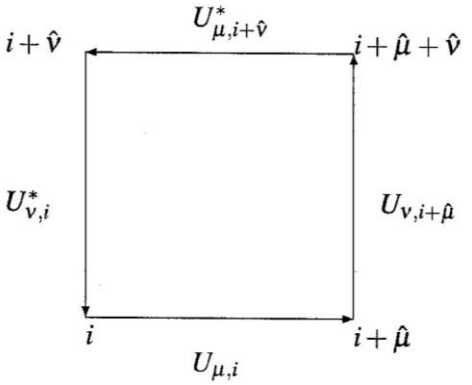

It is straightforward to see that the product of matrices in the Wilson action can be written as a sum over all plaquettes:

$$S_{gauge}(U) = -\beta \sum_{i,\mu>\nu} P_{i,\mu\nu}$$

The sum in the right hand side can be computed in QCDLAB by the following routine:

```
function p=Plaquette(U);
% computes unnormalised plaquette
p=0;
%globals
global beta N E
for mu=1:4;
for nu=mu+1:4;
    E1=E(:,(mu-1).3.N+1:mu.3.N); E2=E(:,(nu-1).3.N+1:nu.3.N);
    U1=U(:,(mu-1).3.N+1:mu.3.N); U2=U(:,(nu-1).3.N+1:nu.3.N);
    U1=U1.E1; U2=U2.E2;
    p=p+real(trace(U1.U2.U1'.U2'));
end
end
```

It follows directly the definition of the action in terms of sparse matrices, which makes the computation very efficient. Since the color trace is unnormalized in the routine the Wilson action is computed by calling `-beta/3.Plaquette(U)`.

2.4. Dirac operator

Let *D(U)* be the Wilson formulation of the Dirac operator describing one quark flavor with bare mass m in the background gauge field configuration *U*:

$$D(U) = (m+d)I - \frac{1}{2}\sum_{\mu}[(U_{\mu}E_{\mu})\otimes(1-\gamma_{\mu}) + (U_{\mu}E_{\mu})^{*}\otimes(1+\gamma_{\mu})]$$

where d = 4 and γ_μ are 4 x 4 Dirac matrices obeying the Dirac-Clifford algebra in the Euclidean signature:

$$\left\{\gamma_{\mu},\gamma_{\nu}\right\} = \delta_{\mu\nu}$$

We assume also periodic boundary conditions in each direction. To see why it works we set U_μ = I and go to momentum space, in which case $E_\mu(p)=e^{ip\mu}$ and therefore:

$$D(p) = m + i\sum_{\mu}\gamma_{\mu}\sin p_{\mu} + \sum_{\mu}(1-\cos p_{\mu})$$

It is clear that for small momenta $D(p) \to m + i\not{p} + p^2/2 + O(\not{p}^3)$, whereas at other corners of the Brillouin zone there are 15 additional heavy flavors with masses *m* + 2, *m* + 4, *m* + 6, *m* + 8 and spin structure described by different sets of gamma-matrices. Therefore, at small momenta, Wilson fermions describe a single flavor of fermions and break chiral symmetry even at *m* = 0 by the $p^2/2$ term. We will discuss this issue further in later sections. Here is the routine that implements Wilson fermions:

```
function A=Wilson(U,mass);
% Constructs Wilson-Dirac lattice operator
% global mass N N1 N2 N3 N4 E1 E2 E3 E4 GAMMA5
N1=6; N2=6; N3=6; N4=12; N=N1.N2.N3.N4;
% gamma matrices
gamma1=[0, 0, 0, -i; 0,0,-i,0; 0,i,0,0; i,0,0,0];
gamma2=[0, 0, 0, -1; 0,0,1,0; 0,1,0,0; -1,0,0,0];
gamma3=[0, 0, -i, 0; 0,0,0,i; i,0,0,0; 0,-i,0,0];
gamma4=[0, 0, -1, 0; 0,0,0,-1; -1,0,0,0; 0,-1,0,0];
% Projection operators
P1_plus=eye(4)+gamma1; P1_minus=eye(4)-gamma1;
P2_plus=eye(4)+gamma2; P2_minus=eye(4)-gamma2;
P3_plus=eye(4)+gamma3; P3_minus=eye(4)-gamma3;
P4_plus=eye(4)+gamma4; P4_minus=eye(4)-gamma4;
% Shift operators
p1=[N1,1:N1-1];p2=[N2,1:N2-1];p3=[N3,1:N3-1];p4=[N4,1:N4-1];
I1=speye(N1); I2=speye(N2); I3=speye(N3); I4=speye(N4);
T1=I1(:,p1); T2=I2(:,p2); T3=I3(:,p3); T4=I4(:,p4);
E1=kron(kron(kron(kron(T1,I2),I3),I4),speye(3));
E2=kron(kron(kron(kron(I1,T2),I3),I4),speye(3));
E3=kron(kron(kron(kron(I1,I2),T3),I4),speye(3));
```

```
E4=kron(kron(kron(kron(I1,I2),I3),T4),speye(3));
%
U1=U(:,0.3.N+1:1.3.N);
U2=U(:,1.3.N+1:2.3.N);
U3=U(:,2.3.N+1:3.3.N);
U4=U(:,3.3.N+1:4.3.N);
%
% Upper triangular
A=      kron(U1.E1,P1_minus);
A=A+kron(U2.E2,P2_minus);
A=A+kron(U3.E3,P3_minus);
A=A+kron(U4.E4,P4_minus);
% Lower triangular
A=A+kron(U1.E1,P1_plus)';
A=A+kron(U2.E2,P2_plus)';
A=A+kron(U3.E3,P3_plus)';
A=A+kron(U4.E4,P4_plus)';
A=(mass+4).speye(12.N)-0.5.A;
```

2.5. A first algorithm

One special task in QCDLAB is the exponentiation of su(3) algebras. The concrete form of an su(3) algebra associated to a SU(3) gauge field in the fundamental representation is a 3 x 3 anti-Hermitian traceless matrix. We have the following task: given a block diagonal matrix P_μ of order $3N$ with non zero *su*(3) algebra blocks we would like to compute the gauge field matrix:

$$U_\mu = e^{P\mu}$$

without using loops over the lattice sites. Here is an algorithm that completes this task:

```
function U=Exp_su3(P);
% exponentiate su(3) algebras
% using power expansion and Horner's algorithm
global N
%
P1=P(:,0.3.N+1:1.3.N);
P2=P(:,1.3.N+1:2.3.N);
P3=P(:,2.3.N+1:3.3.N);
P4=P(:,3.3.N+1:4.3.N);
%
Id=speye(max(size(P1)));
u1=Id; u2=Id; u3=Id; u4=Id;
n=24;
for k=n:-1:1;
   u1=Id+P1.u1/k;
   u2=Id+P2.u2/k;
   u3=Id+P3.u3/k;
   u4=Id+P4.u4/k;
end
U=[u1,u2,u3,u4];
```

It is an implemetation of the exponential power expansion:

$$e^{P\mu} = \sum_{k=1}^{n} \frac{P_\mu^k}{k!} + O\left[P_\mu^{(n+1)} \right]$$

truncated at order n = 24 using the Horner algorithm. The order is chosen such that the resulting gauge fields are SU(3) matrices in the working precision of GNU Octave. If in doubt, the user should use the routine `Unitarity_check`. There are more efficient implementations if we were to write the routine in C++. In this case one can exponentiate *su*(3) algebras one at a time using the algorithm behind the expm function of the GNU Octave.

3. QCD path integral

In this paper we focus in the simulation of pure Yang-Mills theory. Simulation of lattice QCD in this approximation, known as the quenched approximation, neglects screening coming from quark-antiquark pairs. It delievers very fast QCD properties such as the linear rising potential and hadron spectrum. Therefore, our task is the evaluation of the path integral:

$$Z = \int \prod_{\mu,i} dU_{\mu,i} e^{-S_{gauge}(U)}$$

where $dU_{\mu,i}$ denotes the the SU(3) group integration measure, which is asummed to be gauge invariant. Its concrete form is unimportant in the algorithms used in QCDLAB.

3.1. Hybrid Monte Carlo Algorithm

The HMC algorithm [Duane et. al. 1987] starts by introducing *su*(3) conjugate momenta matrices P_μ to gauge fields. Gauge field configurations are generated by integrating classical field equations with Hamiltonian:

$$H(P,U) = -\frac{1}{4} tr \sum_{\mu} P_{\mu}^2 - \frac{\beta}{6} \sum_{\mu\nu} tr(U_\mu E_\mu)(U_\nu E_\nu)(U_\mu E_\mu)^*(U_\nu E_\nu)^*$$

The extra one half in the normalization of the kinetic energy comes from the normalization of Gell-Mann matrices, which are adopted as *su*(3) algebra generators in the calculation of momentum matrices. The kinetic energy is computed by the following routine:

```
function y=T(P);
%   computes the kinetic energy of H
global N
p1=P(:,0.3.N+1:1.3.N);
p2=P(:,1.3.N+1:2.3.N);
p3=P(:,2.3.N+1:3.3.N);
p4=P(:,3.3.N+1:4.3.N);
y=-(trace(p1^2)+trace(p2^2)+trace(p3^2)+trace(p4^2))/4;
y=real(y);
```

The first equation of motion is:

$$\dot{U}_\mu = P_\mu U_\mu$$

Since H is an integral of motion, the second equation is derived by the equation:

$$0 = H = -\frac{1}{4} \sum_{\mu} trP_\mu \dot{P}_\mu - \frac{\beta}{6} \sum_{\mu\nu} (\dot{U}_\mu E_\mu)(U_\nu E_\nu)(U_\mu E_\mu)^*(U_\nu E_\nu)^* + h.c.$$

Substituting for $\dot{U}_\mu$ the first equation of motion:

$$0 = H = -\frac{1}{2} \sum_{\mu} trP_\mu \left\{ \frac{1}{2} \dot{P}_\mu + \frac{\beta}{3} \sum_{\nu(\neq\mu)} \left[P_{\mu\nu}^{(1)} + P_{\mu\nu}^{(2)} \right] \right\} + h.c.$$

with $$P_{\mu\nu}^{(1)} = (U_\mu E_\mu)(U_\nu E_\nu)(U_\mu E_\mu)^*(U_\nu E_\nu)^*$$

$$P_{\mu\nu}^{(2)} = (U_\mu E_\mu)(U_\nu E_\nu)^*(U_\mu E_\mu)^*(U_\nu E_\nu)$$

one gets the second equation of motion:

$$\frac{1}{2}\dot{P}_\mu = -\frac{\beta}{3}\sum_{\nu(\neq\mu)}\left[P^{(1)}_{\mu\nu} + P^{(2)}_{\mu\nu}\right]$$

Since $P_{\mu\nu}$ matrices are 1 x 1 loops around adjecent plaquettes that share a common link, they are block diagonal matrices of 3 x 3 blocks. However, these blocks are not guaranted to be *su*(3) valued. Therefore, the force exerted at the gauge field $U_{\mu;\mu}$ is the traceless anti-Hermitian part of $\dot{P}_{\mu,i}$:

$$F_{\mu,i} = \frac{1}{2}\left(\dot{P}_{\mu,i} - \dot{P}^*_{\mu,i}\right) - \frac{1}{3}tr_C\,\frac{1}{2}\left(\dot{P}_{\mu,i} - \dot{P}^*_{\mu,i}\right)$$

The force is implemented in the following routine:

```
function F=Force_su3(U);
%globals
global beta N E
F=[];
for mu=1:4;
M=sparse(zeros(3.N));
for nu=1:4;
if (mu~=nu),
E1=E(:,(mu-1).3.N+1:mu.3.N);
E2=E(:,(nu-1).3.N+1:nu.3.N);
U1=U(:,(mu-1).3.N+1:mu.3.N);
U2=U(:,(nu-1).3.N+1:nu.3.N);
U1=U1.E1; U2=U2.E2;
M=M+U1.U2.U1'.U2'+U1.U2'.U1'.U2;
endif
end
f=M-M';
% subtract trace
diag_f=diag(f); tr_f=sum(reshape(diag_f,3,N));
tr_f=kron(transpose(tr_f),ones(3,1));
f=f-sparse(diag(tr_f))/3;
F=[F,f];
end
F=-beta/3.F;
```

Having the equations of motion the next step is to build a trajectory using the leapfrog integration scheme:

$$U_\mu(t+\frac{\Delta t}{2}) = e^{P_\mu(t)\Delta t/2}U_\mu(t)$$

$$P_\mu(t+\Delta t) = P_\mu(t) + F_\mu(t+\Delta t/2)\Delta t$$

$$U_\mu(t+\Delta t) = e^{P_\mu(t+\Delta t)\Delta t/2}U_\mu(t+\Delta t/2)$$

with a Δt step size and a trajectory length τ. At $t = 0$ $su(3)$ momenta are taken to be Gaussian su(3) algebras: given eight independently distributed standard Gaussian variables at each lattice site and direction the routine `algebra_su3` computes the corresponding momentum matrices. Note the half step updates of guage fields: it is expected that the force requires more flops than the exponentiation.

The algorithm ends by correcting for the non-conservation of the Hamiltonian using Metropolis et.al. with acceptance probability:

$$P_{acc}(\{P(0),U(0)\} \to \{P(\tau),U(\tau)\}) = \min\left\{1, e^{-[H(\tau)-H(0)]}\right\}$$

Upon rejection, one goes back to $t = 0$ and refreshes momenta. This ends the description of the Hybrid Monte Carlo algorithm. One implicit and important assumption of QCDLAB is that the rand function of GNU Octave suffices its purpose. The simulation routine of QCDLAB is:

```
function [acc,Plaq,U1,stat]=SU3(NMC,U1,iconf);
%globals
%global beta N N1 N2 N3 N4 E
beta=5.7; N1=6; N2=6; N3=6; N4=12; N=N1.N2.N3.N4;
E=ShiftOperators(N1,N2,N3,N4);
%Starting configuration
if (iconf~=2),
   U1=GaugeField(iconf); %iconf=0/1 (cold/hot)
endif
% Start Hybrid Monte Carlo
ntest=0; Plaq=[]; stat=[]; acc=0;
NMD=20; deltat = 0.025;
for mc = 1:NMC;
   p=randn(8,4.N); % Refresh momenta
   P=algebra_su3(p);
% Compute H1
H1=T(P)-beta/3.Plaquette(U1);
% Propose U2 using MD evolution
% U2=U1;
% MD loop
for md=1:NMD;
 U2=MultSU3(Exp_su3(P.deltat/2),U2); % Advance fields half step
 P=P+Force_su3(U2).deltat; % Advance momenta full step
 U2=MultSU3(Exp_su3(P.deltat/2),U2); % Advance fields half step
end
% Compute H2
   H2=T(P)-beta/3.Plaquette(U2);
% Metropolis test
R=min([1,exp(-(H2-H1))]);
random=rand;
istat=[random,R,H2-H1]; stat=[stat;istat];
if random<R,
   U1=U2;
   acc=acc+1;
   plaq=Plaquette(U1)/N/6/3; Plaq = [Plaq;plaq];
 end
```

```
end
acc=acc/NMC
```

Now we have enough programs to start exploring QCD. In the next section we begin with the string tension computation.

4. QCD string

In QCD, the energy between two static charges at large enough separation R follows the string law:

$$V(R) = KR ;$$

where K is the string tension. On the lattice we measure the dimensionless string tension $K = a^2 K$, where a is the lattice spacing. Using the string tension value from the Regge slopes, K = (440 MeV)^2, one can set the physical scale:

$$a = \frac{197 MeVfm}{440 MeV}\sqrt{K} ,$$

where 197 MeV fm = 1 is the energy-length conversion factor. Scale setting can be performed using any other physical quantity such as a hadron mass. QCD is compared to experiment by extrapolating dimensionless ratios of physical quantities at vanishing lattice spacing keeping the physical lattice size large enough to fit the physics. But how do we measure the string tension? We use an important lattice observable, the Wilson loop, which we deal with next.

4.1. Wilson loop

We already know how to measure a 1 x 1 Wilson loop, or the plaquette. Alghough one can measure all sorts of Wilson loops on the lattice, we restrict ourseleves to rectangle Wilson loops of dimensions R x T . Let V_1 and V_2 be the product of matrices along the R and T directions respectively:

$$V_1 = \underbrace{(U_1 E_1)...(U_1 E_1)}_{R \ times}, \ V_2 = \underbrace{(U_2 E_2)...(U_1 E_2)}_{T \ times} .$$

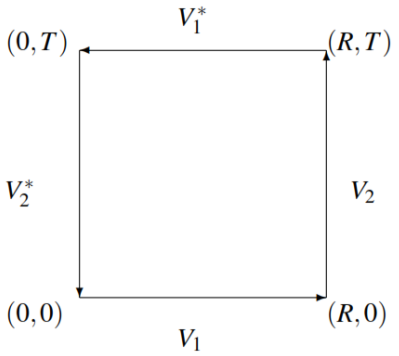

Then, the (unnormalized) R x T Wilson loop is:

$$W(R,T) = \sum_{\mu \neq \nu} \mathrm{Re}\, tr V_1 V_2 V_1^* V_2^*$$

The following routine is a direct implementation of the formula.

```
function w=Wloop(R,T,U,N1,N2,N3,N4);
% computes rectangular Wilson loop
E=ShiftOperators(N1,N2,N3,N4);
N=N1.N2.N3.N4;
w=0;
for mu=1:4;
for nu=1:4;
 if (mu!=nu),
  E1=E(:,(mu-1).3.N+1:mu.3.N); E2=E(:,(nu-1).3.N+1:nu.3.N);
  U1=U(:,(mu-1).3.N+1:mu.3.N); U2=U(:,(nu-1).3.N+1:nu.3.N);
  U1=U1.E1; U2=U2.E2; V1=speye(size(U1));
  for r=1:R;
     V1=V1.U1;
  end
  V2=speye(size(U2));
  for t=1:T;
   V2=V2.U2;
  end
  w=w+real(trace(V1.V2.V1'.V2'));
 end
end
end
```

4.2. Area law

The vacuum expectation value of *R x T* Wilson loop is the correlation function of the static quark-antiquark propagator separated with T lattice sites. Since, the large time behavior is dominated by the ground state contribution:

$$W(R,T) = \langle W(R,T) \rangle \simeq e^{-V(R)T}$$

the string behavior of the potential *V(R)=KR* is observed if the Wilson loop falls off exponentially with the area of the loop RT. A direct way to measure the string tension is by means of Creutz ratios:

$$\chi(R,T) = -\log \frac{W(R+1,T+1)W(R,T)}{W(R+1,T)W(R,T+1)}$$

at large R and T values. Note that W 's are sample averages and error propagation is not straightforward. A proper way to compute the error is using partial sample averages. This requires a large sample volume, which is often not available. An important trick, used as a short cut, is data resampling, or the so called *bootstrap* resampling. We will expain shortly, a bootstrap variant which is widely used in lattice QCD, the *jackknife* method.

4.3 Jackknife resampling

Let us suppose we are given the real data vector x with volume n. The resampled jackknife data is the linear map:

$$x^{(J)} = \overline{x} - \frac{x - \overline{x}}{n-1}$$

which conserves the sample average $\overline{x}$. If we require further the conservation of variance:

$$Var\left[x^{(J)}\right] = Var(x) \;\Leftrightarrow\; C\left\|x^{(J)} - \overline{x}\right\|^2 = \frac{1}{n-1}\left\|x - \overline{x}\right\|^2$$

we should should choose the normalization factor *C=n–1*. As it is clear by inspection, the elements or $x^{(J)}$ are partial sample averages of x:

$$x_i^{(J)} = \frac{1}{n-1}\sum_{k(\neq 1)} x_k$$

This way, we gain n 1 more sample averages of primary data than in the case without resampling. Thus, the physical quantity of interest, for example a Creutz ratio, is computed for all individual elements of $x^{(J)}$ as opposed to a single sample average that was available originally. If y is the vector such estimations, its sample variance normalization is inherited from the corresponding variance of resampled data:

$$Var(y) = (n-1)\left\| y - \bar{y} \right\|^2 .$$

The QCDLAB routine that computes Creutz ratios is `creutz_ratios`. Applying it to a small sample of 10 Wilson loops of maximal linear size 4, obtained on 6^3x12 lattices, we get:

$$\chi(2,2) = 0.37(1), \quad \chi(3,3) = 0{:}28(2), \quad \chi(4,4) = 0.46(33)$$

with the corresponding estimation of the lattice spacings, in fm units:

$$a_{(2,2)} = 0.272(3), \quad a_{(3,3)} = 0.24(1), \quad a_{(4,4)} = 0.30(11).$$

Normally we should rely on the results of large Wilson loops. We see however, that the $a_{(4,4)}$ value has a large error, so that the compromise is to select the $a_{(3,3)}$ value as the estimation of our scale.

4.4 Quark-antiquark potential

A standard way to measure the string tension on the lattice is measuring the quark-antiquark potential. In order to extract the potential from the Wilson loops one usually relies on effective potentials:

$$V_{eff}(R,T) = -\log \frac{W(R,T+1)}{W(R,T)}$$

For fixed R we select as *V(R)* the median value of $V_{eff}(R,T)$ over all *T* sizes of Wilson loops, whereas the corresponding error is computed using the jackknife method. These data are fitted to the general form:

$$V(R) = V_0 + \frac{\alpha}{R} + KR$$

where V_o and α are two more constants in addition to the string tension K. Such a procedure is coded in the routine `effective_potentials`. Using the same set of Wilson loops as in the case of Creutz ratios the routine produces the 3-sigma band plot:

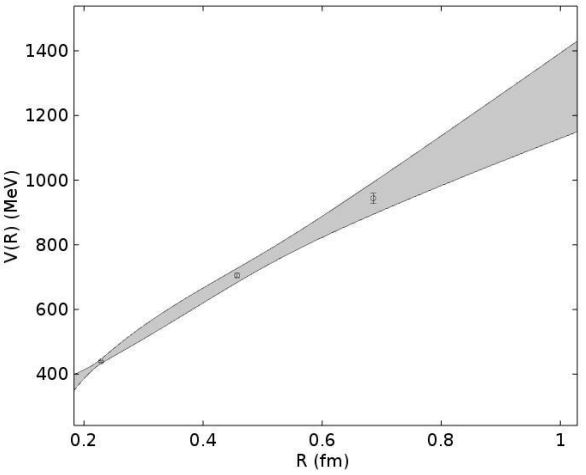

as well as the results:

$$\chi = 0.26(3),\ \alpha_{pot} = 0.23(1)\ \text{fm}.$$

From the plot we see that the potential is of the order of 1 GeV if it is extrapolated at 1 fm separation. We observe also that the results are consistent with those obtained using Creutz ratios.

5. Hadron spectrum

A basic computation in lattice QCD is the hadron spectrum. We will ilustrate it in the case of low lying mesons such as the pion and rho. Quark propagators are computed using the `quark_propagator` routine. It calls the BiCGstab algorithm [Van der Vorst, 1992, Gutknecht, 1993] as a Dirac solver:

$$q = D^{-1}b$$

where D is the Wilson operator and b a point source at the origin of the lattice for each color and Dirac spin. Therefore, at each lattice site x the propagator q_x is a 12x12 matrix. The pion and rho propagators are defined as:

$$G_{\pi,x} = Trq_x q_x^* \ , \quad G_{\rho,x} = Tr\gamma_5\gamma_k q_x \gamma_k \gamma_5 q_x^* \ ,$$

where the trace and Hermitian conjugation is performed in the tensor product space of color and spin. We sum over space-like lattice sites in order

to get particle masses. For example, at long Euclidean time separation T the pion propagator is dominated by its ground state contribution:

$$G_{\pi,T} = \sum_{\vec{x}} G_{\pi,(T,\vec{x})} \simeq Ce^{-m_\pi T}$$

Since we simulate with periodic boundary conditions in all directions the propagator de-cays exponentially also with respect to reflected times, which are translated by the lattice size N_4:

$$G_{\pi,T} \simeq C\left[e^{-m_\pi T} + e^{-m_\pi (N_4 - T)}\right] \propto \cosh\left(T - \frac{N_4}{2}\right)$$

Therefore, the routine `pion_propagator` symmetrizes propagators with respect to the origin, which is actually at T = 1:

```
N1=6;N2=6;N3=6;N4=12;
N=N1.*N2.*N3.*N4;
pion=sum(abs(q).^2,2);
pion=sum(reshape(pion,12,N));
pion=sum(reshape(pion,N4,N1.*N2.*N3),2);
pion(2:N4/2)=(pion(2:N4/2)+pion(N4:-1:N4/2+2))/2;
pion(N4/2+2:end)=[];
```

5.1 Effective masses

In complete analogy to the quark-antiquark potential we compute the effective masses of mesons as:

$$M_{eff}(T) = -\log\frac{G_{\pi,T+1}}{G_{\pi,T}}$$

and take the median value over all T values as the actual M_{eff}. The meson masses squared are then fitted against the bare quark masses using a quadratic model:

$$M_{eff}^2 = c_o + c_1 m + c_2 m^2 ;$$

where c_o, c_1, c_2 unknown constants. With Wilson fermions we define the chiral limit at the vanishing pion mass. This procedure can be implemented by first calling the routine `effective_masses` with pion data to find the critical quark mass m_c. Then, the routine is called with rho data and critical quark mass as input. It returns the lattice spacing using M_r = 770 MeV. Finally, the routine is called once more with pion data and the lattice spacing as input. Using the same configurations as before we get the 3-sigma band plot for pion and rho masses:

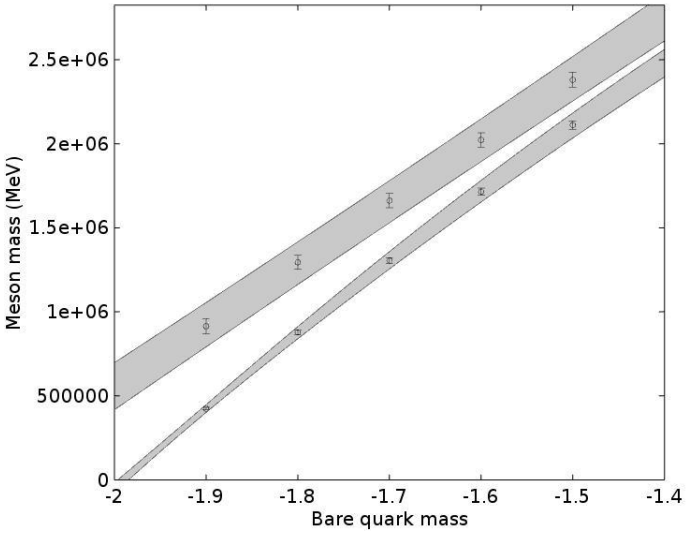

We have used a linear fit for the *rho* and a quadratic fit for the *pion*. The plot shows that the pion mass squared vanishes linearly with the quark mass in the chiral limit:

$$M_\pi^2 = c_1(m - m_c) + c_2(m^2 - m_c^2)$$

The nonzero value of m_c is an artifact of Wilson fermions. For chirally symmetric fermions there should be no such artificats like the critical bare mass. We these data, the estimated lattice spacing:

$$a_\rho = 0.19(1) \text{ fm}$$

and the one estimated using the quark-antiquark potential are 4-sigma away from each other. This discrepancy illustrates various systemtatic errors, the finite lattice spacing and lattice size being the most important ones.

6. Autocorrelations

An important issue that one must take into the consideration in error reporting are auto-correlations in the Monte Carlo time series. If $x^{(1)} = (\vartheta_1, \vartheta_2, ..., \vartheta_n)$ is the time series vector of an observable ϑ one measures the autocorrelation function between $x^{(1)}$ and the time forwarded samples $x^{(1)}, x^{(2)}, ..., x^{(t)}$:

$$f_{j,\vartheta} = C \sum_{k=1}^{n-t+1} \left(x_k^{(1)} - \overline{x}^{(1)} \right) \left(x_k^{(j)} - \overline{x}^{(j)} \right) \ , \ \text{j=1,2,…,t}$$

as well as the integrated autocorrelation time $\tau_{\text{int},\vartheta}$ [Sokal, 1992]:

$$\tau_{\text{int},\vartheta} = \frac{1}{2} + \sum_{j=2}^{n} \left(1 - \frac{j-1}{n} \right) f_{j,\vartheta}$$

The normalization constant C is chosen such that $f_1 = 1$. The right hand side may be approximated by the sum:

$$\tau_{\text{int},\vartheta} \approx \frac{1}{2} + \sum_{j=2}^{t} f_{j,\vartheta}$$

assuming that the data volume is much larger than the cutoff *t*. QCDLAB routine that computes autocorrelations is `Autocorel`:

```
function [tau_int,f]=Autocorel(x,t);
% x: data vector of length N
% t: forward time
% tau_int: integrated autocorrelation time
% f: autocorrelation function
x=x(:);
N=max(size(x));
x1=x(1:N-t+1);
x1=x1-mean(x1).ones(N-t+1,1);
f=zeros(t,1);
for j=1:t;
xj=x(j:N-t+j);
xj=xj-mean(xj).ones(N-t+1,1);
f(j)=x1'.xj/(N-t+1);
end
f=f/f(1);
tau_int=1/2+sum(f(2:t));
```

A proper estimation of autocorrelations should also ensure that the integrated autocorrelation times are small compared to *t*, and the corresponding error is computed on a large data set. In our simulation example, plaquette decorrelates in 5(2) Hybrid Monte Carlo trajectories and saved configurations are separated by 100 trajectories.

In summary, we have described briefly the main routines of QCDLAB, version 2.0, as well as its use.

REFERENCES

[Gross,Wilczek,1973] D. J. Gross, Frank Wilczek, Ultraviolet Behavior of Nonabelian Gauge Theories, Phys. Rev. Lett. 30 (1973) 1343.

[Politzer, 1973] H. D. Politzer, Reliable Perturbative Results for Strong Interactions?, Phys. Rev. Lett. 30 (1973) 1346.

[Wilson, 1974] K. G. Wilson, Confinement of Quarks, Phys. Rev. D10 (1974) 2445.

[Kogut,Susskind,1975] J. B. Kogut, L. Susskind, Hamiltonian Formulation of Wilson's Lattice Gauge Theories, Phys. Rev. D11 (1975) 395.

[Creutz 1979] M. Creutz, Confinement and the Critical Dimensionality of Space-Time, Phys. Rev. Lett. 43 (1979) 553-556.

[GNU Octave, 2018] https://www.gnu.org/software/octave/.

[Duane et. al. 1987] S. Duane et. al., Hybrid Monte Carlo, Phys. Lett. B195 (1987) 216.

[Van der Vorst, 1992] H. A. Van der Vorst, Bi-CGSTAB: A Fast and Smoothly Converging Variant of Bi-CG for the Solution of Nonsymmetric Linear Systems, SIAM J. Sci. and Stat. Comput. 13(2) (1992), 631.

[Gutknecht, 1993] M. H. Gutknecht, Variants of BICGSTAB for Matrices with Complex Spectrum, SIAM J. Sci. Comput. 14(5) (1993) 1020.

[Sokal, 1992] A . D. Sokal, Bosonic Algorthms, in Quantum Fields on the Computer, M.

Creutz, editor, World Scientific (1992) 211.

MANAGEMENT OF RADIOACTIVE WASTE IN ALBANIA

Dritan PRIFTI, Elida BYLYKU and Brunilda DACI
Institute of Applied Nuclear Physics, University of Tirana, Albania

ABSTRACT

In Albania like throughout the world, radioactive sources are used in medicine, industry, agriculture, research, and teaching; they are also used in some military applications. A new radioactive waste storage facility for the management and temporary storage of radioactive waste was set up in 1999 at the Institute of Applied Nuclear Physics (IANP), Tirana, Albania. Radioactive waste and sources of non-nuclear origin have been put into this facility for processing and temporary storage in accordance with the national / international radioactive waste acceptance criteria. Albania has a legal and regulatory framework according to international standards in the field of radioactive waste management where the basic law is the law no. 8025, dated 9.11.1995 "On protection from ionizing radiation" amended with no. 9973, dated July 28, 2008. The Radiation Protection Commission (RPC) is the Regulatory Body that defines the policies related to the treatment of radioactive waste and sources in Albania. The Radiation Protection Office (RPO) has been established as the executive body of the RPC and a national inventory of radioactive waste and sources has been created. IANP is the institution responsible for the processing and management of all radioactive waste and disused sources, produced in Albania. In addition, it is licensed by the RPC for the import - export, transportation, treatment, conditioning and temporary storage of radioactive sources and wastes. IANP has in use and temporary storage radioactive sources of category I-V and performs transport of radioactive materials in accordance with the new regulation on transport in Albania, No.815, dated 16.11.2016 "On the safe transport of radioactive materials". Treatment of radioactive waste and sources is carried out in accordance with Decision no. 638, dated 7 September 2016, of the Council of Ministers "On the adoption of the regulation on the safe handling of radioactive waste in the Republic of Albania". The security assessment of the storage facility for temporary storage and management of radioactive waste is made considering its impact on employees, the public and the environment and in accordance with the Decision of the Council of Ministers no. 877, dated 30.10.2015, on the adoption of the regulation "On security of radioactive sources in the Republic of Albania". The storage capacity of this facility will be sufficient for Albania's needs over the projected 30-year operating period. A study will be carried out based on the Decision No.435 dated 14.10.2015 "On approval of

the document of strategic steps for the safe management of radioactive waste in the Republic of Albania" for the location and construction of a radioactive waste disposal facility in our country. The present study is based on the guidelines and recommendations of the International Atomic Energy Agency (IAEA).
Keywords: radioactive waste; radioactive sources; treatment; conditioning; temporary storage

2. INTRODUCTION

A new radioactive waste storage facility (RWSF) was set up in 1999 at the IANP for processing and temporary storage of radioactive wastes and disused sealed radioactive sources (DSRS) in accordance with National / International waste acceptance criteria (WAC) (Decision no. 638, 2016; IAEA-TECDOC-1515, 2006). The safety assessment of this facility is based on its impact to workers, public and environment (Law No. 8025, 1995; IAEA, SG No. WS-G-6.1, 2006; Regulation Nr.313, 2012).

The site receiving LLW/ILW of non-nuclear power plant origin (health care, industry, agriculture, education, research) has been operating since 1971 with a capacity of 60 m^3, reinforced by concrete / bricks vaults accommodating solid spent sources into drums. The decommissioning of old interim storage facility in IANP began due to the urbanization of the area—at a 10-meter distance. For that reason, the staff of IANP had transferred all plastic bags, lead containers and 200-liter drums conditioned with ^{226}Ra, ^{137}Cs, ^{60}Co into the new Radioactive Waste Storage Facility (IAEA SSS No. WS-R-5, 2006).

The temporary storage facility of LLW / ILW operates based on the IAEA Recommendations and the daily practice considering the country specific features. The Institute of Applied Nuclear Physics (IANP), Tirana, Albania, is the only authority in the country in charge for the collection, import - export, transport, pre-treatment, treatment, conditioning and temporary interim storage of radioactive sources and radioactive waste licensed by the Radiation Protection Commission (RPC) as the National Authority. This institution collaborates with the RPC for all radioactive sources entering Albania and carries out contracts with users for the conditioning of DSRS. The facility is designed as recommended by the IAEA (2014). Photo 1 and 2 show the two principal areas inside the facility; the Operational area and Temporary Interim Storage area. The storage facility for waste management was designed, constructed and supported financially by Albanian Government and the equipment has been provided by an IAEA Project.

Photo 1: Operational area.

Photo 2: Temporary Interim Storage area.

2. MATERIALS AND METHODS

2.1. National Legal and Regulatory Framework

A national legal and regulatory framework has been approved in Albania, providing among others the safety and security objectives, based on internationally agreed principles for a consistent level of institutional control in all steps of the waste management scheme.

Albania has in place a set of regulations for the safety, security and radiation protection to ionizing sources:

Law No. 8025, date 9.11.1995 "On Ionizing Radiation Protection" amended No. 9973, July 28-th 2008.

Regulation on "Categorization of radioactive sources in the Republic of Albania", Decision No. 09, date 07 January 2010 of Council of Ministers.

Regulations on "Licensing and inspection of activities with sources of ionizing radiation" Decision No.10, Date 07 January 2010 of Council of Ministers.

Regulation on "Safe handling with ionizing radiation sources", Decision No. 543, Date 7 July 2010 of Council of Ministers.

Decision No 344, date 29 April 2011 of Council of Ministers. - Regulation on "Protection of the employees professionally exposed to ionizing radiation sources".

Regulation on "Public protection from the discharges in the environment, determination of sampling, regions and frequency of measurement" Decision No 313, date 09 May 2012 of Council of Ministers

Regulation on "Public safety to exposures caused from ionizing radiation sources" Decision No 481, date 25 July 2012 of Council of Ministers.

Guidelines nr 1526/2, dated 13.04.2012 "Over the procedures of physical movement for radioactive materials, goods and reaction in case of incident with radioactive sources in CPs".

Regulation on "Safety on Medical exposure with ionizing radiations" No 229 date 20 March 2013.

Decision No 877, date 30.10.2015 of Council of Ministers. -Regulation on "Physical protection of the radioactive materials in the Republic of Albania",

Regulation No.957 date 25.11.2015 "For permitted levels of Radon concentration in buildings, and radionuclide's concentration in goods for public protection"

Regulation on "Safe management of radioactive waste in the Republic of Albania", Decision No. nr. 638, date 7.9.2016 of Council of Ministers.

Regulation on "Safe transport of radioactive materials", Decision No.815, date 16.11.2016 of Council of Ministers.

The IANP is licensed quinquennially by the RPC for the collection, import - export, transport, pre-treatment, treatment, conditioning and interim storage of radioactive sources and radioactive waste by the RPC as the National Authority.

2.2 Applications of Radioactive Materials/Sources in Albania

2.2.1 Industrial Applications

Geophysical/geochemical enterprises, metallurgical factories, oil-well companies etc, have in use for industrial purposes sealed radioactive sources. These radioactive sources are used in gauges that measure the evenness of asphalt during road paving. Sealed sources are also used in gamma radiography to check pipe welds. Industrial sources for density, level, thickness, weight, humidity, gauges measurements are widely used in our country. In NDT applications the radioactive source is placed inside the pipe at point of the weld to check the weld quality.

2.2.2 Medicine Applications

Nuclear Medicine Laboratories and Hospitals have in use radiotherapy and brachy-therapy radioactive sources like ^{60}Co, ^{137}Cs, ^{192}Ir or use ^{99}Mo / ^{99m}Tc

generators, ^{131} etc. In medicine radiation is used to kill cancer cells and shrink tumors in a patient. The sealed radioactive source that produces this radiation is part of a special piece of equipment called a tele-therapy machine. Another cancer treatment, called brachy-therapy, uses a small radioactive source that can be implanted in or near the tumor.

2.2.3 Military Chemistry Divisions

Usage of sealed radioactive sources in Albania begun in the early ’60 years supplied by the Russian Federation with calibration of dosimetric devices in some military divisions. These sources were mainly ^{226}Ra, ^{60}Co and ^{90}Sr. Regarding the DSRS used by military units of Ministry of Defense, the IANP/RPC have been contacted officially and after the agreement between the Ministry of Defense and IANP, it was confirmed that all DSRS have been stored / conditioned in IANP.

2.2.4 Agriculture

In agriculture, sealed radioactive sources are used to irradiate seeds and food. To prevent early sprouting, crop seeds can be exposed to short bursts of radiation in irradiators. Iradiators are also used to sterilize food and prevent food borne diseases. In irradiators, the sources are in fixed positions and housed within the radiation shield. The shield contains a rotor and during operation, the rotor turns 180 degrees and the sample chamber is exposed to radiation. Exposure rates during sample's irradiation are typically from 0.05 to 0.1 mR / hr. In irradiators with moving sources, the sources are mounted on shielded operating rods which are moved from the completely shielded "off" position to the "irradiate" position (wet-source-storage panoramic irradiators). Exposure rates are typically from 0.1 to 0.5 mR / hr.

2.3 Categorization of Radioactive Sources.

In Albania, the Safety Guide provides a categorization system for radioactive sources used in research, industry, medicine, agriculture and education (Table 1). In addition, it is applied for radioactive sources used in military / defense programs.

Table 1. Categorization of Radioactive Sources in Albania.

Category	**Practices**	**Activity Ratio (A/D)**	**Source Activity (Bq)**	**Radionuclide's**
1	Radioisotope thermoelectric generators, Irradiators, Tele-therapy sources, Fixed, multi beam tele-therapy	**A/D ≥ 100**	100 – 500TBq or 2,5 – 12,5 kCi	^{90}Sr,^{60}Co, ^{137}Cs, ^{60}Co (400 PBq), ^{137}Cs (600 PBq)
2	Industrial gamma radiography sources High/Medium dose rate BT	**1000>A/D≥10**	10 –100 TBq	^{137}Cs, ^{60}Co, ^{192}Ir , ^{137}Cs, ^{192}Ir
3	Fixed industrial gauges… Well loggings gauges	10>**A/D**≥1	1 – 10 TBq	^{137}Cs, ^{60}Co, ^{192}Ir ,^{137}Cs
4	Low dose rate BT sources Industrial gauges not inc HAS, bone densitometers Static eliminators	1>**A/D**≥0,01	1 – 10 GBq	^{137}Cs, ^{60}Co, ^{192}Ir, ^{137}Cs
5	Low dose rate BT sources XRF fluorescence Mossbauer practices Electron capture devices	**A/D**≥0,01 and **A** > **exempt**	40 MBq – 40 GBq	^{55}Fe, ^{57}Fe, ^{238}Pu, ^{241}Am, ^{109}Cd, ^{147}Pm , ^{63}Ni,etc.

2.4 Storage / Disposal Options in Albania

Table 2 reports the Albanian schema of national strategy for radioactive waste management.

Table 2. The Albanian national strategy for radioactive waste management

Half life	**Activity**	**Preferred**	**Options**	**Alternative**	**Options**
$T_{1/2}$	**(Bq)**	**Processing**	**Final step**	**Processing**	**Final step**
<100 days	All	Decay	Clearance	Conditioning Standard waste package	Disposal Near Surface Repository
>100 days	$< 10^6$	Conditioning Standard waste package	Disposal	Packaging for transport	Return at supplier or (other export)
< 30 years			Near Surface Repository		
>100 days	$> 10^6$	Packaging for transport	Return at supplier or other-export	Conditioning special waste package	Disposal Deep Repository
< 30 years					
> 30 years	$< 10^3$	Conditioning Standard waste package	Disposal Near Surface Repository	Packaging for transport	Return at supplier or other -export
> 30 years	$> 10^3$	Packaging for transport	Return at supplier or other -export	Conditioning Special waste package	Disposal Deep Repository

3. RESULTS AND DISCUSSION

3.1 Safety Assessment of Radioactive Waste Storage Facility

The building of the radioactive waste storage facility is considered suitable for the waste processing and storage. The site of the building is considered suitable in terms of possible external effects; the close vicinity of population to the site is not considered to represent a problem for the safety.

Building structures are stable and endurable to withstand degradation processes over the operation period envisaged and also disruptive events (earthquakes) that may occur during the operational period. There are passive safety features: i) protecting against floods by passive drainage systems and concrete barriers, ii) the building and the roof, in particular, will prevent water entering into the storage facility, iii) safety inside the storage facility does not rely on active systems like ventilation (which is only needed in the waste processing section of the building during the work) and, iv) wastes are protected by several physical (embedding in concrete, building structure, fences around the institute) and organisational (access control) barriers.

The layout of the building is in accordance with generic IAEA design and suitable for the planned operations (IAEA, 2014). The storage capacity will be sufficient for the needs of Albania over the anticipated operation period of 30 years. Radiation protection of public and workers is ensured using this building for waste processing and storage (Law No. 8025, 1995; Decision No. 08, 2010; Regulation Nr.313, 2012). The building is equipped with entrance and exit for emergency situations. Visible signs of radioactivity are located,

inside and outside this building. Lighting system inside the building and outside is very efficient.

The building is equipped with elements of high security system. Inactive area is separated from the operational areas with a high security door. Entry and exit in the premises of the operational area and other areas is done by inserting the input code (PIN). Movement of staff inside the premises is under continuous monitoring of the cameras, which are connected to the central system for monitoring the movements in the main entrance. Acoustic signal and data on the light is strong and immediate functional if any unknown person touches or violates these environments (Regulation No. 877, 2015). Retention rate and readiness in an emergency is carried out by high security system that is already in this building.

There are different procedures and emergency plans applicable in case of radiological emergencies inside the territory of IANP.

3.2 Procedures

i. The procedures to be followed are:
ii. Procedure for Entry and Exit at the Institute of Applied Nuclear Physics (IANP).
iii. Procedure for Entry and Exit at the Management and Storage Facility of Radioactive Waste and Sources.
iv. Procedure for Entry and Exit at the Secondary Standard Dosimetry Laboratory
v. Procedure for Entry and Exit at the Irradiation Laboratory
vi. Procedure for Acceptance of Radioactive Materials
vii. Procedure for Collection of Radioactive Materials
viii. Procedure for Pretreatment of Radioactive Materials
ix. Procedure for Treatment of Radioactive Materials
x. Procedure for Conditioning of Radioactive Materials
xi. Procedure for Transport of Radioactive Materials.

3.3 Radiological Emergency Plans

Radiological emergency plans are as following:

i. Radiological Emergencies Plan for the Transport of Radioactive Sources,
ii. Radiological Emergencies Plan for the First Category Radioactive Source, Cs-137
iii. Radiological Emergencies Plan for the Third Category Radioactive Source, Cs-137
iv. Radiological Emergencies Plan for the Radioactive Waste Storage Facility
v. General Radiological Emergencies Plan for Institute of Applied Nuclear Physics (IANP).

3.4 Current Status of Radioactive Waste Storage Facility

The facility represents a solid concrete construction with outside walls between 20 and 40 cm thick. All main entrances to the facility are protected with double security locks. The alarm system is monitored by cameras at the main entrance by policeman. The picture 3 shows the current RWSF.

Photo 3: Radioactive Waste Storage Facility.

Residential area is located 10 meters from the IANP. The surrounding wall of the IANP is 2 m high. The storage facility has been designed for the VIIIth degree of seismicity MSK-64; therefore no detrimental impacts from earthquakes are to be expected. There are no faults close to the site and geo-technical conditions are appropriate. In addition, no major industries with risk of explosion locate in the vicinities. Moreover, railway lines and the airport are at a considerable distance from the IANP (over 10 and 20 km, respectively).

3.5 Radioactive Waste Streams

The main radioactive waste streams in Albania are: i) scrap metals, ii) disused sealed radioactive sources (nuclear medicine, industrial applications, research activities) and, iii) radioactive waste from nuclear medicine applications.

3.6 Radioactive waste treatment methods

Waste treatment technologies in use are: i) size reduction, ii) chemical precipitation, iii) compaction and, iii) cementation in 200 L drums.

4. CONCLUSIONS

Management and treatment of radioactive waste is not a static process. Review of programs that deal with the problems for radioactive waste storage facilities is a permanent task of the staff working in this field. Rhythms of activities with radioactive sources in a near future in our country will be added, and, our study for them provides filling and closing of the works in the premises of temporary storage in IANP planned for the year 2030. For this reason is needed to undertake a study on the location and construction of a final disposal facility of radioactive waste in our country.

The present study is based on the guidelines and recommendations of the IAEA for the design and construction of such buildings or special places for storage of radioactive waste with low and intermediate activity near the soil surface. For the DSRS should be provided for their return to the manufacturer after the end of working hours (consumption). In cases where return is not provided or is not feasible, and in other cases of unknown origin, the treatment of these radioactive waste or DSRS will be performed by IANP. Acceptance of these DSRS will be made on the basis of a draft agreement between IANP and interested companies.

Specialists working in this field in our country will gain more experience during the new project "Upgrading of the radioactive waste storage building according to international standards" for the Technical Cooperation Programme Cycle 2018-2019 with IAEA Support.

REFERENCES

INTERNATIONAL ATOMIC ENERGY AGENCY Development of Specifications for Radioactive Waste Packages IAEA-TECDOC-1515, October 2006, https://www-pub.iaea.org/MTCD/Publications/PDF/te_1515_web.pdf.

INTERNATIONAL ATOMIC ENERGY AGENCY, Safety Standards- Storage of Radioactive Waste, Safety Guide No. WS-G-6.1, VIENNA, 2006, https://www-pub.iaea.org/MTCD/Publications/PDF/Pub1254_web.pdf.

INTERNATIONAL ATOMIC ENERGY AGENCY, Nuclear Energy Series, No-NW-T-1.4 Modular Design of Processing and Storage Facilities for Small Volumes of Low and Intermediate Level Radioactive Waste including Disused Sealed Sources, VIENNA, 2014, https://www-pub.iaea.org/MTCD/Publications/PDF/Pub1628Web-18312413.pdf.

INTERNATIONAL ATOMIC ENERGY AGENCY, IAEA SAFETY STANDARDS SERIES No. WS-R-5 Decommissioning of Facilities using Radioactive Material, Safety Requirements, VIENNA, 2006, https://www-pub.iaea.org/MTCD/Publications/PDF/Pub1274_web.pdf.

Law No. 8025, date 9.11.1995 "On Ionizing Radiation Protection" amended No. 9973, July 28-th 2008, http://www.ishp.gov.al/wp-content/uploads/2015/materiale/L.%20Nr.80252.pdf.

Regulation Nr.313 dated 9.05.2012 "On protection of the public from environmental emissions, the definition of sampling, regions and frequency of measurement'', http://www.ishp.gov.al/rrezatimet-jonizuese/rregullore-2/.

Regulation No.877 dated 30.10.2015 for the Physical Security of Radioactive Materials in the Republic of Albania, http://www.ishp.gov.al/rrezatimet-jonizuese/rregullore-2/.

Decision no. 638, date 07.09.2016, of the Council of Ministers "On the approval of the regulation on the safe handling of radioactive waste in the Republic of Albania", http://www.ishp.gov.al/rrezatimet-jonizuese/rregullore-2/.

THE SCHOLAR VIEWPOINTS ABOUT GEOLOGICAL FRAMEWORK OF MIRDITA OPHIOLITE ZONE IN ALBANIA

Shyqyri ALIAJ [1] and Salvator BUSHATI[2]

ABSTRACT

National syntheses and different scholar's studies about the geology of Albania have been collected and their opinions on the Mirdita zone framework are here reviewed. Most of the scholars pointed out that Mirdita zone involves the ophiolites with their sedimentary cover and, the boundary with Korabi zone passes after the eastern margin of the ophiolites which extends from Kukësi-Peshkopia region in the north to Mali i Thatë in the south. Some others concluded that: i) the Mirdita zone is composed of an ophiolitic subzone and a carbonatic subzone developped in both ophiolite sides, and ii) the border between Mirdita and Korabi zones passes east of Mirdita ophiolites, at the eastern margin of Middle Triassic-Jurassic limestones, and continues in the Peshkopia region. Some others underlined that Mirdita zone is composed of these two units: i) Triassic –Jurassic ophiolites with their sedimentary cover, and ii) subzone units at the periphery and at the basement of the ophiolites, and that the border between the Mirdita and Korabi zones passes after the boundary between Gjallica and Çaja subzones, which follows in the Kukësi-Peshkopia region. The border between Mirdita and Korabi zones probably passes through "Drini fault" either as a normal contact or after a nappe boundary passing immediately east of ultramaphic massifs where many examples of Mirdita ophiolite nappe underlying the Korabi one are shown. Some scholars consider the Mirdita ophiolite nappe overthrusting the Korabi ophiolite nappe and both of them overthrusting Krasta flysch. Most of the Albanian geologists have stated that the genesis of Mirdita ophiolites relates to Mirdita or Krasta (=Pindos) oceanic basin. Few of them consider it originating in Vardar oceanic basin and brought into their current position during the Middle-Late Jurassic time. The geophysicists stated that Mirdita ophiolites are nappe setting completely detached from their roots.

Keywords: Mirdita zone framework, geological syntheses, foreign and native scholar thoughts

[1] Retired from Former Institute of Seismology, Albanian Academy of Sciences
[2] Section of Natural and Technical Sciences, Albanian Academy of Sciences

1. INTRODUCTION

The main tectonic syntheses about the Geology of Albania were made by Nopcsa (1921; 1929), Bourcart (1925), Nowack (1929), Zuber (1938, 1940), Biçoku *et al*., (1965, 1967, 1969, 1970), Shehu *et al*., (1983; 1990) and Xhomo *et al.* (2002b, 2005). In the forthcoming section, the national geological syntheses from Nopcsa (1921, 1929) to Xhomo *et al*. (2002b; 2005) are here reviewed.

In addition to national syntheses, many scholars made researches and studies about the geology of Albania with subsequent publication in the form manuscripts and books. The viewpoints of Aubouin and Ndojaj (1965), Belostockij (1960-1978), Melo (1966-2002), Aliaj (1984-2018), Çollaku *et al.* (1990; 1991), Çollaku (1992), Qirinxhi *et al.*, (1990, 1991), Bushati (1994;1997) and Frashëri *et al*. (1990; 2009) are also here examined.

2. THE REVIEW OF GEOLOGICAL FRAMEWORK OF MIRDITA OPHIOLITES BASED ON GEOLOGICAL SYNTHESES (FROM NOPCSA (1921-1929) TO XHOMO *et al.*, (2002-2005)

The geological syntheses are in the forthcoming paragraphs analysed into two periods based on the Acad. Biçoku's division of geological researches and studies history: a) geological syntheses performed by foreign scholars during the first half of XX century, and b) geological syntheses made by the Albanian State institutions after 1945 (Biçoku 2004).

Main geological syntheses about the geologic structure of Albania were made by Nopcsa (1921; 1929), Bourcart (1925), Nowack (1929), Zuber (1938, 1940), Bicoku *et al.* (1965; 1967; 1969; 1970), Shehu *et al.* (1983; 1990) and Xhomo *et al.* (2002; 2005).

2.1 Geological syntheses performed by foreign scholars during first half of XX century

The history of the geological syntheses performed by the foreign geologists lies in the first half of the XX century when Nopcsa, Bourcart, Nowack and Zuber came to Albania and started their work.

Nopcsa (1905-1929) compiled the Geologic Map of Northern Albania at the scale 1:200.000 and published the monographic study "Geology and Geography of Northern Albania" (1929) with Schematic Map of Tectonic Zoning of Dinarides included in it.

Nopcsa was the first scholar who divided the tectonic zones and showed the overthrusts in Northern Albania in 1906. The scientific studies on the geology of Albania allowed him to make the first classical synthesis about the geology of Dinarides in 1921.

Nopcsa, based on deep geological knowledge, separated in Northern Albania, the following tectonic zones: Durmitor, Plate of Albanian Alps and Cukali zones to the north of Shkodra-Peja transform fault and Shar-Dag (=Korabi), Mirdita Nappe, Cukali-Olonos and Littoral Chains to the south of Shkodra-Peja transform fault.

The tectonic relations among tectonic zones are of overthrust type, with the exception of the border between Mirdita and Shar-Dag zones (1929). Mirdita Nappe is limited with Shar-Dag (=Korabi) through a great fault, called by Nopcsa "Drini Fault", which has been considered by him to be one of the longest faults in the Dinarides system (Figure 1).

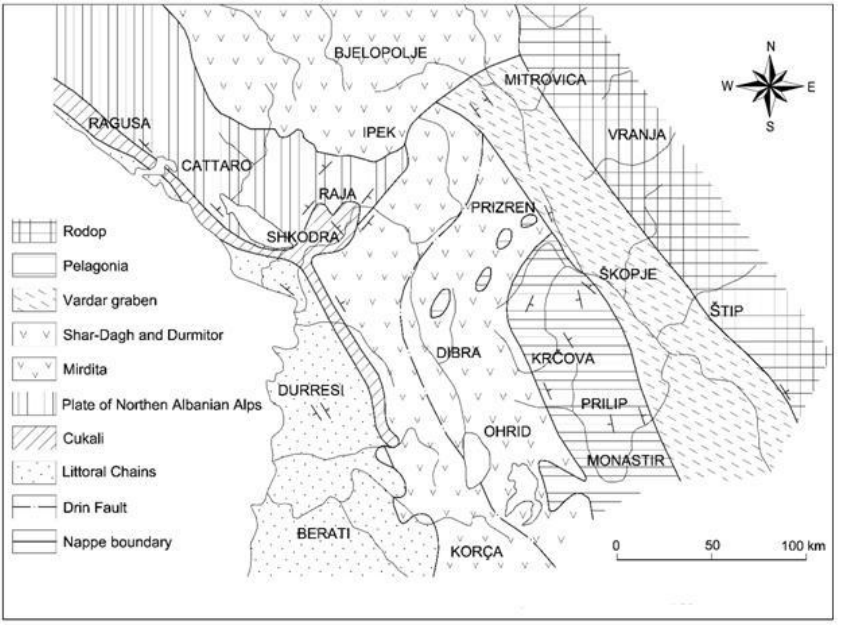

Fig. 1: Map of Tectonic Zoning of Dinarides (Nopcsa 1929).

He presented Mirdita Nappe as an ophiolitic pre-Gosaw nappe, displaced and overthrusted to the west up to Littoral Chains. In addition, he stated that the origin of Mirdita Nappe should investigated at about 90 km to the east, in Prizreni, Kosovo. Undoubtedly, Nopcsa for many and many years held a virtual monopoly on the Albanian geology, a contribution accepted by most of his colleagues, like Nowack and Zuber (Aliaj and Shkupi, 2000).

Bourcart (1916-1926) together with a group of French geologists, carried out for many years geological and tectonic studies in the Korça region with the subsequent publication of more than 20 papers. Here, we could mention: "The geologic map of South-Eastern Albania at the scale 1:200.000"

published in Paris in 1921 and the studies "The Albanian borders administrated by France (1916-1920)", "Contribution on the geology and geography of Middle Albania" (Paris,1922), "The new obervations on tectonics of Middle Albania" (Paris, 1925) and "The new observations on structure of Adriatic Dinarides" (Madrid, 1926).

Bourcart (1925) reported about the nappe building character, especially of Albanian ophiolites, while for the border between Mirdita ophiolites and Korabi zones he supported the Nopcsa assumtions.

Nowack (1919-1929), based on geologic works carried out by Nopcsa and Bourcart, and on his geological mappings and studies on different regions of Albania, compiled the "Geologic map of Albania, at the scale 1:200.000", published in Salzburg in 1925, and the scientific work "Geologic outlook on Albania" published in Berlin in 1929. His researches covered the entire territory and the results were subsequently published.

Peza (1967) re-sketched the Tectonic Scheme of Albania of Nowack based on the explanations in the text accompanying Geologic Map of Albania (1925). Nowack's Tectonic Zonation of Albania include, from East to West, the following zones: Drin-Korabi, Serpentinite, Cukali-Olonos, Dalmatian-Montengrin Coastal Chains, Lower Epirus, Albania and Adriatic-Ionian to the south of Shkodra-Peja transform fault, and to the north of it: Durmitor, Plate of Northern Albania, Cukali-Olonos and Dalmatian-Montengrin Coastal Chains (Peza 1967). Nowack presented in details the division of Nopcsa Lateral Chains in the south of Shkoder-Peje transform fault. The tectonic relations between Mirdita and Cukali-Olonos zones are shown of overthrust type, while for the border between Mirdita and Korabi zones Nowack supported the Nopcsa thought.

Zuber (1927-1943) carried out many geological researches and studies in Albania, mainly in oil field and ore prospecting areas. He carried out the geologic mappings at the scale 1:25.000, 1:50.000 and 1:75.000 and also detailed studies on different regions of Albania. Here, could be especially mentioned 45 geologic maps at the scale 1:50.000 compiled by Zuber for many Albanian regions, as on the oil prospecting regions of western Albania as well as on ore prospecting regions from Puka to Korça areas etc. Biçoku(2007) said that Zuber published the results of many of his geological works and studies in Albania.

Zuber was involved in the following geologic works and studies: Geologic Map of Albania at the scale 1: 200.000 (Kuçovë, 1943), still unpublished, Tectonic Map of Albania at the scale 1: 400.000 with 7 geologic cross-sections (Roma, 1938), Geologic Map of Central Albania at the scale 1:75.000 (Kuçova, 1932), Geologic Map of Devolli basin and Dumre at the scale 1: 75.000, On Geology of Albanian Oil (Roma, 1937), and On Tectonics and Geologic Evolution of Ore-bearing Deposits of Albania (Roma, 1940).

Zuber carried out also geological works and studies for oil prospecting in coastal part of Montenegro and Greece (Biçoku 2007). Here, we can mention the work of Zuber "Notes on Geology and Oil-bearing of Greece" (manuscript 1944, translated in Albanian by Prof. Papa and published by Tirana University 1965).

The figure 2 depicts the Zuber's Tectonic Map at the scale 1:400.000 (1938) where the Nappe zones including Shar-Dag, Durmitor, Cukali, Albanian Alps and Albanian ophiolite zones; the Frontal nappe zones including Krasta, Gjani and Frashëri Flysch zones; Coastal Folds or Parautochthonous zones comprising present Kruja and Ionian zones, and "Adria" zone (Sazani zone and geologic structure under waters of Adriatic Sea) big tectonic units could be distinguished.

Zuber was the first among the foreign scholars who noted the Albanian ophiolite nappe, which often referred to as Ophiolite nappe, that underlies the Shar-Dag (=Korabi zone) nappe in the Peshkopia region.

Zuber conceived the idea of tectonic nappe content of all main tectonic zones in the northeast of frontal nappe flysch zones which is shown in the tectonic ideal section across the Southern Italy and Balkan Folds, passing south of Shkodra-Peja transform fault, where the Pelagonia, Shar-Dagh (Korabi), Albanian ophiolite (Mirdita) and Cukali (Krasta) nappe zones overlie successively one over the other as roof-tiles from NE to SW (Figure 3).

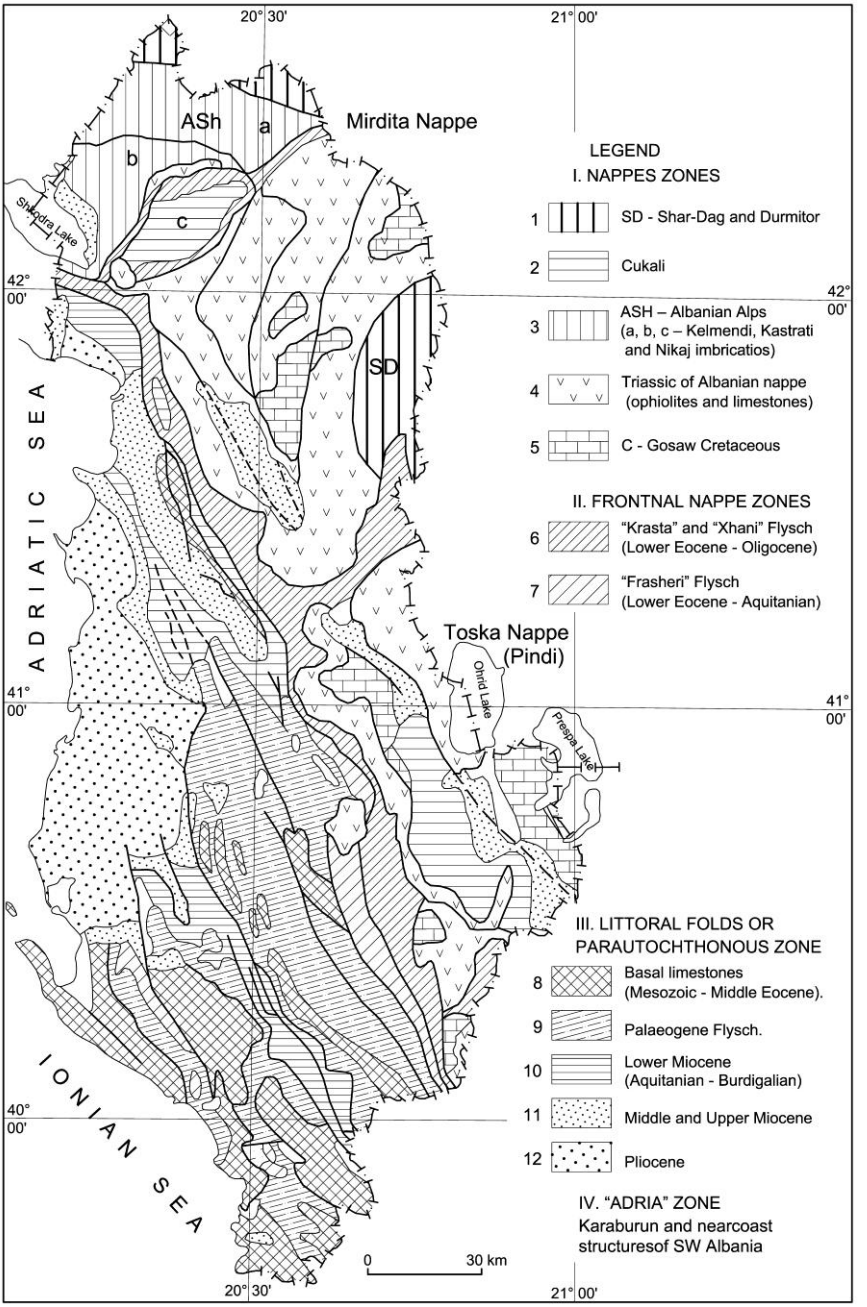

Fig. 2: Tectonic Map of Albania (Zuber 1940).

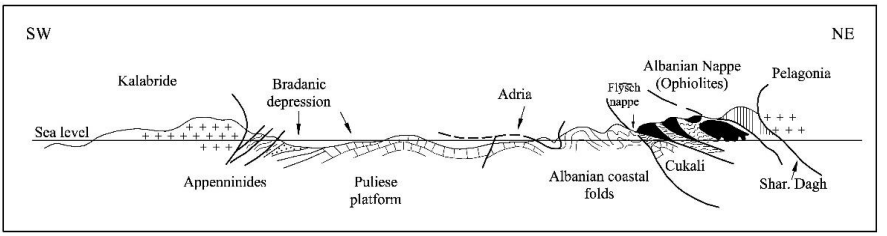

Fig. 3: Ideal section across Southern Italy and Balkan Folds (Zuber 1940).

The ophiolitic nappe could be divided into two separate nappes: Mirdita and Toska ophiolite nappes showing that the Toska nappe overlies the Mirdita one (Zuber 1940).

2.2 Geological syntheses performed by the Albanian specialists after 1945

Biçoku *et al*. (1965; 1967; 1969; 1970), Shehu *et al.* (1983; 1985; 1990) and Xhomo *et al.*, (2002; 2005) have carried out geological synthesis.

The compilation of the first Geologic Map of Albania at the scale 1:200.000 began in the second half of the1959, when a group of eminent personalities in the area came together to work in the area and latter joined by the specialists former USSR under the leadership of the Russian geologist Belostockij. When the relations with the former USSR were interrupted in 1961, all the Russian specialist working in Albania were exluded from the working team.

Given the situation, a new group with specialists from the Albanian Geological Survey was set up in 1962 under the supervision of Acad. Prof. Biçoku and Prof. Pumo. This group carried out from 1963 to 1966 field geological works and studies in the unmapped or weakly mapped regions to verify the geological borders and stratigraphic units and clarify the incertanties about the stratigraphy, magmatism and tectonics of the country (Biçoku 2004). The Geologic Map of Albania at the scale 1:200.000 was compiled from 1950 to 1965 based on 70 geologic maps at different scales: 1:25.000, 1:50.000, 1:100.000 and 1:200.000 which were compiled in line with the geological works and studies carried out in the first half of XX century. The Geologic Map of Albania was published by the Enterprise of School, Cultural and Sportive Means "Hamdi Shjaku", Tirana (1967). The explanatory text "Geology of Albania" in Albanian (1970) and in French "*La géologie de l'Albanie*" (1974) were published by "Naim Frashëri" Publishing House, Tirana, Albania. The "Tectonic Map of Albania" at the scale

1:500.000 was published by the Enterprise of School, Cultural and Sportive Means "Hamdi Shjaku" Tirana in 1969.

In the Tectonic Map of Albania at the scale 1:500.000 (Biçoku *et al*., 1969) and Tectonic Scheme of Albania (Biçoku and Papa, 1965 with some changes; Biçoku *et al*., 1970) are delineated these structural-facial or tectonic zones of Albania: i) *Internal zones*: Korabi, Mirdita and Gashi, and ii) *External zones*: Albanian Alps, Krasta-Cukali, Kruja, Ionian and Sazani zones (Figure 4).

The Tectonic Map of Albania at the scale 1:500.000 (Biçoku *et al*., 1969) along with the Scheme of Albania position in the regional framework present the tectonic zones and their internal structure. The structural types (anticlines, synclines and monoclines) in all tectonic zones and the anticlinal and synclinal chains in the framework of the external tectonic zones are presented. The main tectonic faults, either those delimiting tectonic zones, either those cutting internal structure of different zones, are also shown in the tectonic map.

Korabi zone extends from Drini i Zi basin, including Korabi mountainous massif in the north to the south, in the east of Shebeniku massif to the Ohrid Lake, including Mali i Thatë Mountain in south. The tectonic relations between Mirdita and Korabi zones are shown as a normal contact which passes after the eastern margin of ultramafic massifs, partly of thrust type complicated by a system of normal faults, while those between Mirdita and Krasta-Cukali zones are drawn by thrust fault (Biçoku *et al*., 1970; Papa 1971).

The tectonic zones that could be here distinguished are K- Korabi, M- Mirdita, G- Gashi, A- Albanian Alps, K-C- Krasta-Cukali, Kr- Kruja, J- Ionian and S-Sazani.

The compilation of the second Geologic Map of Albania at the scale 1:200.000 dates in 1978, when a group of specialists under the supervision of Prof. Shehu, PhD. Lleshi and Prof. Xhaçka was set up. The working team was composed of many specialists from the Institute of Geologic Researches, Tirana, Institute of Oil and Gas, Fier, Geologic Enterprises, Faculty of Geology and Mining, Seismological Centre of the Albanian Academy of Sciences and Geology-Geodesy Enterprise. Many geological mapping and redaction works and the observations in problematic centers, associated with stratigraphic, paleontological and geophysical studies, were carried out from 1978 to 1982.

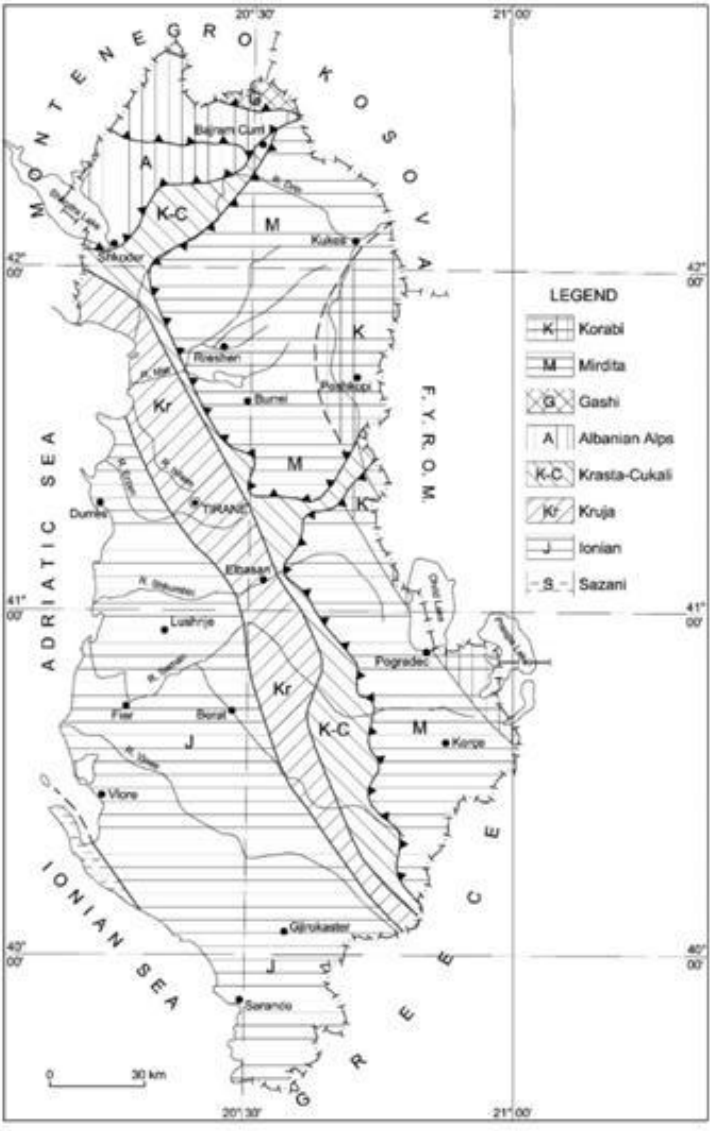

Fig.4: Tectonic Scheme of Albania (Biçoku and Papa 1970).

The Geologic Map of Albania at the scale 1:200.000 was compiled based on detailed geologic mappings, thematic and generalization studies, complex works for oil and gas and for useful minerals carried out up to 1982. It is published by the Enterprise of School, Cultural and Sportive Means "Hamdi

Shijaku", Tirana (1983), and its explanatory text published by the "Mihal Duri" Publishing House, Tirana (1990).

Biçoku 2004 stated that the Tectonic Map of Albania at scale 1:200.000 was compiled in the manuscript in 1985 by a working team involving geologists from the Institute of Geologic Researches and Faculty of Geology and Mining under the supervision of Shallo *et al*., (1985) and published in Johannesburg, South Africa in 1999.

The Tectonic Map of Albania at the scale 200.000 (1999) along with the Tectonic Scheme of Albania has been properly compiled based on tectonic principles. They show the tectonic zones and their internal geologic structure. Main topics that are presented in the Tectonic Map of Albania (1999) are: i) Variscian Tectogenic Cycle: the regions affected by the Late Variscian Tectogenesis, ii) Alpine Tectogenic Cycle into which are distinguished the following tectogeneses: Late Jurassic, Late Cretaceous, Late Eocene, Late Middle Oligocene, Burdigalian-Tortonian, Late Miocene and Late Pliocene, iii) alpine cycle formations, iv) Jurassic Ophiolite Unit and, v) structural symbols.

Shallo *et al.*, (1985) distinguished these two subzones within the Mirdita zone: i) the ophiolitic subzone and, ii) the carbonatic subzone consisting of 'peripheral complex' or 'carbonate periphery' on both sides of Mirdita ophiolites. The stratigraphic section of Korabi zone begins with the Ordovician-Devonian basement units, unconformably overlain by 'Verrucano' facies of Permian-Lower Triassic, passing upwards into volcano-sedimentary deposits of Early-Middle Triassic and shallow-water carbonates of Middle Triassic to Late Jurassic. The extent of Korabi zone follows in Peshkopi region (Figure 5).

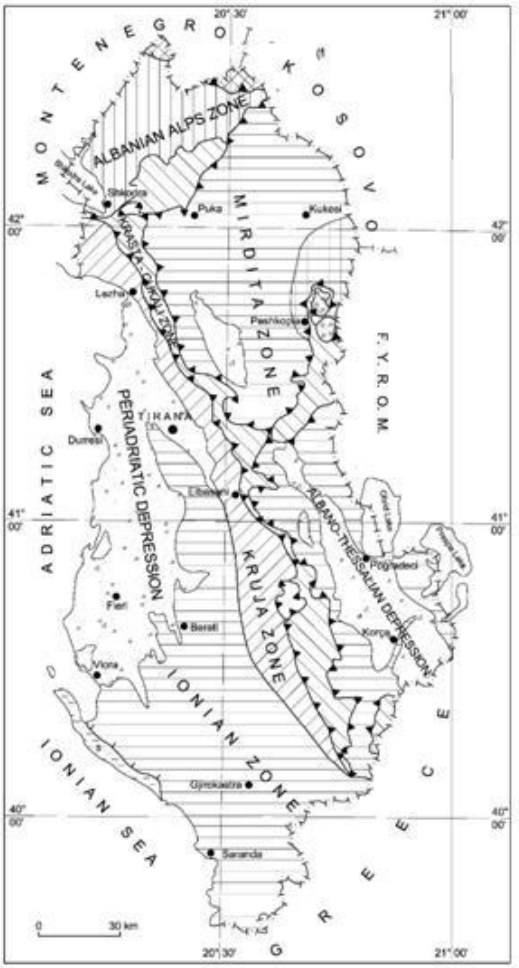

Fig. 5: Tectonic Scheme of Albania (Shallo *et al*., 1999).

The denomination of tectonic zones made by Biçoku and Papa (1970) were also here used. The difference lies in the Korabi zone which extends only in the Peshkopia region and has a normal contact with the Mirdita zone.

The border between Mirdita and Krasta-Cukali zones is of thrust type. The border between Mirdita and Korabi zones is presented as a normal contact following the eastern margin of carbonate periphery in the Peshkopia region (Tectonic Scheme of Albania, incorporated in the Tectonic Map of Albania, 1999). It was drawn in the same manner by Dede *et al*., (1971) who consider the boundary between the Mirdita and Korabi zones at the contact between

the Middle Triassic carbonatic limestones and Lower Triassic terigenous deposits.

For the compilation of the last Geologic Map at the scale 1:200.000 in 1995, a large number of specialists from the Institute of Geologic Researches in Tirana, Institute of Oil and Gas, Fier and the Faculty of Geology and Mining, University Polytechnic of Tirana, in collaboration with the Department of Geophysics together with Geological Regional Branches of Tirana, Rubiku, Shkodra, Kukësi, Peshkopia, Puka, Bajram Curri, Bulqiza, Burreli, Korça and Pogradeci was set up under supervision of Xhomo, Prof. Kodra, Xhafa and Prof. Shallo.

The same denomination of tectonic zones used by Biçoku and Papa (1970) has been used in general, but two new units are here mentioned; the South Adriatic Basin and Ostreni zones and Korabi zone with the Kukësi-Peshkopia region extention.

The Geologic Map at the scale 1:200.000 was compiled in 2002 based on all geologic mapping and research studies carried out up to 1999 and the geological works and researches made especially for the compilation of this map. It was printed by the "Huber Kartografie" in Munich, Germany in 2005 while its explanatory text the "Geology of Albania" by the Albanian Geological Survey in 2002.

The map 6 shows the tectonic zonation of Albania: the Kruja, Cukali, Albanian Alps, Vermoshi and Gashi to the north of Shkodër-Peja transform fault, and Sazani, South Adriatic Basin, Ionian, Kruja, Krasta, Ostreni, Mirdita and Korabi zones to its south. Korabi, Mirdita and Gashi tectonic zones included into the internal zones which are in the monographical work "Geology of Albania" and in the Tectonic Scheme of Albania reported. In addition, the division of the Albanides into the western and eastern Albanides was also included (Xhomo *et al*. 2002).

Xhomo *et al*., (2002) stated that Mirdita Zone represents a super-zone with graben-like palaeogeographic architecture formed during the continental rifting associated and followed by the Upper Anisian continental break-up and narrow "oceanic" extension during the Middle Triassic-Early Liassic and Middle-Upper Jurassic time. The closing of Mirdita "oceanic" basin occurred during the Middle Jurassic-beginning of Upper Jurassic due to the bi-divergent interoceanic and marginal paleo-emplacement. At the end of the Late Eocene, Mirdita Zone overthrusts the flysch deposits of the external tectonic units.

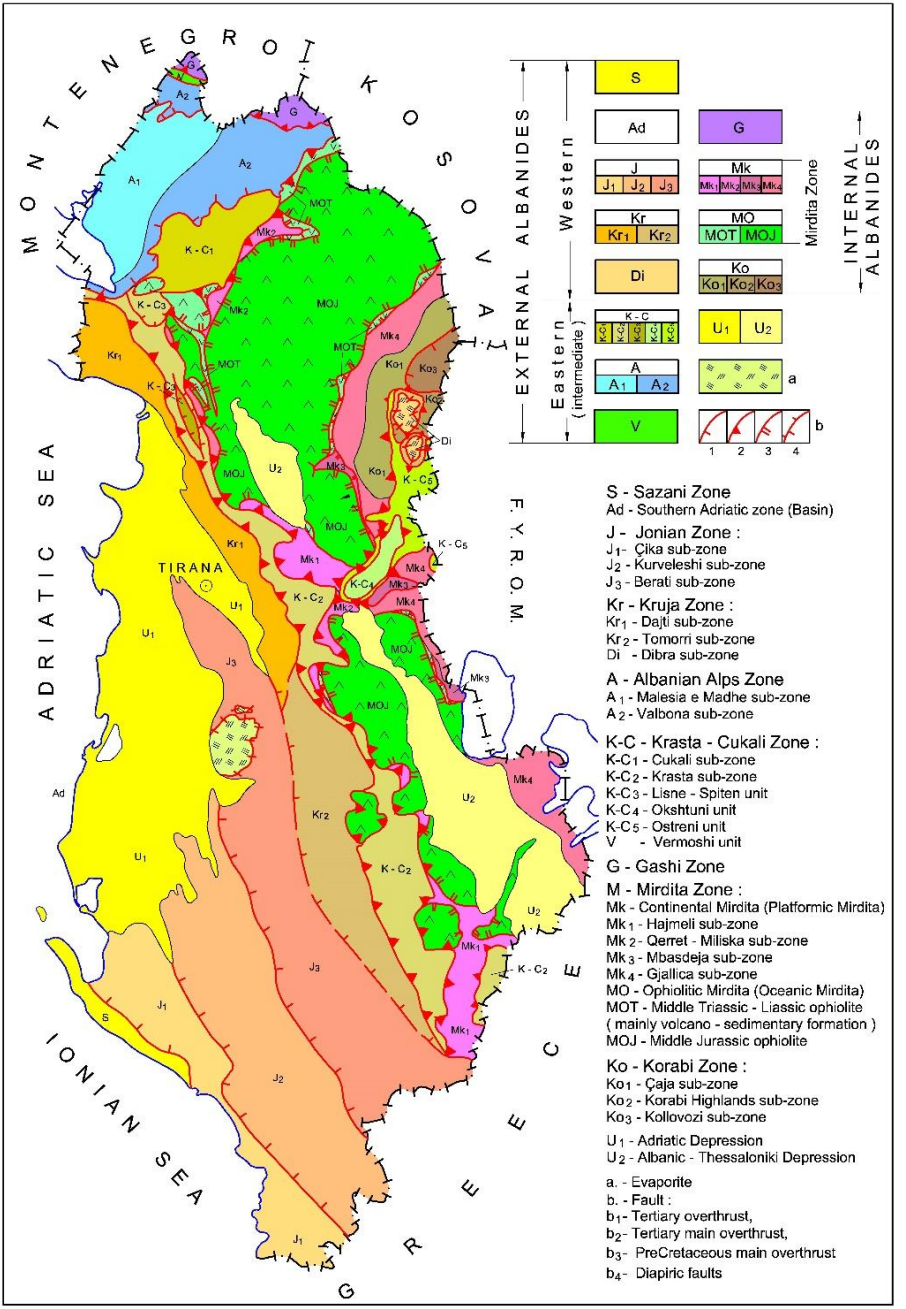

Fig. 6: Tectonic Scheme of Albania (Xhomo *et al*. 2005).

Two main geologically different units could be distinguished in the Mirdita Zone: i) the Triassic and Jurassic ophiolites and their sedimentary cover, and ii) the subzone units at the periphery and at the basement of the ophiolites. The Hajmeli and Qerret-Miliska subzones could be distinguished at the western periphery of ophiolites, while the Gjallica and Mbasdeja subzones at its eastern periphery.

In the Korabi zone, Malësia e Korabit and Kollovozi subzones could be distinguished from west to the east the Muhurr-Çaja. The main characteristics of Korabi zone is the wide extension of Lower Paleozoic deposits and the presence of pelagic carbonates of Middle Triassic- Middle Jurassic (Xhomo *et al*., 2002).

The border between Mirdita and Korabi zones passes after the boundary between Gjallica and Çaja subzones and follows in the Kukësi-Peshkopia region. Mirdita zone has transitory relations with the Korabi zone and both of them overthrust Dibra, Ostreni and Krasta units.

Xhomo and Kodra (2002) presented the tectonic scheme of Albania (Figure 6) and the tectonic cross-section through the Albanides fold and thrust belt, into which show that the Korabi nappe overthrusts the Ostroni unit overlying the Dibra Unit (=Kruja zone), whereas the Mirdita ophiolites overthrust the continental ophiolite periphery to the east (Pz-Mz) and to the west (Mz), and both Mirdita and Korabi nappes overlie the Ostreni nappe that is supposed to be an imbrication of regional extension.

As an ophiolite nappe, Mirdita zone completely covers the Krasta subzone in the south-eastern Albania. Mirdita zone is separated by Labinot-Dibër transversal sector into two ophiolite parts: Northern Mirdita and Southern Mirdita ones. In northern Mirdita, close to the Shkodër-Peja transform fault, an ophiolite wide belt of north-eastern extent is established.

3. THE CONTRIBUTION OF INDIVIDUAL SCHOLARS ABOUT THE MIRDITA ZONE FRAMEWORK

Some geologists and geophysicists carried out researches and studies about the regional geology of Albania, with subsequent publication of their results related to the tectonics of Mirdita and Korabi zones. The results concerning the framework of Mirdita are of great interest for the scholars.

The opinions of the scholars like Aubouin and Ndojaj (1964), Belostockij (1960-1978), Melo (1966-2002), Aliaj (1987-2018), Kodra (1986-2016), Çollaku *et al*. (1990, 1991), Çollaku (1992), Qirinxhi *et al*. (1990, 1991), Bushati (1994, 1997) and Frashëri *et al*. (1990, 2009) are in the forthcoming pharagraph introduced.

Aubouin and Ndojaj (1964) published an important study titled "Regard sur la géologie de l'Albanie et sa place dans la géologie des Dinarides". The

relations between Mirdita and Korabi isopique zone's border is considered as a normal one passing after eastern margin of ophiolites and extended from the Kukësi-Peshkopia region in the north to Mali i Thatë Mountain in the south. Mirdita/Subpelagonian and Krasta/Pindos nappes are delimited by frontal thrusts.

Belostockij (1960-1978) published one paper in Albanian (1960) and eight others in Russian (1963-1977), and the book "Stroenie i formirovannie tektoniçeskih pokrovov" (1978) (234 pgs) where his researching experience of more than 15 years on nappe topics and related issues were reported based on field observations carried out in the Albanian sector of Dinarides and the wide literature on tectonic nappes in different regions of terrestrial globe, especially in the European Alps (Belostockij 1978).

As his papers on Albanian geology are of high interest for the Albanian scholars, they are here mentioned: "Mbi manifestimet e tektonikës gravitative në Shqipëri". Bul. UT Shk. Nat. Nr 4, O tektoniçeskih pokrovov i gravitacionih strukturah zapadnoj çasti centralnih Dinarid. St. 1: Tektoniçeskie pokrovi. Bul MOIP, Otd. Geol., No 6, 1963, O tektoniçeskih pokrovov i gravitacionih strukturah zapadnoj çasti centralnih Dinarid. St. 2: Gravitacionnie strukturi. Bul MOIP, Otd. Geol., No 1, 1964, Tektoniçeskie pokrovi Dinarid. Izv. ANSSSR, Serija geol., No 2, 1965, Tektoniçeskie pokrovi v basene r. Devoll v Dinaridah. Geotektonika, No 6, 1967, Uslovija osadkonakoplenija i tektoniçeskaja obstanovka v zone Mirdita (centralnij sector Dinarid) v melovoe vremja. Izv. Vish. Uçeb. Zav., Geologija i Razvjedka, No 10, 1968, Tektoniçeskie pokrovi, zoni melanzha i haotiçeskih struktur. V knige: Oçerki struktjurnoj geollogi slozhnodislocirovannih tolsh. M. Nedra, 1970, Nekotorie voprosi kinematiki sharjazhej. V knige: Oçerki struktjurnoj geollogi slozhnodislocirovannih tolsh. M. Nedra, 1977 and K probleme ofiolitov v Dinaridah. Izv. ANSSSR, Serija geol., No 9, 1969. Belostockij I.I., Kolbancev R.V.

The separated zones are: i) Pelagonian, ii) Subpelagonian with its northern continuation, iii) Durmitor, iv) Komani-Fierza (block), v) Pindos and, possibly, the internal zones of early flysch, vi) High karst, vii) External zones of Hellenides and their north-eastern continuation, vii) Molasse depression, ix) Gypse cupola and, x) borders of structural zones (Nappe complexes) and frontal lines of separate nappes.

In a special chapter of the book titled "Morphologic-kinematic nappe characteristics" (60 pps), is reported about the nappe tectonics in Albanian sector of Dinarides evidenced at boundaries of nappe complexes or main structural zones. Tectonic nappes following the outer extremities of Korabi zone are clearly analyzed. In this chapter cases related to nappe tectonics in different sectors of Albania are detailed. The following paragraph reports about the Selishta sector, different sectors of Korabi allochthon, nappes of

Subpelagonian (=Mirdita) zone, the examples of allochtonous structures at forehead of both internal and external zones and Devolli nappe packet into which the covering of some tectonic zones is evidenced.

The sectors of geological observations carried out by Belostockij in all the tectonic zones of Albanian sector of Dinarides are marked in the tectonic map and reported in the paragraph ”Different sectors of Korabi allochthon” (Figure 7).

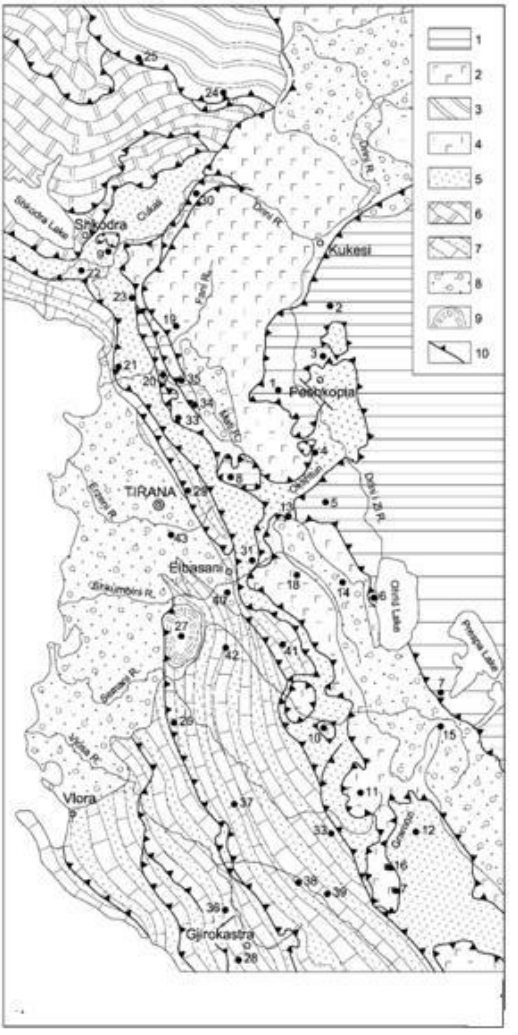

Fig. 7: Tectonic Map of Albanian Sector of Dinarides into which are shown by numbers the observed areas in different zones (Belostockij 1978).

The allochthtonous Triassic limestones overlying the ophiolites of Subpelagonian zone (=Mirdita zone) are observed in many places from Selishta sector to the south, as in Okshtuni river valley, in Klenja and Luniku areas. More to the south, in Shebeniku and Jabllanica Mountains, as well as in western coast of Ohrid Lake, the external contour of Korabi zone is of allochthonous nature. Here, the Triassic limestones are nappe overlying the ophiolite complex. To the south and south-east from here, the front of Korabi allochthon in many places is covered under the Upper Miocene and Pliocene-Quaternary deposits, but in the field of Triassic limestones small tectonic windows into which outcrops the ophiolitic mélange, for example that of Zvezda pass in Mali i Thatë Mountain, near the Prespa Lake could be observed. The data of the Peshkopia-Korabi sector extending in northern frame of Dibra big halfwindow with which the Okshtuni halfwindow is connected are of special interest.

The Northern Dinarides, Albanian sector and Thessalian sector of Hellenides geological cross-sections with enough depth, showing reliable building of Dinarides allochthonous complex of nappe sheets are presented in (Belostockij 1978).

In these cross-sections are distinguished two levels having different basic geological building: an upper level or "suprastructure" within which is shown the observed geological building of all tectono-stratigraphic units, and lower level or "infrastructure" which is drawn with specific root zones responding deep sector parts from which has originated main allochthonous sheets. The compilation of the such geological hypothetic cross-sections of Dinarides was based on the characteristics of each allochthonous complex and the tectonic windows here noted.

In the Albanian sector are shown from east to west the following nappe units of allochthonous complex: Vardar, Pelagonian, Subpelagonian, intermediary unit and Pindos nappe sheets. The relations of tectono-stratigraphic zones in root level or "depth relations" in Albanian sector can be compared with those in Thessalian sector, if under Mirdita allochthonous complex exists an intermediary hypothetic zone with enough width. Belostockij stated that Komani-Fierza nappe can be interpolated as a vestige for the existence of such absent structural-facial unit. Guri i Topit zone is well interpolated as an absent intermediary tectono-stratigraphic unit between Krasta and Mirdita zones (Aliaj 2018).

Qerreti-Miliska subzone of Mirdita zone north-east extending, taking place in the same Komani-Fierza sector, has been later distinguished by Prof. Kodra (2002a; 2016). Qerreti-Miliska subzone in general has a similar stratigraphic profile with that of Guri i Topit zone, but it has tectonic setting between Mirdita and Cukali zones and not between Mirdita and Krasta zones.

The root level zones of nappe sheets presented in the Albanian sector cross-section are the followings: Subpelagonian (=Mirdita) ophiolite nappe under Pelagonian zone pre-Cembrian cristaline basement, Intermediary (=Guri i Topit) zone under Subpelagonian zone root level and Pindos zone under Intermediary (=Guri i Topit) zone root level. The Gavrovo and Ionian zones are presented as autochthonous units which thrust westwards above their Paleozoic basement (Belostockij 1978).

As already said, Belostockij was an eminent personality in the field of tectonics. Here, we can mention his contribution to the regional geology of Albania, especially in nappe tectonics being the fundamental key for a better understanding of the geological building of Albania.

Melo (1966-2002), an eminent personality in the field of tectonics in Albania, has reported in many different scientific activities and published many papers about the tectonic structure of Albania and particularly about thrust and nappe tectonics.

The geological relations of flyschoid nummulitic sequence with surrounding and overlying deposits in Korabi region (Melo 1966), Geology and tectonics of Gramoz unit in Helmes-Shtike-Kozel sector and relations with Mirdita zone (Melo and Kote 1973), The Peshkopi-Labinot extent of flysch tongue and the opinions for its paleotectonic and tectonic setting (Melo 1982), Tectonic nappes in the Milot-Lezhë sector of Krasta subzone (Melo and Kanani 1984), Thrust and nappe tectonics in Albanides (Melo *et al*., 1985), Thrust and nappe tectonics in geological structure of Albanides (Melo *et al*., 1990; 1991a), Tectonic windows of the external zones in the eastern regions of Albanides (Melo *et al*., 1990; 1991b) and Tectonic structure of Albania (manuscript, Melo 2002) are some of his most important scientific papers. Melo authored the book "The building and geotectonic evolution of Albanides" (1986) and many other teaching books for the students of the Faculty of Geology and Mining, Polytechnic University of Tirana.

The nappe structures could be met in many sectors of our country like Peshkopia region, Lezha-Miloti sector, Albanian Alps region and contact area of Korabi zone with Mirdita one (Melo and Kanani 1984; Melo 1985; Melo *et al*., 1991a). The Peshkopia region presents the classic one having evidences of nappe structures. There are observed two nappe sheets one over another overlying Kruja 'autochthon'. Melo *et al*. (1990; 1991a) pointed out that Korabi allochthon overlies the Dibra unit, which, through Shëngjergji flysch tongue connects with the Krasta zone. In Peshkopi region the following nappe sheets are distinguished: Upper nappe of Korabi zone on the top, and lower Krasta nappe overlying Kruja autochthon composed of gypsum and Eocene-Oligocene flysch deposits. Upper Korabi nappe is composed of three separate nappes. The synform anticlines and antiform synclines at the limestone belt to the east of Mirdita ophiolites testify for their allochthonous setting. Melo *et*

al. (1991a) pointed out that Mirdita ophiolitic nappe can't be considered as brought from Vardar ophiolite zone. The Mirdita ophiolites resulted from the closing of the Mirdita oceanic basin separated by Pelagonian zone from the Vardar oceanic basin.

Melo *et al*., (1991b) described in details tectonic windows of the external zones in Peshkopi region as follows: Okshtuni window of Krasta zone, and the Kërçishti, Mali i Bardhë, Peshkopi and Dibra e Madhe windows of Kruja zone. The general characteristics of nappe structures which overthrust the Kruja and Krasta tectonic windows evidenced in the region from Orenja in the south to Veleshica stream in the north are shortly treated here (Melo *et al.* 1991b). The following pile of nappe sheet could be met from the bottom to the top in the eastern regions of Albania: i) the autochthonous Kruja zone windows outcropped from Dibra e Madhe to Mali i Bardhë under the nappe of Krasta zone, ii) the nappe sheet of Krasta zone is built by the Albian-Cenomanian flysch, Upper Cretaceous limestones and the Maastrichtian-Lower Eocene flysch, iii) the nappe sheet of Tithotian-Valanginian marly flysch unit, which outcrops under the field of Triassic-Jurassic limestones and Lower Paleozoic terrigenous formations in Trebisht, Zerqan windows etc. which may be belonging to the nappe of Korabi zone, and its allochtonous setting over the Maastrichtian-Lower Eocene flysch of Okshtuni tectonic window belonging to Krasta zone, and iv) the nappe sheets of Korabi and Mirdita zones.

Melo (2002) through the his study "Tectonic structure of Albania", rich in graphs pointed out especially topics concerning the nappe boundaries of the Eastern Albanides tectonic zones, into which the following ones are included: Korabi, Mirdita, Gashi, Albanian Alps (including also the Vermoshi subzone) and Krasta-Cukali allochthonous zones overlying one another: the Gashi zone over Vermoshi and Albanian Alps ones, and the Albanian Alps zone over Krasta-Cukali one to the north of Shkodra-Peja transform fault, and the Korabi-Mirdita zone over Krasta-Cukali one to the south of Shkodra-Peja transform fault. The Eastern Albanides with Krasta zone at their front, through a nappe boundary of regional character, are delimited with the Western Albanides having Kruja zone at their back.

The main tectonic elements of Korabi and Mirdita zones are: the Korabi Paleozoic nappes, and the ophiolitic belt with two peripheral Triassic-Jurassic limestone belts of Mirdita zone. Prof. Melo considers the Korabi zone nappe structure to be located only in the Peshkopi region and is composed of three nappe subzones, from down to the top: Grama (it is also known as Radomira), Çaja-Muhurri and Kollovozi nappe subzones. From structural view-point, the Paleozoic deposits of Korabi zone constitute the monoclinal nappes accompanied with tectonic imbrications. The three Korabi subzone nappes compose the upper Korabi nappe overlying the lower Krasta nappe, which

covers the Kruja autochthon outcrop in Mali i Bardhë, Peshkopia, Kërçina and Dibra e Madhe tectonic windows. This geological situation testifies the allochthonous setting of internal zones of Eastern Albanides (Krasta, Mirdita and Korabi) over the Western Albanides zones (Figure 8).

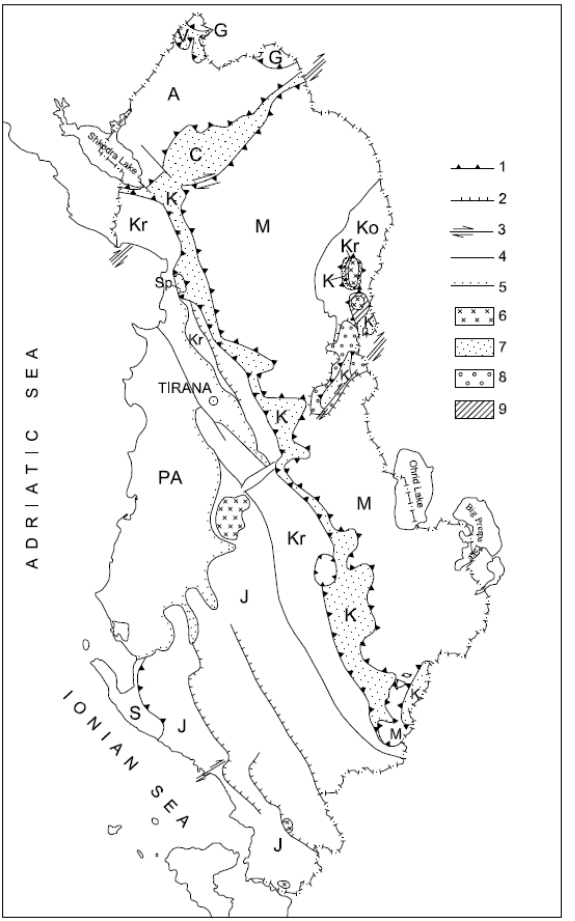

Fig. 8: Tectonic zonation of Albania (from Melo 2002). Internal tectonic zones: G- Gashi, Ko- Korabi, M- Mirdita. External tectonic zones and subzones: V- Vermoshi, A- Albanian Alps, C-Cukali, Kr-Krasta, Sp-Spiteni subzone, K- Kruja, J- Ionian and S- Sazani. PA-Periadriatic Depression. 1- Overthrust of nappe character having great displacement amplitude, 2- Thrust fault having average displacement amplitude, 3- Dextral strike-slip, 4- Western boundary of Korabi and Kruja zones, 5- Periadriatic depression boundary, 6- diapiric cupola, 7- Krasta and Cukali zones, 8- Early Cretaceous flysch in a debatable position and 9- Eocene-Oligocene age (?) Flysch of an intermediary zone between the Kruja and Krasta zones.

The Mirdita zone structure consists of two peripheral Triassic-Jurassic limestone belts and the ophiolitic belt in its center. The eastern limestone belt in the border of the Paleozoic section of Korabi zone with the ophiolites and it is followed from Koritniku Mountain in the north to Mali i Thatë and Ivan Mountains in the south. The boundary between ophiolites and the eastern limestone belt is interpreted as a complicated contact, somewhere underlying and somewhere overlying the limestone belt. In the southern Albania, from Përrenjasi to Bilishti area, the Triassic limestone blocks overlying the ultrabasic rocks are could be observed many km from the limestone belt front. The serpentinite belts of some hundred meters wide and tens km long are observed within limestone belt. The serpentinites are originally located at the ophiolite basement and are transported via nomal faults, sometimes resulting from early rifting before thes opening of the Mirdita Ocean and simetimes as olistoliths.

The western limestone belt is placed at the ophiolite front from Leskoviku to Shkodra overlying the Krasta flysch and then follows up to Tropoja overlying the Cukali and Albanian Alps flysch deposits. The western limestone belt is somewhere up to some km thick and somewhere else up to disapearing, bringing the ophiolites directly over the Krasta flysch. The ophiolitic belt in Central Mirdita region presents an ophiolite megasyncline structure with ultrabasic massifs in flanks and gabbro and volcanic rocks in the center.

There are two scenarios for the Mirdita zone origin from Vardar Ocean or from Mirdita Ocean. As Mirdita ophiolitic zone and the Korabi ophiolitic zone are displaced as a common nappe over Krasta zone for a distance of many km, they could be considered as nappes without roots. Melo (2002) pointed out that whichever scenario can be for the Mirdita ophiolitic origin, as rooted in Mirdita zone or with its roots in the Vardar zone, the ophiolite nappe in our country can be followed some km into the depth.

Aliaj (1987-2018) carried out many researches and studies about the geological and neotectonic structure as well as of seismotectonics of Albania with subsequent publication of the results inside and outside the country. He authored and co-authored 3 books and more than 100 papers. Here, we can mention some important publications: Plunged folds in frontal part of Korabi nappe: Fushë Lurë-Selishtë Sector, their neotectonic deformation (1984), Examples of nappe structures in the internal zones of Albanides and their neotectonic deformation (1987), Plunged folds at the frontal part of the Korabi zone: Selishtë-Resk region (1991), Tectonic windows of the external zones in the region of Peshkopia (Eastern Albania) (1993), Nappe structures in south-eastern Albania (1994a), Mirdita oceanic basin was located westwards of Korabi zone (=Pelagonian zone) (Aliaj and Meço 1994b) and Guri i Topit zone – An intermediary tectono-stratigraphic unit between the

external and internal Albanides (2018). In addition, he co/authored many books: "Geology of Albania" (in English, by Meço, *et al*., 2000), "Seismicity, Seismotectonics and Seismic Hazard Assessment in Albania" (in Albanian with Extended English Summary by Aliaj *et al*., 2010) and "Neotectonics of Albania" (in Albanian, Aliaj 2012) and coauthored some teaching books for the students of Faculty of Geology and Mining, Polytechnic University of Tirana, Albania.

Researches and study works about the nappe tectonics were out years ago in the frontal part of Korabi zone and the results could be found in (Aliaj 1984; 1987; 1991). Many examples of nappe structures observed in the internal zones of Albania are given in the paper of Aliaj (1987), reporting also their neotectonic deformation through normal faulting tectonics. The main results about the overturned west plunged folds in frontal part of Korabi nappe in Fushë Lurë-Selishtë sector (Aliaj 1984) could be found in (Aliaj 1987). At Shemri Mountain, east of Selishte village, an east verging overturned west plunged syncline, built by Triassic-Jurassic limestones covered by Permian-Lower Triassic terrigenous deposits could be clearly seen. The syncline and anticline overturned folds are also observed going to the west to Qafë Murra, where the Triassic-Jurassic limestones overlie somewhere on ultrabasic rocks, somewhere on effusive and somewhere on Tithonian-Valanginian flysch, which cover the ophiolites. In the Fushë-Lura geological cross-section, such overturned west plunged folds are also observed.

In Mali me Gropa region, two nappe sheets could be met: i) upper nappe composed of Triassic-Jurassic limestones of Korabi zone, and ii) the lower nappe consisted of Mirdita ophiolites unconformably overlain by the Tithonian-Valanginian flysch which in turns overthrusts the Krasta flysch nappe (Aliaj 1987).

In the region around Ohrid and Prespa Lakes, many examples of nappe structures as in the sector from Lin village at the coast of Ohrid Lake to the west of Qafë-Thanë could be observed. Here, the Korabi zone Triassic-Jurassic limestones, slightly west dipping, allochthonously overlay the ophiolites of Mirdita zone and Near Qafë-Zvezde, along the road to Great Prespa Lake, in Zagradec at Small Prespa Lake and from Zagradec to Bitincke, the Triassic limestones overlain by Eocene deposits overlie the ultrabasic rocks. The north-west extending anticline structure of horst shape in Mali i Thatë Mountain and in the Prespa lakes region built by Triassic-Jurassic limestones can be formed due to the diapirism of ophiolites underlying it.

A small tectonic window of Krasta zone within Mirdita ophiolite nappe field outcrops in Rungaja valley, west-southwest of Vithkuqi village. In the Leskoviku-Erseka region is characterized by the development of Mirdita

tectonic nappe of small thickness, tens to hundreds of meters, represented by ophiolites and Triassic-Jurassic limestones navigating on Ionian and Kruja flysch (Aliaj 1987).

The east-verging overturned west plunged folds built by Triassic-Jurassic limestones and Permian-Lower Triassic terrigenous deposits observed at the frontal part of the Korabi zone in Selishtë-Resk region, was reported in the "Symposium on Thrust tectonics" held in Tirana in 1990 and published in 1991. These typical overturned folds are located in an up to 8-10 km wide belt in the frontal part of Korabi zone, directly to the east of Mirdita ophiolite massifs, along the four geological cross-sections: Qafë Murrë-Shemri Mountain, Fushë Lurë-Vila Mountain, ZallReç-Vila village and TejDrin-Resk cross-sections. The common characteristic of all cross-sections is their overturned stratigraphic succession composed of Middle Triassic-Jurassic limestones in the lower part and Permian-Lower Triassic terrigenous deposits in the upper part, disrupted by normal faults. Many serpentinite belts of tens meters wide and some km long, are observed in the carbonatic periphery to the east of Mirdita ophiolites. The author pointed out that the Korabi nappe of overturned Permian-Jurassic sequence overlie the Mirdita ophiolites.

The east-verging overturned west plunged folds in frontal part of Korabi zone were developed in a retrocharriage manner: the W-E back movement of Middle Triassic-Jurassic limestones in the lower part and Permian-Lower Triassic terrigenous deposits in the upper part has been caused from the strong barrier of Cretaceous basal conglomerates and neritic limestones, which transgressively cover the ophiolites. To the east of overturned cascade folds, the conjugated small folds observed in Silurian-Devonian schist and sandstone deposits at Muhurri Bridge passing the Drini i Zi River, show the E-W movement of rock masses. These data are a means to address the end Cretaceous nappe emplacement of Korabi zone over the Mirdita ophiolites (Aliaj, 1991).

Aliaj (1993) was focused on the "Tectonic windows of the external zones in the region of Peshkopi (Eastern Albania)". A horst structure has been developed to the east of Dibra graben depression from the Kërçinë and Velivar mountains in the south up to Mali i Bardhë Mountain in the north where some Kruja and Krasta tectonic windows Mali i Bardhë, Banjat e Peshkopisë, Kërçishti and Dibra e Madhe windows north of Kruja zone Okshtuni window northeast of Krasta zone crop out within Korabi zone. Krasta nappe window that crops out in Velivar and Kërçinë mountains and to the east of Albanian state border, overthrusts the "autochthon" of Kruja zone (Aliaj 1993).

The tectonic windows of Kruja and Krasta zones in the region of Peshkopi (eastern Albania), have been formed due to the Pliocene-Quaternary extensional tectonics, accompanied by normal faulting and evaporite

diapirism which created cupola pattern horsts and favoured the erosion of the Mirdita and Korabi upper nappe sheets, which are seen only at the margins of these windows. The ophiolite bodies found along the normal faults at frontal part of Korabi zone up to Korabi Highland and along nappe boundaries surrounding the tectonic windows, could be considered as pulled up from the Mirdita ophiolites underlying the Korabi zone. These data show that Mirdita ophiolites underlie the Korabi nappe structures, proving perfectly that the Mirdita oceanic basin located to the west of Korabi zone.

Aliaj and Meço (1994), in the "Mirdita oceanic basin was located eastwards of Korabi zone (=Pelagonian zone)" are focused on the Mirdita ophiolite origin, first of all by analyzing the ophiolitic outcrops on the surface at about 25 km to the east of big ultramafic massifs, and the data showing that the Mirdita ophiolites underlie the Korabi nappe. New data obtained from the observations in the "Grama nappe" could be here found. The sequence of Middle-Upper Triassic limestones overthrusting the effusive rocks transgressively overlain by the flysch deposits considered of Upper Jurassic-Lower Cretaceous could be met at Tomini stream, about 1 km to the north of Peshkopia. The Grama nappe structure has been interpreted as consisting of two nappe sheets: upper Korabi nappe consisting of Middle Triassic–Middle Jurassic limestones and lower Mirdita nappe consisting of the effusive rocks overlain transgressively by the Upper Jurassic-Lower Cretaceous flysch (Aliaj and Meço 1994).

Meço and Aliaj (2000) in the book "Geology of Albania" published in Germany pointed out that "the Mirdita Zone overthrusts the Krasta Zone and is itself overthrust by the Korabi Zone"; such nappe relations are also pictured in the Tectonic Zonation of Albania showing that the Korabi nappe overthrust the Mirdita one (Figure 9).

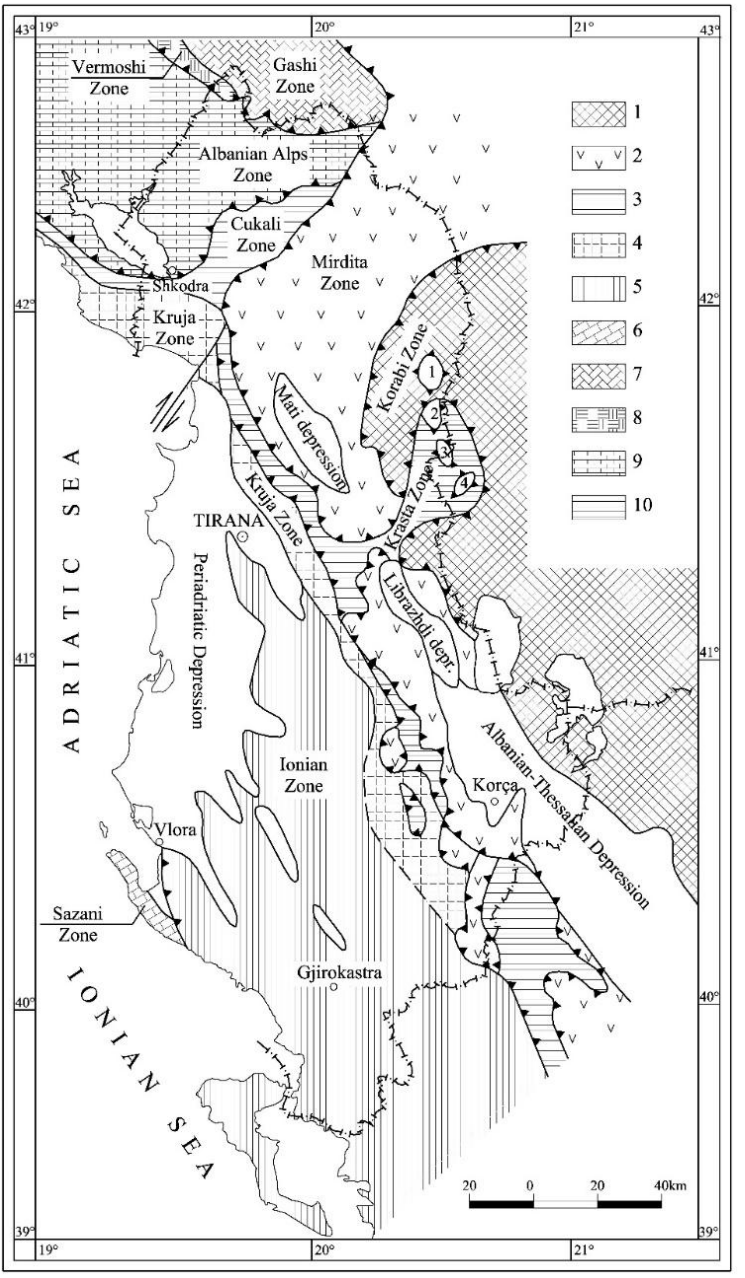

Fig.9: Tectonic map of Albania (Meço and Aliaj 2000)Tectonic zones: 1- Korabi, 2- Mirdita, 3- Krasta, 4- Kruja, 5- Ionian, 6- Sazani, 7- Gashi, 8- Vermoshi, 9- Albanian Alps, 10- Cukali. 1, 2, 3, 4- tectonic windows of Kruja zone.

Aliaj (2018) reviewed in the paper "Guri i Topit zone – An intermediary tectonic-stratigraphic unit between the external and internal Albanides" the data about the relation between the external and internal zones and especially between Mirdita and Korabi zones. It is important to mention that the distinction of the Guri i Topit zone is an additional proof that the Mirdita oceanic basin locates to the west of Korabi zone. The side by side development of Krasta, Guri Topit and Mirdita zones, the setting of Guri Topit Flysch Zone (Beotian zone in Greece) between the Krasta (Pindos) zone and the Mirdita (sub-Pelagonian) zone and the accumulation of flysch sequences in the Krasta and Guri Topit zones conditioned by the sedimentary hiatuses in South of Mirdita zone can be regarded in favor of the location of Mirdita oceanic basin to the west of Korabi zone.

Aliaj (1987; 1991; 1993; 2018), Aliaj and Meço (1994) and Meço and Aliaj (2000) investigated in details all the aforementioned data pointing out that the following nappe sheets could be met within the Korabi zone, from top to bottom: i) Korabi nappe, Mirdita ophiolite nappe transgressively covered by the Tithonian-Valanginian flysch, and ii) Krasta nappe overlying the Kruja "autochthon".

Kodra (1976-2016) is an eminent tectonist and the best expert of geology of the Mirdita and Korabi zones. Many of his geological works and studies on these zones have been referred to in many geological reports, monographic studies and research papers. The most important papers related to the topic of the paper in process of publication are mentioned below: About Jurassic Age of volcano-sedimentary formation of Mirdita zone (Kodra 1976), Ophiolites in the framework of geotectonic evolution of internal Albanides (Kodra and Gjata 1982), Geology and mineral resources perspective in the Resk-Shistavec region. PhD thesis (Kodra 1986), Paleogeographic and geotectonic evolution scheme of internal Albanides during the Triassic and Jurassic (Kodra 1987), Mirdita continental crust rifting and first phases of Mirdita oceanic spreading (Kodra 1988), Mesozoic evolution of internal Albanides, rifting phases and Mirdita oceanic spreading (Kodra and Gjata 1989), Paleotectonic emplacement of Mirdita zone ophiolites (Kodra and Bushati 1989), Tectonic windows of external zones within eastern regions of Albanides (Melo *et al.*, 1991), La formation volcano-sedimentaire du jurassique superieur: temoin de l'ouverture du domaine ophiolitique dans les Albanides internes (Kodra *et al.*, 1993), Mesozoic volcanism in Albania (Kodra *et al.*, 1995), Tectonic history of Mirdita ocean basin (Albania) (Kodra *et al*., 2000), Geology of Albania (Xhomo *et al*., 2002), Geologic Map of Albania at the scale 1:200.000 (Xhomo and Kodra 2005), Geology of Kosova (Elezaj and Kodra 2008) and The Albanides Setting in the Dinaric-Albanian-Hellenic Belt and Their Main Geological Features (Aliaj and Kodra 2016).

A special contribution to the stratigraphy and the structure of Mirdita and Korabi zones has been given by Kodra (see the references). The position of volcano-sedimentary formation at the bottom part of carbonate section, the amphibolite placing as the metamorphic sole of Jurassic ophiolite massifs and radiolarite cherts at the top of carbonate section of pelagic facies parallelly to the neritic facies of Upper Triassic-Lower Jurassic limestones are evidenced by Kodra (1976). Kodra and Gjata (1982) individualized the Mirdita zone in the framework of a Mirdita megastructure with oceanic subduction, giving the idea of the closing of the Mirdita oceanic basin by the marginal bi-divergent paleo-emplacement of ophiolites.

Based on the topic of the paper below should be emphasised Kodra opinions related to the geologic framework of Mirdita zone as he has presented in the papers and monographic studies, without any comments.

Kodra et al., referring to (Melo *et al*., 1990; 1991) made an original interpretation for the nappe sheet structure across the Mirdita and Korabi zones (Figure 10). In the eastern regions of Albania the following pile of nappe sheets, from down to top could be met: i) the autochthonous Kruja zone windows outcropped from Dibra e Madhe to Mali i Bardhë under the nappe of Krasta zone, ii) the nappe sheet of Krasta zone, iii) the nappe sheet of Tithotian-Valanginian marly flysch unit, which outcrops under the field of Triassic-Jurassic limestones and Lower Paleozoic terrigenous formations in Trebisht, Zerqan windows etc. might belong to the nappe of Korabi zone, and its allochtonous overset the Maastrichtian-Lower Eocene flysch of Okshtuni tectonic window belonging to Krasta zone, and iv) the nappe sheets of Korabi and Mirdita zones.

Peshkopia region is among the classic areas with nappe structures. There are evidenced two nappe sheets located over one another as well as over the "autochton unit". The upper nappe belongs to the Korabi zone which overthrusts the lower one represented by the Krasta zone. Both covers the "Kruja autochtonous unit" that outcropped in Mali i Bardhë tectonic window. The nappe of Mirdita ophiolites eastwards overthrusts the Triassic-Jurassic limestones and both Korabi and Mirdita nappes as a common nappe are displaced towards the west over Krasta zone for a distance of tens km (Figure 10).

The geologic profiles of the Geologic Map of Albania at the scale 1:200.000 (2005) show that Mirdita ophiolites overlie the Triassic-Jurassic carbonate formation towards the Korabi zone. In the explanatory text of Geologic Map of Albania (2002) the authors reported about the tectonic cross-section through the Albanides fold and thrust belt (Figure 11) .

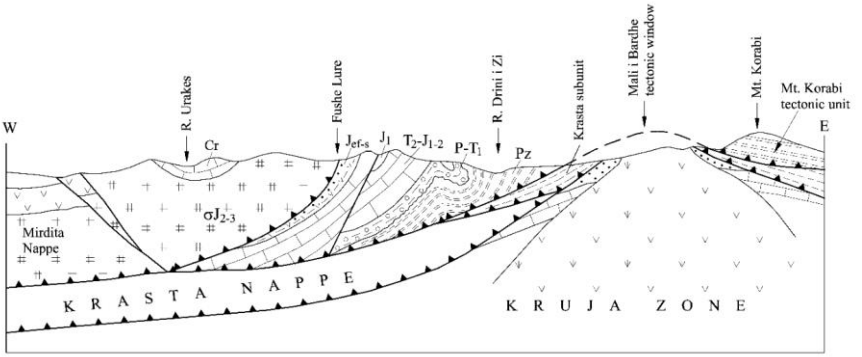

Fig. 10: Geological cross-section through the Mirdita and Korabi nappes (Kodra *et al*., referring to (Melo *et al*., 1990, 1991).

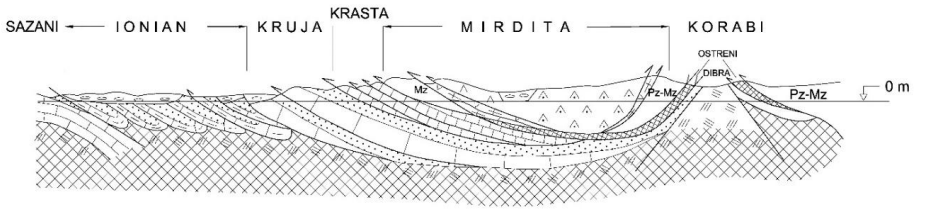

Fig. 11: Tectonic cross-section through the Albanides fold and thrust belt (Xhomo and Kodra 2002).

The Korabi nappe overthrusts the Ostroni unit overlying the Dibra Unit (=Kruja zone), whereas the Mirdita ophiolites overthrust the continental ophiolite periphery to the east (Pz-Mz) and to the west (Mz), and both Mirdita and Korabi nappes overlie the Ostreni nappe that is supposed to be an imbrication of regional extension (Figure 11).

Aliaj and Kodra (2016) referring to Kodra (2016) stated that the main markers of the internal tectono-stratigraphic units of the Albanides are the Triassic and Jurassic ophiolites of Mirdita and Vardari zones with the Korabi-Pelagonian microblock between them. Kodra (2016) distinguished two main different units in the geology of the Mirdita Zone: i) the Triassic and Jurassic Ophiolites with their Middle-Upper Jurassic, Jurassic-Cretaceous and younger sedimentary cover, and ii) the tectonic subzones with sedimentary and volcano-sedimentary formations at the basement and at the periphery of the ophiolites. The Hajmeli and Qerret-Miliska subzones could be noted in the western periphery of ophiolites, while the Gjallica and Mbasdeja subzones in its eastern periphery. Each of them has the value of a real tectonic zone, but

he have maintained including them into the graben megastructure of Mirdita Zone.

Kodra (2016) distinguished two subzones in the Korabi Zone, from west to east: Muhurr-Çaja and Malësia e Korabit (M.Ç-MK) and Kollovozi (Sharri) Subzones. The Muhurr-Çaja and Malësia e Korabit are shown as separate subzones by Xhomo *et al*., (2002). The southern half of Korabi-Pelagonian mikroblock during the Triassic and Jurassic times was developed under a platform condition (Pelagonian platform), while the northern half under basin conditions (Korabi Basin: Muhurr-Çajë-Malësi e Korabit - Kastoria and Kollovozi-Sharri-Flambouro units).

The Mirdita Zone represents a super-structure zone resulted from a basin graben-like architecture. The continental rifting during the Early-Middle Triassic time was associated and followed with continental break-ups of the Vardari and the Mirdita basins during the Late Anisian time and the oceanic time from the the Ladinian to the Middle Jurassic time. The genesis of the Mirdita ophiolites might have occurred in the Mirdita graben megastructure in southwest of Korabi-Pelagonian Microblock and northeast of Hajmeli (Koziakas) platform. The compressional deformation stages and tectonic style of Mirdita oceanic basin closure are characterized by interoceanic and marginal bi-divergent paleo-emplacement during Middle Jurassic until beginning of Late Jurassic time (Figure 12).

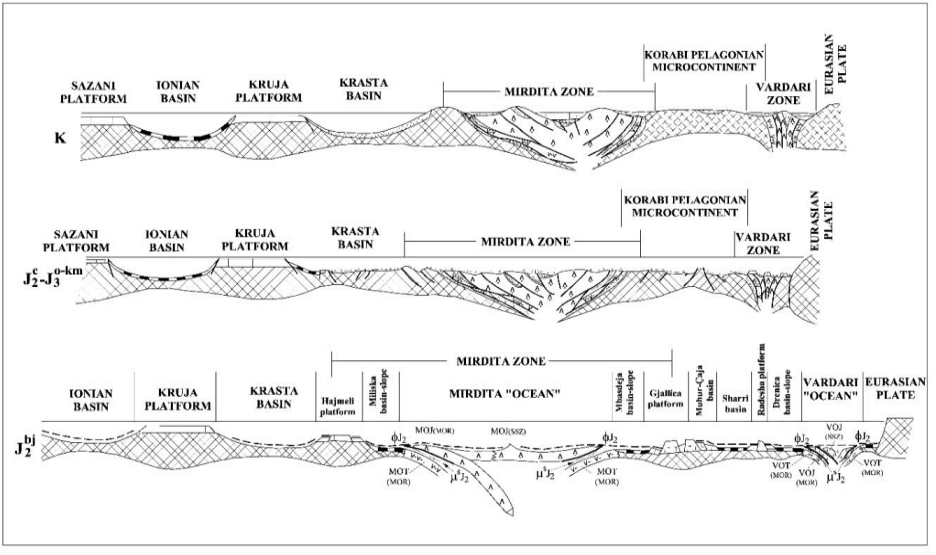

Fig. 12: Reconstruction scheme of the Mesozoic tectonic evolution of Albanides (Kodra 2016).

The Middle-Upper Jurassic and Jurassic-Cretaceous time period was related mainly to compressional deformations that led to the closure of the Vardari and Mirdita ocean basins. Kodra (2016) defined three Mirdita deformation stages during this time period. The first deformational stage belongs to bi-divergent interoceanic paleo-emplacement of the Jurassic ophiolites over the volcano-sedimentary sequence of Triassic ophiolites. Metamorphic sole between the Jurassic ophiolites and the Triassic ones are of Middle Jurassic age. Kodra has named this stage as Mirdita Middle Jurassic Stage 1 (M-1 J_2) (Figure 12). The second deformational stage belongs to the time interval of Callovian-Oxfordian, that is named as Mirdita Callovian-Oxfordian Stage 2 (M-2 J_2^c-J_3^{ox}). The main closure of the Mirdita oceanic basin occurred during the second stage. Third deformational stage is more complex. After Callovian-Oxfordian time, the extensional and compressional regime modes were present in different parts of the Mirdita Zone. They are expressed by the presence of radiolaritic cherts and flysch-flyschoidal deposits of the Oxfordian-Hauterivian age, and by quite clear distinguished emplacement under water washing and structural unconformity of the Upper Tithonian-Valanginian deposits. During the Hauterivian time almost a total rising of the Mirdita Zone occured, but there were also areas where the deposition of Hoterivian-Barremian conglomerates and Aptian platformic limestones continued. The mass rock's displacement during the third stage mainly occurred from northeast to the southwest. At the third deformational stage, named as Mirdita Late Jurassic-Early Cretaceous Stage-3 (M-3 J_3-K_1), the full closure of Mirdita oceanic basin happened.

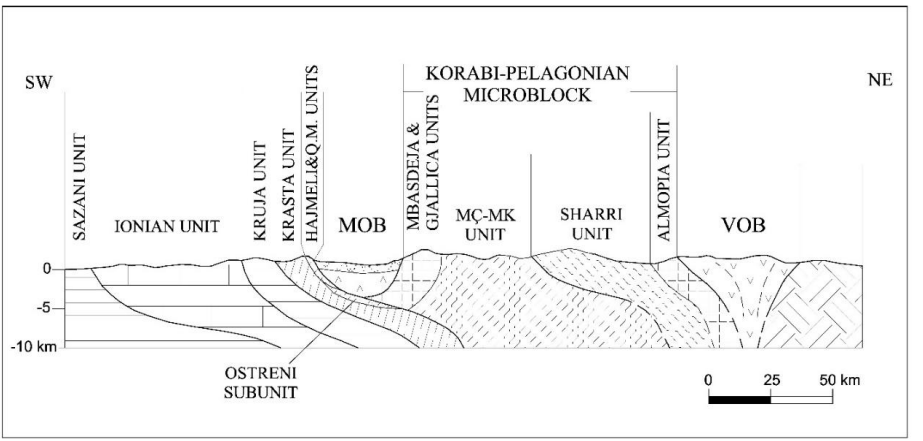

Fig. 13: The cross-section through the present-day geological structure of Albanides (from Kodra 2016).

Kodra (2016) presented a cross-section through the present-day geological structure of Albanides, into which the Mirdita Ophiolite Belt (MOB) overthusts the Krasta zone overlain by the Ostreni subunit, and eastwards thrusts the Mbasdeja and Gjallica units that underlies it (Figure 13).

Çollaku *et al.,* (1990; 1991) and Çollaku (1992) in the symposium "Thrust Tectonics in Albania" held in TiranaNovember 1990, the paper "A propos de la position structural des ophiolites Albanaises: un profil W-E de Rubik a Korabi", published in 1991 under title "Sur l'allochtonie des Albanides: apport des données de l'Albanie Septentrionale". Çollaku *et al*., (1990) published the paper "Sur l'allochtonie des zones internes Albanaises: mise en évidence de fenêtres à l'arrière de la nappe ophiolitique de Mirdita (Albanie)" and Çollaku (1992) presented his thesis in the University Paris 6 "Evolution geodinamique de l'Albanie septentrionale: Structuration cenozoique: Mise en place des ophiolites et metamorphismes associés".

Çollaku *et al*., (1991) stated that Mirdita and Korabi zones present the separate nappes and Mirdita ophiolites overthrust the Triassic carbonatic series of Korabi zone. The synthetic cross-section of Albanides expresses the end Jurassic nappe setting of Mirdita ophiolites, brought from Vardar ophiolite zone, and Tertiary thrusting (end of Lower Miocene) of both Korabi and Mirdita nappes over Krasta flysch unit as well as the gypsum rising in tectonic windows (Çollaku 1992).

Çollaku *et al*., (1990; 1991) confirmed in NE Albania the existence of the tectonic windows of the external zones underlying the following nappe sheets from below to top: Ionian (?) and Kruja autochthonous zones outcropped in tectonic windows, Krasta-Cukali (Krasta subzone) nappe, the nappe of the Upper Jurassic-Lower Cretaceous flysch unit (Radomira flysch unit), Korabi nappe and the Mirdita ophiolite nappe. The Krasta flysch in Shëngjergji corridor with a NE-SW trending, is covered by the nappe of Upper Jurassic-Lower Cretaceous flysch. The Upper Jurassic-Lower Cretaceous flysch is crushed between the parautochthon of Slatin (Mali i Bardhë) window and the Korabi nappe into the Rasa e Zezeë-Radomirë-Kall-Dipjakë half window where it outcrops. The Upper Jurassic-Lower Cretaceous flysch unit, underlying the Korabi nappe, is a useful picket that can be used to connect it with both Bosnian zone of Bosnia and Beotian zone of Greece.

Qirinxhi *et al*. (1990;1991) presented in the Symposium "Thrust Tectonics in Albania" held in Tirana, in November 1990, the paper "Review on relations of Albanides tectonic zones and main features of their inner structure", published in 1991. Qirinxhi *et al*., (1990; 1991) concluded that the tectonic zones in Albania are thrust and overthrust westward. Korabi zone overthrusts Mirdita one and both overthrust external zones of Albanides. In addition, he and his colleagues pointed out that Korabi zone is built by overturned folds consisting of Paleozoic-Triassic formations complicated by thrust and

overthrust faults, which have disrupted the boundaries of Korabi nappes and their internal structure. Mirdita zone is mainly composed of ophiolites. Most scholars considered the relations of Mirdita ophiolites with Korabi zone as normal, but one observes that Korabi Paleozoic-Triassic formations overthrust serpentinites and the Upper Jurassic-Lower Cretaceous flysch unit, which are considered as belonging to Mirdita zone. Therefore, these are its eastern tectonic "tail" of Mirdita zone. The extention of Mirdita ophiolites NE, close to the Shkodra-Peja transform fault is interpreted by them as being formed due to the ophiolite nappe displacement toward the west.

Bushati (1985; 1988; 1994; 1997) presented at the University of Leeds, UK, the study "Geotectonic ophiolite position in the Inner Albanides based on gravity data" in the framework of Global Gravity Map (GETHEC Group) in 1994. Three years later, he finished the study "Map of magnetic field anomalies of Albania at the scale 1:200.000".

The Mirdita ophiolitic belt is characterized by intensive Bouguer anomalies and very turbulent magnetic field of relatively low intensity anomalies. The high gradients and their mosaic shape clearly show the gravity anomalies in the Mirdita zone. The local positive anomalies go up to 48-50 mgal, typical of Mirdita ophiolites. The ophiolite massifs are mapped by different Bouguer gravity anomalies: in the Tropoja ultrabasic massif by the amplitude of 50 mgal, and 48 mgal in Bulqiza massif, 30 mgal in Shebeniku massif and 10 mgal in southern margin of the ophiolite belt. The gravity field of Bulqiza massif has an asymmetric shape, where the deepest part, about 6 km, belong to the eastern part of the massif and 1.1 km to its western margin. The gravity data show that the ophiolite belt is genetically unique, divided into two parts by Shëngjergji corridor of Krasta flysch tongue. The thickest part of the ophiolite belt is 14 km in the Kukës ultramafic massif and towards its west and south, the thickness decreases by 2 km. The gradual decreasing gradient of gravity field towards the east characterizes the Korabi zone.

The contact to the west of Korabi zone gravity field with the gravity field anomalies of the Mirdita ophiolitic belt passes after the Ohrid-Qarrishta-Qafë Murra-Kukësi seismogenic deep fault line.

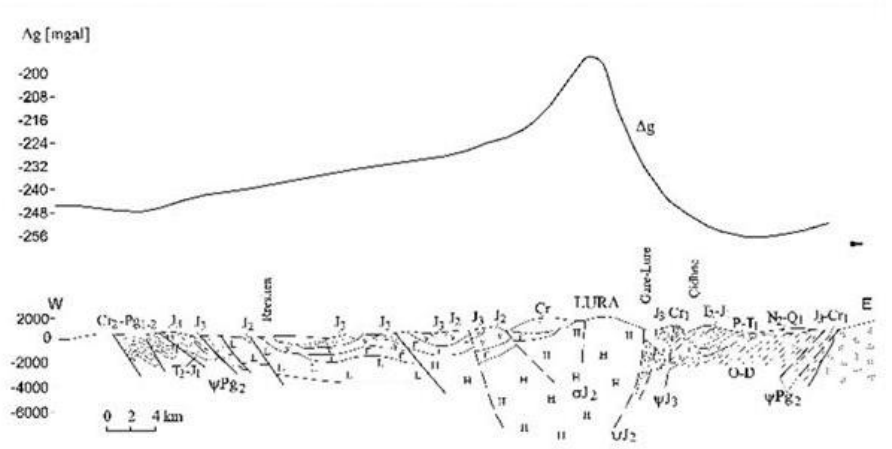

Fig. 14: Geological-geophysical cross-section from Rresheni through Lura ultrabasic massif up to Korabi heights (Bushati and Xhomo 1994).

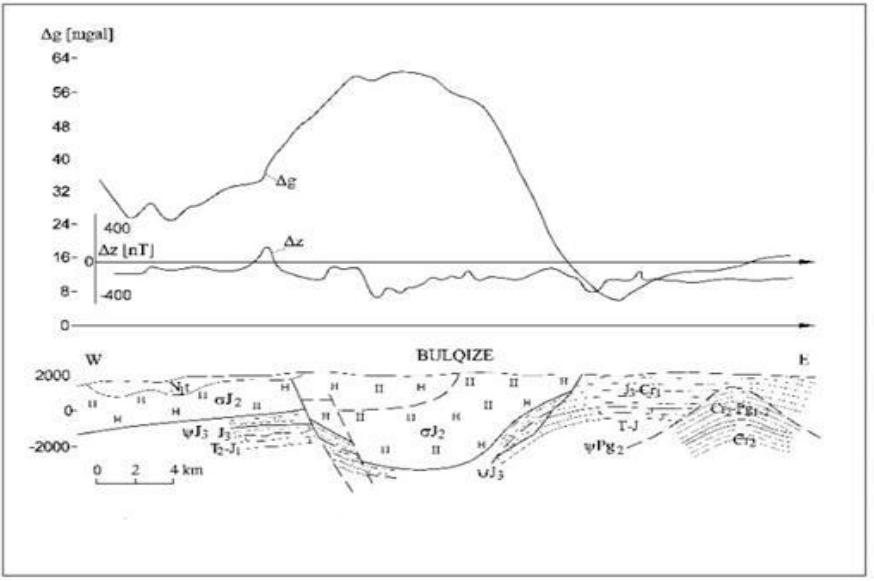

Fig.15: Geological-geophysical cross-section from Klosi through Bulqiza ultrabasic massif up to Shupenza village (Bushati and Xhomo 1994).

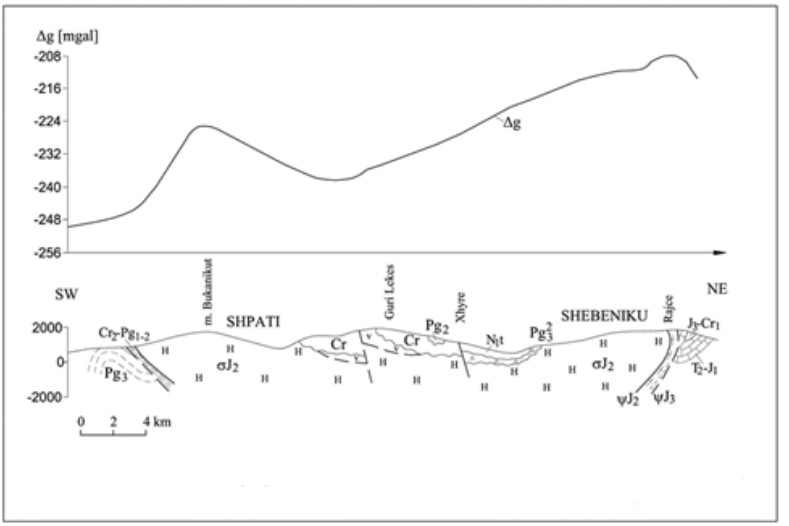

Fig. 16: Geological-geophysical cross-section through Shpati and Shebeniku ultrabasic massifs (Bushati and Xhomo 1994).

The complex geophysical data show that the serpentinized ultrabasic rocks underlie the Burreli molasse depression proving the connections between the eastern and western ultramafic belts of Albania. The eastern margin of the ophiolite massifs is in general west-dipping. The presented gravity cross-sections support the allochthonous setting of the Mirdita ophiolites completely detached from their roots (Figure 14-16).

Bushati (1997) stated that the Mirdita ophiolitic belt is characterized by a turbulent magnetic field of relatively low intensity. The ophiolitic massifs have the magnetic anomalies of high amplitude, up to 800 nT in Kukësi ophiolitic massif, while towards the south, ultrabasic massifs, like Lura, Puka and Bulqiza, Shebeniku and Shpati are represented by low anomalies up to 400 nT (see Map of Magnetic Field anomalies of Albania at the scale 1:200.000, Bushati 1997).

Magnetometric mappings at the scale 1:200.000 or 1:100.000 were not used to fix the magnetic anomalies of the sedimentary formations of the Mirdita ophiolitic periphery and Korabi and Krasta-Cukali zones.

More detailed magnetometric surveys at the scale 1:25.000, carried out in Korabi area (Kospiri *et al*., 1986), showed that all the ultrabasic outcrops could be noted through the magnetic anomalies fixed above them as in Biçaja, Stanët e Preshit, Piramida 2 etc. The covered ultrabasic bodies overlain by deluvial or proluvial deposits can be fixed too by the magnetic anomalies up to 200 nT, e.g., Bjeshka e Shehut, Fusha e Panaireve, Burimet e Radomirës etc. Some of covered ultrabasic bodies with the magnetic anomalies above them were verified by boreholes, e.g., Bjeshka e Shehut, where the

serpentinites or very serpentinized peridotites along a normal fault were met from 11.25 m to 25.00 m deep, under the deluvial deposits consisted of limestone rocks fragments (Kodra *et al*., 1986).

Frashëri and Bushati presented in the Symposium "Thrust Tectonics in Albania" held in Tirana, in November 1990, the paper "Some aspects on the relations of ophiolites with the surrounding rocks based on geophysical data" which was published in 1991. Later on, Frashëri and Bushati (2009) published the paper "Geophysical outlook on structure of the Albanides".

Frashëri *et al*., (2009) concluded that the Mirdita ophiolitic complex causes a gravity anomaly chain and a turbulent magnetic field of relatively low density, and the geophysical evidences support the allochthonous character of the ophiolite belt. Gravitational data report that the thickness of ophiolite massifs varies from 6 to 14 km to the east and less than 2 km to the west.

4. THE SUMMARY OF SCHOLAR OPINIONS ABOUT THE MIRDITA ZONE FRAMEWORK

In stead of conclusions, opinions about the Mirdita zone framework of some of the scholars are here briefly reported.

Nopcsa (1921; 1929) was the first scholar who performed the tectonic zoning of Dinarides showing that the relations among Dinarides tectonic zones are of overthrust type, with the exception of the border between Mirdita and Shar-Dagh zones passing through the "Drini Fault". He considered the Mirdita Nappe as an ophiolile pre-Gosaw nappe.

Zuber (1938; 1940) was the first of foreign scholars who distinguished that "Albanian ophiolite nappe", which often is called "Ophiolite nappe", underlies the Shar-Dagh (=Korabi zone) nappe in the Peshkopi region.

Zuber has formulated the conception of tectonic nappe building of all tectonic zones lying to the northeast of frontal nappe flysch zones which is shown in tectonic ideal section across the Southern Italy and Balkan Folds, passing south of Shkodra-Peja transform fault, where from NE to SW the Pelagonia, Shar-Dagh (Korabi), Albanian ophiolite (Mirdita) and Cukali (Krasta) nappe zones overlie successively one over the other like roof-tiles.

Biçoku *et al*., (1965, 1970) and Papa (1971) underlined that the Mirdita zone overthrusts the Krasta-Cukali flysch unit and it delimits with the Korabi one through a normal contact which passes after the eastern margin of ultramafic massifs.

Shehu *et al*., (1983; 1985; 1990) and Shallo (1985, 1999) distinguished two subunits of Mirdita zone: An ophiolite subzone and another carbonate subzone in both ophiolite sides. The Mirdita zone overthrusts the Krasta-Cukali zone and its border with Korabi zone, which extends in Peshkopi

region, is indicated as normal contact following the eastern margin of carbonatic periphery.

Xhomo and Kodra (2002; 2005) distinguished two main units of the Mirdita zone: i) Triassic- Jurassic ophiolites and their sedimentary cover, and ii) subzone unit at the periphery and at the basement of the ophiolites (the Hajmeli and Qerret-Miliska subzones in the west and Gjallica and Mbasdeja subzones in the east). The Muhurr-Çaja, Korabi Highlands and Kollovozi Subzones could be in the Korabi zone distinguished. The border between Mirdita and Korabi zones passes after the border between the Gjallica and Çaja subzones drawn as a normal contact that follows in the Kukësi-Peshkopia region. Mirdita zone has transitory relations with the Korabi zone and both of them overthrust Dibra, Ostreni and Krasta units.

Xhomo and Kodra (2002) presented the tectonic scheme of Albania and the tectonic cross-section through the Albanides fold and thrust belt where the Korabi nappe overthrusts the Ostroni unit by overlying the Dibra Unit (=Kruja zone). The Mirdita ophiolites overthrust the continental ophiolite periphery to the east (Pz-Mz) and to the west (Mz), and both Mirdita and Korabi nappes overlie the Ostreni nappe. This is supposed to be an imbrication of regional extension.

Aubouin and Ndojaj (1964) considered the border between the Mirdita and Korabi zones as a normal one passing after eastern margin of the ophiolites which extends from Kukësi-Peshkopia region in the north to Mali i Thatë Mountain in the south. Mirdita/Subpelagonian and Krasta/Pindos nappes are delimited by frontal thrusts.

Belostockij (1960-1978) reported about the nappe tectonics in Albanian sector of Dinarides evidenced at boundaries of nappe complexes or main structural zones. Especially the tectonic nappes following the outer extremities of Korabi zone are analyzed in details. He has reported about the Selishta sector, different sectors of Korabi allochthon, nappes of Subpelagonian (=Mirdita) zone, the examples of allochthonous strucrures at forehead of both internal and external zones and Devolli nappe packet into which the covering of some tectonic zones is evidenced. All sectors of observations are marked in the Tectonic Map of Albanian Sector of Dinarides (Figure 6). The allochthtonous Triassic limestones overlying the ophiolites of Subpelagonian zone (=Mirdita zone) are observed in many places from Selishta sector in the north to Mali i Thatë Mountain in the south.

The following nappe units of allochthonous complex could be met in the Albanian sector from east to west: Vardar, Pelagonian, Subpelagonian, intermediary unit and Pindos nappe sheets. Belostockij showed the root levels zones of nappe sheets evidenced in the Albanian sector.

Melo (1966-2002) pointed out that the Peshkopia region is among the classic areas with nappe structures. He distinguished these main tectonic

elements of Korabi and Mirdita zones: i) the Korabi Paleozoic nappes, and ii) the ophiolite belt with two peripheral Triassic-Jurassic limestones belts of Mirdita Zone. The Korabi Paleozoic nappe located in the Peshkopia region consists of three subzone nappes, from bottom to top: Grama (it is also known as Radomira), Çaja-Muhurri and Kollovozi nappes. The Korabi nappe is considered as the upper nappe which overlies the lower Krasta nappe covering the Kruja zone tectonic windows.

In the Tectonic Zonation Scheme of Albania (Melo, 2002) the border of Mirdita zone with the Korabi zone is presented as normal contact. The Bulqiza ultramafic massif thrusts the Okshtuni tectonic window, whereas the Mirdita zone overthrusts the Krasta zone.

The nappe of Mirdita ophiolites overthrusts the Triassic-Jurassic limestones and both Korabi and Mirdita nappes as a common nappe are displaced towards the west over Krasta zone for a distance of tens km, so they can be considered as nappes without roots. Melo pointed out that whichever scenario allocated to the origin of Mirdita ophiolite,either lying in the Mirdita zone or in Vardar zone, the ophiolitic nappe in our country can be followed some km deep.

Aliaj (1987-2018) stated that the east verging overturned west plunged folds, built mainly by Triassic-Jurassic limestones, overlie the Mirdita ophiolites. They are observed at the frontal part of Korabi zone in the Selishta-Resku region and directly to the east of Mirdita ophiolites.

The tectonic windows of Kruja and Krasta zones observed within Korabi zone in the region of Peshkopi (eastern Albania), have been formed due to the Pliocene-Quaternary extensional tectonics, accompanied by normal faulting and evaporite diapirism which created cupola pattern horsts and favoured the erosion of the Mirdita and Korabi upper nappe sheets, which are seen only at the margins of these windows. The ophiolite bodies found along the normal faults, at frontal part of Korabi zone up to Korabi Highland and along the nappe boundaries surrounding the tectonic windows, could be considered as pulled up from the Mirdita ophiolites underlying the Korabi zone. These data show that Mirdita ophiolites underlie the Korabi nappe structures, proving perfectly that the Mirdita oceanic basin located to the west of Korabi zone.

It is important to mention that the distinction of the Guri i Gopit zone addresses the location of the Mirdidta oceanic basin to the west of Korabi zone.

Meço and Aliaj (2000) in the book “Geology of Albania” pointed out that the Mirdita Zone overthrusts the Krasta Zone and is itself overthrust by the Korabi Zone; such nappe relations are also plotted in the graf of Tectonic Zonation of Albania showing that the Korabi nappe overthrusts the Mirdita one.

Based on the aforementioned data, Aliaj (1987-2018) and Meço and Aliaj (2000) pointed out that within Korabi zone the following nappe sheets could be met, from top to bottom: Korabi nappe, Mirdita ophiolitic nappe transgressively covered by the Tithonian-Valanginian flysch and Krasta nappe that overlies the Kruja zone "autochthon".

Kodra (1976-2016) stated that the main markers of the internal tectono-stratigraphic units of the Albanides are Triassic and Jurassic ophiolites of Mirdita and Vardari zones with the Korabi-Pelagonian microblock between them. He recognized from west to east two main units in the geology of the Mirdita Zone and two subzones in the Korabi Zone: the Muhurr-Çaja and Malësia e Korabit (M.Ç-MK) and Kollovozi (Sharri) subzones. The southern half of Korabi-Pelagonian microblock during the Triassic and Jurassic times was developed in platform condition (Pelagonian platform), while the northern half have been in basin conditions (Korabi Basin: Muhurr-Çajë-Malësi e Korabit - Kastoria and Kollovozi-Sharri-Flambouro units) (Kodra 2016).

The Mirdita Zone represents a super-structure zone resulted from a basin graben-like architecture. The continental rifting during the Early-Middle Triassic time was associated and followed with continental break-ups of the Vardari and the Mirdita basins during the Late Anisian time and the oceanic spreading during the Ladinian till the Middle Jurassic time. The generation place of the Mirdita ophiolites supposed to be the Mirdita graben megastructure in southwest of Korabi-Pelagonian Microblock and northeast of Hajmeli (Koziakas) platform. The compressional deformation stages and tectonic style of Mirdita oceanic basin closure are characterized by interoceanic and marginal bi-divergent paleo-emplacement during Middle Jurassic until beginning of Late Jurassic time. The Middle-Upper Jurassic and Jurassic-Cretaceous time period was related mainly to compressional deformations that led to the closure of the Vardari and Mirdita ocean basins.

Kodra, Xhomo and Melo (in Melo *et al.* 1990; 1991) realized an original interpretation for the nappe sheet structure across the Mirdita and Korabi zones. There are evidenced two nappe sheets located over one another as well as over the "autochton unit". The upper nappe belongs to the Korabi zone which overthrusts the lower one represented by the Krasta zone. Both covers the "Kruja autochtonous unit" that outcropped in Mali i Bardhe tectonic window. The nappe of Mirdita ophiolites eastwards overthrusts the Triassic-Jurassic limestones and both Korabi and Mirdita nappes as a common nappe are displaced towards the west over Krasta zone for a distance of tens km.

Kodra and Xhomo (2002; 2005) in the geologic profiles of the Geologic Map of Albania at the scale 1:200.000 (2005) show that Mirdita ophiolites overlie the Triassic-Jurassic carbonate formation towards the Korabi zone and in the Tectonic cross-section through the Albanides fold and thrust belt is

shown that the Korabi nappe overthrusts the Ostroni unit overlying the Dibra Unit (=Kruja zone), whereas the Mirdita ophiolites overthrust the continental ophiolite periphery to the east (Pz-Mz) and to the west (Mz), and both Mirdita and Korabi nappes overlie the Ostreni nappe that is supposed to be an imbrication of regional extension.

Kodra (2016) has presented a cross-section through the present-day geological structure of Albanides, into which the Mirdita Ophiolite Belt (MOB) overthusts the Krasta zone overlain by the Ostreni subunit, and eastwards thrusts the Mbasdeja & Gjallica units that underlies it.

Çollaku *et al*., (1990; 1991) and Çollaku (1992) concluded that Mirdita and Korabi zones present the separate nappes and that Mirdita ophiolite nappe, brought from Vardar ophiolite zone, overthrusts the Korabi one and both overthrust the Krasta flysch. Çollaku *et al*., (1990; 1991) concluded that in NE Albania is confirmed the existence of the tectonic windows of the external zones underlying the following nappe sheets from below to top: Ionian (?) and Kruja autochthon zones outcropped in tectonic windows, the Krasta-Cukali (Krasta subzone) nappe, the nappe of the Upper Jurassic-Lower Cretaceous flysch unit (Radomira flysch unit), the Korabi nappe and the Mirdita ophiolite nappe. The Krasta flysch in the Shengjergji corridor NE-SW trending is covered by the nappe of Upper Jurassic-Lower Cretaceous flysch. The Upper Jurassic-Lower Cretaceous flysch is crushed between the parautochthon of Slatin (Mali i Bardhe) window and the Korabi nappe into the Rasa e Zeze-Radomire-Kall-Dipjake half window where it outcrops.

Qirinxhi et al. (1990, 1991) arrived in conclusion that the Korabi zone overthrusts the Mirdita one and both overthrust the external zones of Albanides. The Korabi zone is built by the overturned folds composed of Paleozoic-Triassic formations complicated by thrust and overthrust faults, which have disrupted the boundaries of Korabi nappes and their internal structure. The nappe of Korabi zone overthrusting the ophiolites (serpentinites) covered by Late Jurassic-Early Cretaceous flysch deposits is observed in the Veleshica river. Mirdita zone is mainly composed of the ophiolites. Most scholars considered as being normal the relations of Mirdita ophiolites with Korabi zone but it is seen that the Korabi Paleozoic-Triassic formations overthrust the serpentinites and the Upper Jurassic-Lower Cretaceous flysch unit, which are considered as belonging to the Mirdita zone. Therefore these present the eastern tectonic "tali" of the Mirdita zone. The NE extending of Mirdita ophiolites near to the Shkoder-Peje transform fault is interpreted by them as being formed due to the ophiolite nappe displacement toward the west.

Bushati (1985; 1988; 1994; 1997) stated that the Mirdita ophiolitic belt is characterized by intensive Bouguer anomalies and very turbulent magnetic field of relatively low intensity anomalies. The high gradients and their

mosaic shape clearly show the gravity anomalies in the Mirdita zone. The local positive anomalies go up to 48-50 mgal, typical of Mirdita ophiolites. The gravitational data show that the ophiolitic belt is genetically unique, divided into two parts by Shëngjergji corridor of Krasta flysch tongue. The thickest part of the ophiolite belt is 14 km in the Kukës ultramafic massif, and towards its west and south, the thickness decreases by 2 km. The gradual decreasing gradient of gravity field towards the east characterizes the Korabi zone. The contact to the west of Korabi zone gravity field with the gravity field anomalies of the Mirdita ophiolitic belt passes after the Ohrid-Qarrishta-Qaf Murra-Kukësi seismogenic deep fault line.

The complex geophysical data show that the serpentinized ultrabasic rocks underlie the Burreli molasse depression proving the connections between the eastern and western ultramafic belts of Albania. The eastern margin of the ophiolite massifs is in general west-dipping. The presented gravity cross-sections support the allochthonous setting of the Mirdita ophiolites completely detached from their roots.

Bushati (1997) stated that the Mirdita ophiolite belt is characterized by a turbulent magnetic field of relatively low intensity. The ophiolite massifs have the magnetic anomalies of high amplitude, from 400 nT up to 800 nT. The detailed magnetometric surveys, carried out in Korabi area showed that all the ultrabasic outcrops are evidenced through magnetic anomalies fixed above them as in Biçaja, Stanët e Preshit, Piramida 2 etc.

Frashëri *et al*., (1990; 2009) concluded that the geophysical evidences support the allochthon character of the ophiolitic belt. Based on the gravity data, the thickness of ophiolite massifs varies from 6 to 14 km in east and less than 2 km in the west.

REFERENCES

Aliaj Sh. 1987. Shembuj te mbulesave tektonike ne zonat e brendeshme te Albanideve dhe deformimi neotektonik i tyre. *Studime Sizmologjike.* **1**: 117-136.

Aliaj Sh. 1991. Rrudha të zhytura në ballin e zonës së Korabit (Rajoni Selishtë-Resk). *Buletini i Shkencave Gjeologjike*. **1**: 139-147.

Aliaj Sh. 1993. Tectonic windows of the external zones in the region of Peshkopia (eastern Albania). *Geological Society* of *Greece*. **XXVIII/1**: 351-360.

Aliaj Sh. 1994. Nappe structures in southeastern Albania. *Bull. Soc. Geol. Greece*. **XXX/2:** 459-466, Athens.

Aliaj Sh. 1997. Alpine geological evolution of Albania. *Albanian Journal of Natural and Technical Sciences*. **3**, 69-81. Albanian Academy of Sciences.

Aliaj Sh. 2012. Neotektonika e Shqiperise. Shtëpia Botuese KLEAN, f. 292.

Aliaj Sh. 2018. Guri i Topit zone – An intermediary tectono-stratigraphic unit between the external and internal Albanides. In press. *Journal of Natural and Technical Sciences*. Albanian Academy of Sciences. Tirana.

Aliaj Sh, Meço S. 1994. Mirdita oceanic basin was located westwards of Korabi Zone (= Pelagonian Zone). *Ofioliti*. **19 (1):** 97-103.

Aliaj Sh, Shkupi D. 2000. Nopcsa's thought on tectonics of Albania. *Albanian Journal of Natural and Technical Sciences.* **9**: 111-119. Albanian Academy of Sciences.

Aliaj Sh, Koçiu S, Muço B, Sulstarova E. 2010. Sizmiciteti, sizmotektonika dhe Vlerësimi i Rrezikut Sizmik ne Shqiperi. Shtypshkronja "Kristalina KH" Tirane, 310 f.

Aliaj Sh, Kodra A. 2016. The Albanides Setting in the Dinaric-Albanian-Hellenic Belt and Their Geological Features. *Journal of Natural and Technical Sciences. Albanian Academy of Sciences.* **2:** 31-73.

Aubouin J, Ndojaj I. **1964.** Regard sur la géologie de l' Albanie et sa place dans la géologie des Dinarides. *Bulletin de la Société Géologique de France***Ser. 7 VI (5),** 593-624.

Behrmann RB. 1941. Die Ölgeologosche Erschließung Albaniens. *Oel und Kohle* 37, 771, 875.

Belostockij II. 1960. Mbi manifestimet e tektonikes gravitative ne Shqipëri. *Bul. UT Shk. Nat. Nr 4.*

Belostockij II. 1963. O tektoniçeskih pokrovov i gravitacionih strukturah zapadnoj çasti centralnih Dinarid. St. 1:Tektoniçeskie pokrovi. *Bul MOIP, Otd. Geol., No 6.*

Belostockij II. 1978. Stroenie i formirovanije tektoniceskih plokrovov. *M., Izd. "Nedra" c. 234*.

Biçoku T. 2004. Historiku i kërkimeve dhe studimeve gjeologjike të Shqipërisë. *Shtypshkronja "Mësonjtorja" Tiranë. 325.*

Biçoku T. 2007. Kontributi i të huajve në fushën e gjeoshkencave të Shqipërisë. Shtypshkronja "Nënë Tereza" Tiranë, f. 522.

Biçoku T, Pumo E, Papa A, Xhomo A, Qirinxhi A, Çili P, Dede S, Pashko P, Turku I, Pasho S. 1967. Harta Gjeologjike e Shqipërisë në shkallë 1:200.000. Shtypur nga Ndërmarrja e Mjeteve Mësimore, Kulturore dhe Sportive "Hamid Shijaku" Tiranë.

Biçoku T, Pumo E, Papa A, Xhomo A, Qirinxhi A, Çili P, Dede S, Pashko P, Turku I, Pasho S. 1970. Gjeologjia e Shqipërisë. Tekst shpjegues i Hartës Gjeologjike të Shqiperisë në shkallë 1:200.000, Shtëpia Botuese "Naim Frashëri" Tiranë, 343.

Biçoku T, Papa A. 1970. Skema tektonike e Shqipërise sipas Biçoku & Papa (1965) me disa ndryshime, integruar në librin "Gjeologjia e Shqipërisë" (Biçoku *et al.*, 1970).

Bushati S, Dema Sh. 1985. Harta gravimetrike e Shqiperise në shkalle 1:200.000. *Qendra Gjeofizike Tiran*ë.

Bushati S. 1988. Studimi krahinor i fushës së rëndesës në Albanidet e brendëshme në nidhmë të rajonizimit tektonik e metalogjenik. *Disertacion, Fakulteti Gjeologji-Miniera Tiran*ë.

Bushati S. 1994. Geotectonic ophiolite position in the Inner Albanides according to the gravity data. *Presented at University of Leeds, UK, in the framework of Global Gravity Map (Gethec group).*

Bushati S. 1997. Map of magnetic field anomalies of Albania at the scale 1:200.000. *Qendra Gjeofizike Tiran*ë.

Çollaku A, Cadet JP, Melo V, Bonneau M. 1990. Sur l'allochtonie des zones internes albanaises: mise en évidence de fenêtres à l'arrière de la nappe ophiolitique de la Mirdita (Albanie), *C. R. Ac. Sc. Paris, t. 311 (II), 1251-1258.*

Çollaku A, Cadet JP. 1991. Sur l' allochtonie des Albanides. Apport des donnes de l' Albanie septentrionale. *Buletini i Shkencave Gjeologjike. Nr. 1, 255-270.*

Çollaku A. 1992. Evolution *géodynamique* de l'Albania septentrionale: Structuration cenozoique: Mise en place des ophiolites et metamorphismes associes. *Thesis Université. Paris 6.*

Dede S, Shehu R, Çili P. 1971. Albanidet e brendëshme (zonat Korabi, Mirdite dhe Gashi). *Përmbledhje Studimesh. Nr.4, 57-76.*

Frashëri A, Lubonja L, Langora Ll, Bushati S. 1991. Disa aspekte të marrëdhënieve të ofioliteve 7, me shkëmbinjtë përreth, sipas interpretimeve të të dhënave gjeofizike. *Buletini i Shkencave Gjeologjike. Nr 1, 93-98.*

Frashëri A, Bushati S, Bare V. 2009. Geophysical Outlook on structure of the Albanides. *Journal of Balkan Geophysical Society.* **12 (1):** 9-30.

Gjata K, Kodra A, Pirdeni A. 1980. Gjeologjia e disa pjesëve periferike të zonës së Mirditës. *Përmbledhje Studimesh*. **3:** 57-74.

Gjata K, Kodra A. 1982. Magmatizmi pasofiolitik J-Kr dhe ai më i ri, mesataro-acid në vendin tonë. *Buletini i Shkencave Gjeologjike.* **4**: 25-39.

Hoffman N, Reicherter K, Fernandez-Steeger T, Grützner C. 2010. Evolution of ancient lake Ohrid: a tectonic perspective. *Biogeosciences.* **7:** 3377-3386.

Kodra A. 1976. Mbi moshën jurasike të formacionit vullkanogjeno-sedimentare të zonës së Mirditës. *Përmbledhje Studimesh.* **1:** 11-30.

Kodra A. 1981. Shkëmbinjtë jurasikë dhe jurasiko-kretake në rajonet verilindore të Albanideve (në lindje të ofioliteve të zonës së Mirditës). *Përmbledhje Studimesh*. **3:** 31-47.

Kodra* A. 1987.** Skema e zhvillimit paleogjeografik e gjeotektonik e Albanideve t*ë* brendë*s*hme gjat*ë* Triasikut dhe Jurasikut. *Buletini i Shkencave Gjeologjike*. **4:* 23-34.

Kodra A. 1988$_a$. Shkëmbinjtë vullkano-sedimentare në lindje të masivit ultrabazike të Shebenik-Pogradecit vendosen mbi gëlqerorët Triasiko-Jurasik. *Buletini i Shkencave Gjeologjike.* **1**: 169-178.

Kodra A. 1988. Riftëzimi i kores kontinentale mirditore dhe fazat e para të zgjerimit oqeanik Mirditor. *Buletini i Shkencave Gjeologjike*. **4:** 3-14.

Kodra A. 1990. Shkembijte copezore (melanzhe sedimentare) ne formacionin vulkano-sedimentare te Albanideve te brendeshme. *Buletini i Shkencave Gjeologjike.* **2:** 3-14.

Kodra A. 2016. The Internal Tectono-Stratigraphic Units and the Alpine Geologic Evolution. In: Aliaj and Kodra (2016).

Kodra A, Delaj E. 1976. Të dhëna të reja mbi ndërtimin gjeologjik të rajonit të Poravit. *Përmbledhje Studimesh*. **4**: 71-86.

Kodra A, Goci L. 1977. Problematika e ndërtimit strukturor të zonës së Mirditës dhe marrëdhëniet e saj me zonat fqinje. *Përmbledhje Studimesh*. **4:** 109-118.

Kodra A, Gjata K, Pirdeni A. 1979. Nivele të Doger-Malmit ne rajoinin e Martaneshit. *Përmbledhje Studimesh*. **4:** 59-64.

Kodra A, Shehu B, Goci L, Selimi R. 1980. Gjeologjia e pjeses veriore te njesise "Gjallica". *Përmbledhje Studimesh*. **3:** 75-90.

Kodra A, Gjata K. 1982. Ofiolitet në kuadrin e zhvillimit gjeotektonik të Albanideve të brendëshme**.** *Buletini i Shkencave Gjeologjike*. **2**: 49-63.

Kodra A, Gjata K. 1989. Evolucioni mesozoik i Albanideve të brendshëm, fazat e riftëzimit dhe zgjerimi oqeanik Mirditore. *Buletini i Shkencave Gjeologjike.* **4**: 55-66.

Kodra A, Bushati S. 1991. Vendosja paleotektonike e ofiolitive të zonës së Mirditës. *Buletini i Shkencave Gjeologjike.* **1:** 99-107.

Kodra A, Vergely P, Gjata K, Bakalli F, Godroli M. 1993. La formation volcano-sedimentaire du jurassique superieur: temoin de l'ouverture du domaine ophiolitique dans les Albanides internes. Bulletin de la *Société géologique de France*. **164 (1):** 61-67, Paris.

Kodra A, Gjata K, Bakalli F. 1995. The Mirdita oceanic basin from rifting to closure. Workshop "Albanian ophiolites and related mineralizations". Doc. BRGM 244, 9-26 Tirana.

Kodra A, Gjata K, Xhomo A. 2000. Tectonic history of Mirdita oceanic basin (Albania). *Buletini i Shkencave Gjeologjike.* **1**: 5 – 26.

Kodra B, Alliu I, Hoxha V, Meshi N, Kolgjini E, Mazreku A, lKospiri A. 1986. Studim tematiko-përgjithësues e rilevues kompleks për sqarimin e perspektivës të mineralit të hekurit dhe mineralizimeve të tjera në Rajonin e

Radomirës (për periudhën qershor 1984 - mars 1986). *Fondi Qëndror i Gjeologjisë, Shërbimi Gjeologjik Shqiptar.*

Meço S, Aliaj Sh, Turku I. 2000. Geology of Albania. *Gebruder Borntraeger. Berlin. Stuttgart. 246 pp.*

Melo V. 1966. Marrëdheniet gjeologjike të trashësisë flishoidale numulitike me depozitimet rrethuese që vendosen mbi të në rajonin e Korabit. *Bul. UT Ser. Shk. Nat.,* **1:** 45-56.

Melo V. 1982. Perhapja e flisheve ne gjuhen flishore te Peshkopi-Labinotit dhe mendime mbi vendosjen paleogjeografike e tektonike te saj. *Buletini i Shkencave Gjeologjike.* **2:** 19-45.

Melo V. 1986. Ndërtimi dhe zhvillimi gjeotektonik i Shqipërisë. Shtypshkronja e Universitetit të Tiranës. Tiranë.169 f.

Melo V. 2002. Struktura tektonika e Shqipërisë. *Dorëshkrim, studim i brendshëm,* Instituti i Sizmologjisë Tiranë. 28 f. pa figurat.

Melo V, Kote Dh. 1973. Gjeologjia dhe tektonika e njësisë së Gramozit në sektorin Helmes-Shtike-Kozel dhe marredhëeniet me zonën e Mirditës. *Përmbledhje Studimesh.* **4**: 41-51.

Melo V, Kanani J. 1978. Flishi i hershëm i Kretakut në strukturat karbonatike të Njësisë së Krastës për sektorin e Qafë-Shtamës dhe morfologjia e tyre. Përmbledhje Studimesh. 3-4: 57-65.

Melo V, Kanani J. 1984. Mbulesat tektonike të nënzonës së Krastës në sektorin Milot-Lezhë dhe natyra e blloqeve gëlqerore në flish. *Buletini i Shkencave Gjeologjike.* **1**: 7-27.

Melo V, Shallo, M, Aliaj Sh, Xhomo A, Bakia H. 1991a. Tektonika mbihipëse e mbulesore në strukturën gjeologjike të Albanideve. *Buletini i Shkencave Gjeologjike.* **1**: 7 – 20.

Melo V, Aliaj Sh, Kodra A, Xhomo A, Naço P, Lula F, Gjata K, Hoxha V. 1991b. Dritare tektonike te zonave të jashtme ne rajonet lindore të Albanideve. *Buletini i Shkencave Gjeologjike, 1, 21 – 29.*

Nopcsa F. 1921. Beitrag zur Vereilung der Eruptivgesteine. *Foldt. Kozl. 56, 149-160, Budapest.*

Nopcsa F. 1929. Geologie und Geographie Nordalbaniens mit Anhang von H.V. Mzik. Beitrage zur Kartographie Albaniens nach orientalischen Quellen. *Geologica Hungarica, S. Geol., Vol. 3, 1-704, Budapest.*

Nowack E. 1929. Geologische Übersicht von Albanien. (Erläuterung zur geologischen Karte Mabstabes 1:200 000). Salzburg.

Papa A. 1971. Përfytyrimet e sotme mbi strukturën e Albanideve (Një paraqitje e Hartës Tektonike të Shqipërisë në shkallë 1: 200.000). *Përmbledhje Studimesh Nr. 1, 5-22.*

Peza L. 1967. Rajonizimi gjeologo - tektonik i Shqipërisë. Shtypshkronja e Universitetit të Tiranës, Tiranë, f. 118.

Robertson AHF, Shallo M. 2000. Mesozoic – Tertiary tectonic evolution of Albania in regional Eastern Mediterranean context. *Tectonophysics, 316, 197-254.*

Shallo M, Gjata Th, Vranai A. 1980. Përfytyrime të reja mbi gjeologjinë e Albanideve lindore (nen shembullin e rajonit Martanesh-Çermenikë-Klenjë). *Përmbledhje Studimesh. Nr 2.*

Shallo M, Melo V, Xhafa Z, Yzeiri D, Xhomo A, Vranai A, Gjata Th, Kodra A, Sulstarova E, Aliaj Sh, Bushati S, Langora Ll, Lubonja L, Veizi V, Dema Sh. 1985. Harta Tektonike e Shqiperisë në shkallë 1:200.000. Shtypur në Afrikën e Jugut, Riparë nga Xhomo A., Kodra A., Gjata K., Xhafa Z. (1999).

Shehu R, Shallo M, Kodra A, Vranaj A, Gjata K, Gjata Th, Melo V, Yzeiri D, Bakiaj H, Xhomo A, Aliaj Sh, Pirdeni A, Pashko P. 1983. Harta Gjeologjike e R.P.S. të Shqipërise në shkallë 1: 200 000. Shtypur Ndërmarrja e Mjeteve Mësimore, Kulturore dhe Sportive "Hamid Shijaku" Tiranë.

Shehu R, Shallo M, Kodra A, Vranaj A, Gjata K, Gjata Th, Melo V, Yzeiri D, Bakiaj H, Xhomo A, Aliaj Sh, Pirdeni A, Pashko P. 1990. Gjeologjia e Shqipërisë. Teksti sqarues i Hartës Gjeologjike të Shqipërisë në shkallë 1: 200 000. Shtëpia botuese "8 Nëntori", f. 306**.**

Qirinxhi A, Nasi V, Hyseni A, Kokobobo A, Leci V. 1991. Vështrim mbi marrëdhëniet reciproke të zonave tektonike dhe karakteristikat kryesore të ndërtimit të brendshëm të tyre. *Buletini i Shkencave. Gjeologjike*. **1**: 129-137.

Xhomo A. Qirici V, Kodra B, Pashko P, Meço S. 1991. Stili tektonik mbulesor i zonës së Korabit. *Buletini i Shkencave Gjeologjike. 1, 25-42.*

Xhomo A, Kodra A, Gjata K. 2002a. Vendi i gjenezës së ofioliteve të Shqipërisë është baseni oqeanik Mirdita dhe jo baseni Krasta-Cukali (= Pindi). *Buletini i Shkencave Gjeologjike.* **1**, 25 – 42.

Xhomo A, Kodra A, Xhafa Z, Shallo M. 2002b. Monografia: "Gjeologjia e Shqipërisë". *Botim i Sherbimit Gjeologjik Shqiptar Tirane, f. 464.*

Xhomo A, Kodra A, Xhafa Z, Shallo M. 2005. Harta gjeologjike e Shqipërisë në shkallë 1 : 200 000. *Shtëpia botuese Hubber Kartografie, Munih.*

Zuber S. 1938. Carta tettonica dell' Albania 1:400.000. Roma, 1938.

Zuber S. 1940. Appunti sulla tettonica e sull'evoluzione geologica dei giacimenti metalliferi albanesi. *A.I.P.A. Publicazioni scientiffico-tettoniche, fascicolo 1, 63.*

A STATISTICAL ANALYSIS ON THE AFTERSHOCK SEQUENCE FOR JULY 3rd, 2017, BORDER REGION OF MACEDONIA-ALBANIA (M_L=5.0) EARTHQUAKE: AFTERSHOCK PROBABILITY EVALUATION

Rrapo ORMENI
Institute of Geosciences, Energy, Water and Environment, Polytechnic University of Tirana, Albania
Serkan ÖZTÜRK
Gümüşhane University, Department of Geophysics, 29100, Gümüşhane, Turkey

---

ABSTRACT

The aftershock probability method is a powerful way to evaluate the aftershock behaviors in the mainshock-aftershock occurrences and it should be taken into consideration as a significant part of the mainshock-aftershock pattern. There are different physical and statistical processes for the evaluation of aftershock sequences following the mainshock occurrences. In the present paper, the aftershock activity of July 3, 2017 earthquake (M_L5.0) which occurred in the border region of Macedonia-Albania, 14 km of NE of Lin (Albania) and 6 km NW of Jankovec (Macedonia), was statistically analyzed to define the characteristics of aftershock parameters. Aftershock sequence has a time period of 53 days and aftershock catalog is homogenous for local magnitude, M_L. We used 192 aftershocks with local magnitude $M_L \geq 1.9$ for the time interval between July 3, 2017 and August 25, 2017. For the aftershock sequence, magnitude completeness Mc-value was calculated as 2.0 for examples of 10 events/ window by using a moving window approach. Magnitude and time assessments of aftershock distribution show that statistical properties of aftershock sequence may provide some significant scores on the aftershock probability evaluation and earthquake hazard in this part of Macedonia-Albania border region. We used two main aftershock parameters for the probability evaluation and the combination of Gutenberg-Richter and modified Omori laws were utilized. The present paper aims at forecasting the number of strong or large aftershocks that follow the mainshock and calculating the probability of specific magnitude levels of aftershocks. Gutenberg-Richter b-value was calculated as 0.82±0.07 with Mc=2.0 by using maximum likelihood method. The elapse time since mainshock was considered as 0.0201 day, and considering the aftershocks with $M_L \geq Mc=2.0$, temporal decay rate parameters in the modified Omori law were calculated as p=1.22±0.12,

c=0.592±0.285 and K=59.87±19.91 by using the maximum likelihood procedure. The b-value is lower than 1.0 and this small value may indicate a larger stress distribution to build up over time and to be released by future earthquakes. Also, the estimated large p-value shows a fast decay rate of the aftershock activity. Probability for the maximum aftershock magnitude of 4.2 is estimated as 96.94 % and the expected numbers of aftershocks for magnitude size of 3.0 was calculated as about 24. As a remarkable fact, aftershock probability evaluation may support a contribution for disaster prevention measurements in this border region of Macedonia and Albania.
***Keywords*:** Macedonia-Albania, aftershock, probability, modified Omori, Gutenberg-Richter

1. INTRODUCTION

The border region of Macedonia and Albania was struck on July 3, 2017 by a moderate earthquake (M_L=5.0), 14 km northeast of Lin (Albania) and 6 km northwest of Jankovec (Macedonia). The epicenter coordinates were given as 41.15^{o}N and 20.96^{o}E, which is being felt in Macedonia and in south and central Albania. Some strong and large earthquakes in and around this part of Macedonia and Albania border region occurred in last century and these earthquakes were resulted in human victims and enormous material loss (Aliaj *et al*, 2010). Earthquakes are the norm in this part of the world as the African Plate moves northward towards Europe by 4-10 mm annually, with regular earthquakes occurring alongside the Eurasia-Africa plate boundary, mainly in Turkey, Greece, Sicily and Italy (Aliaj *et al*, 2001; 2010). An effective evaluation of aftershock hazard would be necessary for the minimization of the human loss, property damage, and social and economic disruption due to earthquakes. Consequently, detailed analyses of aftershock sequences involving a statistical evaluation on the aftershock sequence of July 3, 2017 Macedonia-Albania border region earthquake has been made to provide the necessary results for the next earthquake hazard. The aftershock probability evaluation method is one of the most effective methods to analyze the aftershock sequences. Earthquakes are generally followed by aftershocks and aftershock probability evaluation can be used as a supplementary part of earthquake hazard studies. Many researchers used different statistical and physical models for different aftershock sequences and several important results were obtained (Sulstarova 1983; 1995; Muco 1986; 1993; Guo and Ogata 1997; Wiemer and Katsumata 1999; Ogata 2001; Bayrak and Öztürk 2004; Kociaj 2005; Öztürk *et al*., 2008; Öztürk and Bayrak 2009; Enescu *et al*., 2011; Ormeni *et al.*, 2011; Chan and Wu, 2013; Nemati 2014; Ávila-Barrientos *et al*., 2015; Ormeni *et al*., 2017; Wei-Jin and Jian 2017; Ansari 2017). An evaluation of aftershock probability refers to statistically expressing and appraising the frequency that an aftershock with a specific magnitude will occur. The modified Omori model (Utsu, 1961) forecasts the

number of aftershocks that will occur. However, it is necessary to combine this model with the Gutenberg-Richter (Gutenberg-Richter, 1944) formula to provide a probability evaluation of aftershock occurrences. Probability of one or more aftershocks by statistical processing in the mainshock-aftershock pattern can be defined based on the combination of Gutenberg-Richter and modified Omori laws. These types of combined processes for aftershock hazard evaluations estimates not only of the probability of the aftershocks occurrence, but also the number of forecasted aftershocks. After the occurrences of strong or large mainshocks, a number of aftershocks may be triggered in a short period, and additional cumulative damage to structures may be caused by large aftershocks. Strong aftershocks may be dangerous because they are generally not predictable, and they can have a potential to cause extensive structural damage. The structure which is already damaged from the mainshock and is not yet repaired may be collapsed or become completely unusable under mainshock-aftershock seismic pattern. This characteristic is quite significant, and the importance of aftershock sequences cannot be ignored. Therefore, hazard estimation based on the aftershock probability has a great importance and urgency to investigate the influence of as recorded mainshock-aftershock seismic sequences on the dynamic response and accumulated damage of structures (Zhang *et al*., 2013). Consequently, the principally this study aims to provide a probability evaluation on the aftershock occurrence based on the combination of Gutenberg-Richter and modified Omori formulae. We estimated the number of the large aftershocks that might follow the mainshock and achieved an aftershock probability assessment so that a randomly chosen event is larger than or equal to a certain magnitude of aftershock. In this context, we applied an application of aftershock probability evaluation methods to aftershock sequence of July 3, 2017 earthquake (M_L=5.0), which occurred in the border region of Macedonia-Albania.

2. Aftershock data

This study focuses on the aftershock sequence of July 3, 2017 earthquake in the border region of Macedonia-Albania for a detailed evaluation of aftershock probability. The aftershock sequence used in this work were provided by the Albanian, Macedonian and Montenegro seismological stations and by the MEDNET, and AUTH networks. A homogenous and complete data of aftershock catalog was supplied for the mainshock with local magnitude M_L=5.0, occurred at 41.15^{o}N and 20.96^{o}E, and at 11:18:20.1 UTC on July 3, 2017. The aftershock sequence of the mainshock contained about a time period of two months, i.e., from the time of the mainshock (July 3, 2017) until August 25, 2017. The aftershock catalog consists of a total of 192 aftershocks with magnitude $M_L \geq 1.9$ in a time interval of 53 days. The

epicenter distribution of aftershock data is in the map of the figure 1 illustrated, and the cumulative number of aftershocks in about a time period of two months is in Graph 1 plotted.

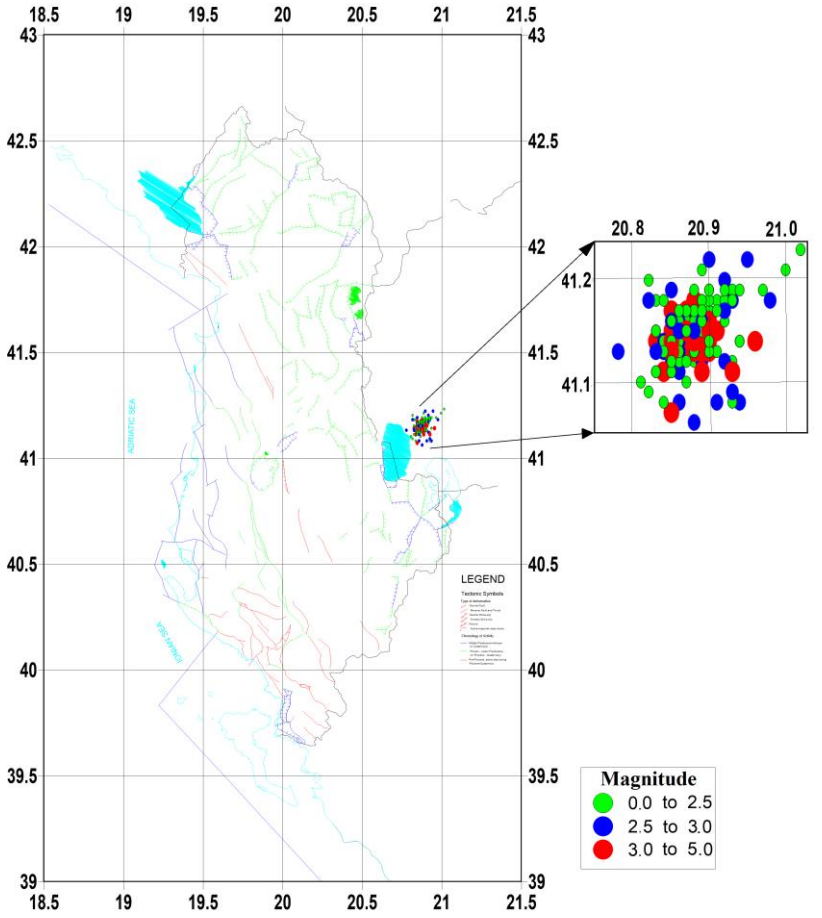

Fig. 1: Seismotectonic map of Albania (Aliaj, 2001), and epicentral distribution of aftershock data of July 3, 2017 earthquake in the border region of Macedonia- Albania. Different color and symbols were used for the data from small to large magnitude levels.

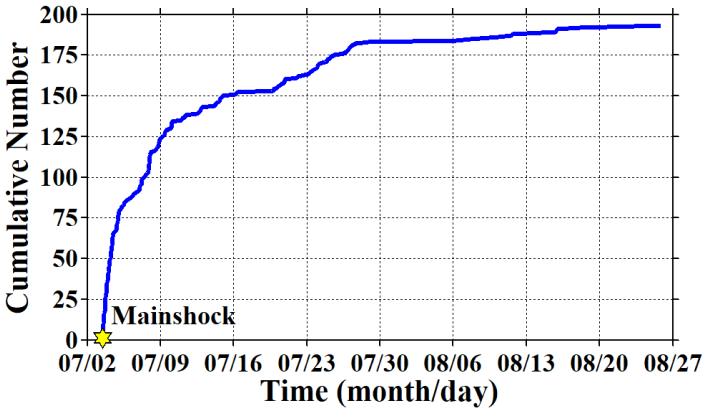

Graph.1: Cumulative number of aftershocks 53 days after the mainshock of July 3, 2017.

3. Brief description of the methods and probability of aftershocks

A number of statistical models have been used to explain the seismic behaviors of earthquakes in space-time-magnitude. There is a significant increase in the modelling of aftershock data in recent years since they occur in a short time period and in a specific region and hence they provide an understanding of source properties of strong or large earthquakes. There are two basic approaches to model the aftershock occurrences: Gutenberg-Richter (G-R) and modified Omori (MO) laws. G-R relation defines the relationship between the frequency of occurrence and magnitude of aftershocks, and MO model defines the occurrence rate of aftershock sequence as a function of time.

The relationship between the magnitude and frequency of occurrence of aftershock sequences can be given as in the following empirical equation:

$$\log_{10} N(M) = a - bM \qquad (1)$$

where $N(M)$ is the cumulative number of aftershocks with magnitudes larger than or equal to M, b-value defines the slope of the frequency-magnitude distribution of aftershocks, and a-value is proportional to the activity level of aftershocks. b-value is one of the most important parameter in earthquake statistics. Utsu (1971) summarized that b-values change roughly in the range 0.3 to 2.0, depending on the different region. Frohlich and Davis (1993) stated that the regional changes of average in an aftershock b-value is accepted as equal to 1.0.

The occurrence rate of aftershock sequence as a function of time can be empirically defined by the modified Omori law (Utsu, 1961) as in the following power law:

$$n(t) = \frac{K}{(t+c)^p} \qquad (2)$$

where *n(t)* is the number of aftershocks per unit time at time *t* after the mainshock. *K*, *c*, and *p*-values are constants. *K*-value depends on the total number of aftershocks in the sequence, *c*-value on the rate of activity in the earliest part of the sequences. There is an opinion that the *c*-value varies from 0.02 to 0.5 and all the reported positive *c*-values result from incompleteness (Hirata, 1969). Of these three parameters, *p*-value is a decay parameter and also the most important one, which varies between 0.6-1.8 (Wiemer and Katsumata, 1999).

It is well known that the number of aftershocks decreases exponentially as the magnitude of aftershocks increases. Expected number of aftershocks $N(T_1, T_2)$ larger than magnitude M during the time from T_1 (beginning time) to T_2 (ending time) is estimated as in the following:

$$N(T_1,T_2) = \int_{T_1}^{T_2} \Lambda(M,s)ds = K\,exp\{-\beta(M-M_{th})\}A(T_1,T_2) \qquad (3)$$

where, K is a parameter from MO formula; b is a parameter of G-R formula and M_{th} is the magnitude of the smallest earthquake (Ogata, 1983). $A(T_1, T_2)$ is given as follow:

$$A(T_1,T_2) = \begin{cases} \dfrac{(T_2+c)^{1-p} - (T_1+c)^{1-p}}{1-p} & (p \neq 1) \\ \ln(T_2+c) - \ln(T_1+c) & (p = 1) \end{cases} \qquad (4)$$

Here, c and p-values are constants from MO law. The probability Q for one or more aftershocks with magnitude M or greater occurring since the mainshock, from the time T_1 to T_2 is calculated by Equations 5 and 6 (e.g., Reasenberg and Jones, 1989):

$$Q = 1 - \exp\left\{-\int_{T_1}^{T_2} \Lambda(M,s)ds\right\} = 1 - \exp\{-N(T_1,T_2)\} \qquad (5)$$

$$Q = \begin{cases} 1 - \exp\left[\dfrac{-Ke^{-\beta(M-M_{th})}}{1-p} \left\{ \dfrac{1}{(T_2+c)^{p-1}} - \dfrac{1}{(T_1+c)^{p-1}} \right\} \right] & (p \neq 1) \\ 1 - \exp\left[-Ke^{-\beta(M-M_{th})} \{ \ln(T_2+c) - \ln(T_1+c) \} \right] & (p = 1) \end{cases} \qquad (6)$$

In these formulations, *p*-value describes the extent of time damping; *c*-value compensates for complex aspects immediately after the main event and *K*-value is approximately proportional to the total number of aftershocks. The β-value represents the relationship of *b* and $\beta = b\ln 10 = 2.30b$ in the G-R formula and it is closely related to the number of small aftershocks/that of large aftershocks ratio. Large β-value indicates relatively small number in large earthquakes. M_{th} is the magnitude of the smallest aftershock processed using the MO or the G-R formulas. It is premised that all aftershocks greater than M_{th} are observed without omissions. T_1 and T_2 represent the beginning and the end of the period during the aftershock probability, respectively. This time interval is evaluated, and both represent elapsed time following the mainshock. It must be kept in mind that Equation 6 does not represent the probability of an aftershock that matches conditions occurring exactly once; it represents the probability of it occurring more than one time.

4. Results and discussions on the estimated aftershock parameters

For the high-quality results in the estimation of the aftershock parameters, it is very important to have a completed data set for all magnitude bands. Analysis of completeness magnitude, *Mc*, is based on the assumption of G-R power-law distribution against magnitude. Completeness magnitude varies systematically in space and time, and particularly the time variations of *Mc*-value after the mainshock can produce erroneous *b* and *p*-value estimations (Wiemer and Katsumata 1999). *Mc*-value can be larger in the early part of the aftershock sequence since the small shocks fall within the coda of larger events. Thus, small shocks may not be located (Bayrak and Öztürk 2004; Ormeni and Öztürk 2017). The estimation of *Mc*-value is a very significant stage for all seismicity-based studies since the usage of the maximum number of aftershocks is necessary for reliable results. The changes in *Mc*-value as a function of time for the aftershock sequence of July 3, 2017 Macedonia-Albania border region earthquake is in Graph 3 plotted. We used a moving time window approach and started at the origin time of the mainshock. *Mc*-value is estimated for samples of 10 events/window. *Mc*-value is relatively

highest and around 3.0 at the beginning time of the sequences (in the first ten hours). Then, it decreases to about 2.1 between 5 and 10 days after the mainshock. However, it decreases again to about 3.0 within ten days from the mainshock. We can easily see from the Graph 3 that *Mc*-value varies between 1.9 and 2.2 ten days after the mainshock. Therefore, we can say that *Mc*-value generally shows a non-stable value in the aftershock sequence. During the period of 53 days, 192 aftershocks were used for July 3, 2017 earthquake. In order to understand how much the *Mc*-value changes according to the sample size, we tried the different sample sizes such as 35, 45, and 75 events/window. We saw that the selection of the sample size does not change the results. Thus, the fluctuations in completeness seen in Graph 2 does not depend on the small sample size.

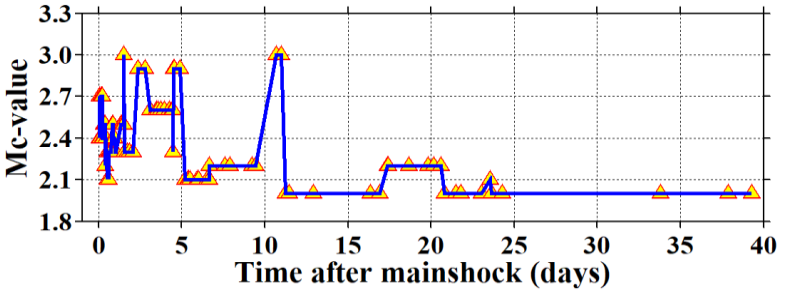

Graph. 2: Completeness magnitude, *Mc*-value, as a function of time for the aftershock sequence of July 3, 2017 Macedonia-Albania border region earthquake. *Mc*-value is estimated for overlapping time windows, including 10 events.

Graph 3 plots the magnitude changes in the time period about two months (53 days) after the mainshock time for July 3, 2017 Macedonia-Albania aftershock sequence. It can be clearly seen from Graph 3 that the greatest aftershock with M_L=4.2 occurred in the five days after the mainshock. However, the occurrences of the aftershocks larger than M_L=3.0 come to an end in 25 days after the mainshock occurrence. There is also a number of aftershocks which magnitudes varies from 3.5 to 4.0 in the first ten days after the mainshock. There is a decreasing trend in the number of aftershocks with magnitude M_L=3.0 after the first 10 days from the mainshock time. Consequently, an average value of magnitude size is densely recorded between 2.0 and 3.0. Graph 4 and 5 show the magnitude histogram and time histogram of the aftershock sequence, respectively. Magnitude level of the aftershock data varies from 1.9 to 4.2, and there is a decrease in the number of aftershocks from the smaller to higher magnitude levels. As seen in Graph 4, the magnitude of the many aftershocks changes between 2.0 to 3.0 and there are some maximums between 2.1 and 2.7. There are 149 aftershocks with

$2.0 \leq M_L < 3.0$. However, the number of aftershocks with $3.0 \leq M_L < 4.0$ is 38, and there are 5 aftershocks with $4.0 \leq M_L$. As a result, the aftershock occurrences with magnitudes $2.0 \leq M_L < 3.0$ are more dominant in the aftershock region. Time histogram of aftershock sequence is also given in Graph 5. The aftershock activity is densely distributed in five days and the number of aftershocks in these days is about 140. There is also an increase in the number of aftershocks between the time interval 15 and 25 days. A stableness can be clearly seen after the first month, and the average number of aftershocks after the first month is less than 5. Thus, these types of evaluations can provide a useful perspective for the description of statistical behaviors of aftershocks which is associated with the aftershock probability evaluation and earthquake hazard in this aftershock region of Macedonia-Albania border region.

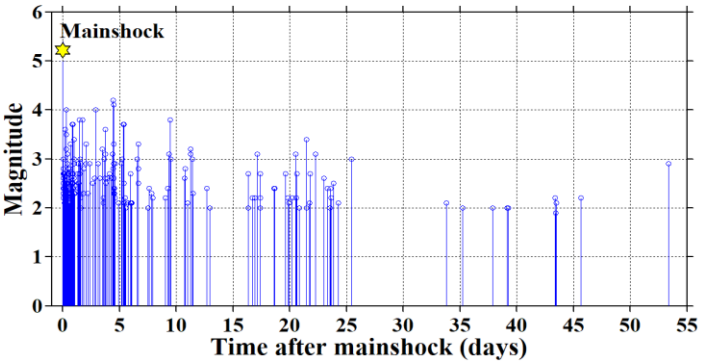

Graph. 3. Changes in magnitude levels during 53 days after the mainshock time for the aftershock sequence of July 3, 2017 mainshock.

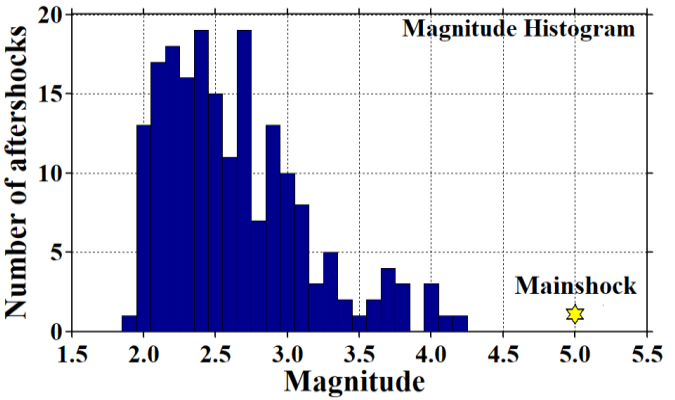

Graph. 4: Magnitude histogram of the aftershock sequence of July 3, 2017 mainshock.

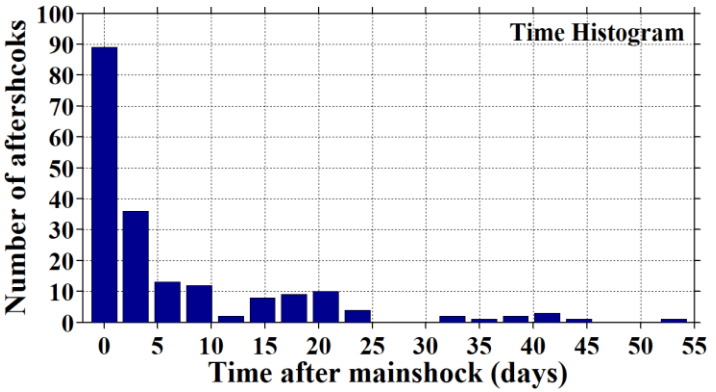

Graph. 5: Time histogram of the aftershock sequence of July 3, 2017 mainshock.

The real implementation of the techniques on aftershock probability evaluation is based on the statistical methods and covers the problem of detecting whether it is possible the exact estimation of the parameters (*K*, *c*, *p*, *b*) for aftershock sequence immediately following a mainshock. If the average values of the aftershock parameters are known, there is a probability that these parameters can be utilized effectively as a preliminary result until the real data is available. For this reason, certain parameters for the aftershock probability evaluation model are compared with the combining of G-R and the MO formulas, and their application range is evaluated. The plot of magnitude-frequency distribution of the aftershocks for July 3, 2017 earthquake is in Graph 6 given. *Mc*-value was calculated as 2.0 for aftershock sequence. The *b*-value and its standard deviation was computed using this *Mc*-value with maximum likelihood method, and *b*-value is estimated as 0.82±0.07. As stated in Frohlich and Davis (1993), this *b*-value is smaller than average value of *b*=1.0 and the smaller *b*-values may be related to the low heterogeneity degree of medium, the higher stress concentration and high strain in this region after the mainshock time. Temporal decay rate of aftershock sequence is in Graph 7 plotted. The *p*, *c* and *K*-values were estimated by using the maximum likelihood method and the occurrence rate was modeled by MO formula. *p*=1.22±0.12, relatively larger, was calculated for aftershock sequence considering minimum magnitude *Mmin*=2.0, T_1=0.0201. The *c*-value was calculated as 0.592±0.285 and *K*-value was calculated as 59.87±19.91. This high *p*-value suggests that aftershock activity after the mainshock shows a fast decay rate as shown also in Graph 1.

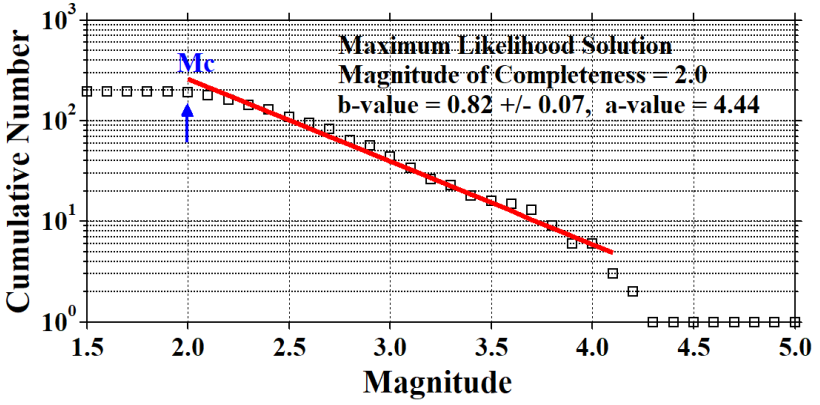

Graph. 6: Gutenberg-Richter relation for aftershocks of July 3, 2017 earthquake. The *b*-value and its standard deviation as well as the *a*-value are given.

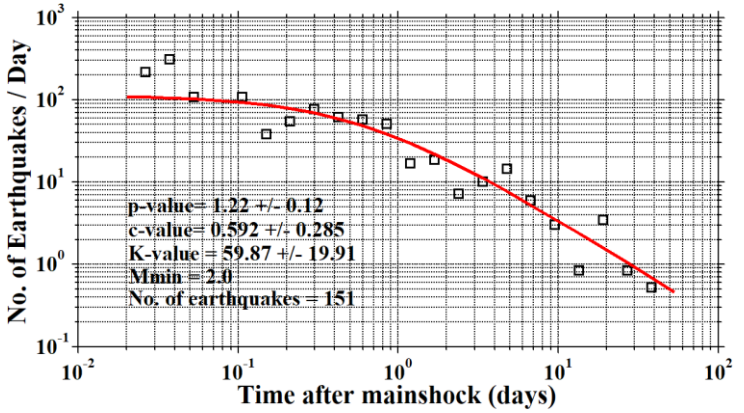

Graph. 7: Aftershock decay rate (per day) in time after mainshock of July 3, 2017 earthquake. *p*, *c* and *K*-values in the modified Omori formula, the minimum magnitude and the number of aftershock used in the estimation are given.

Graph 8 plots the probability of aftershock occurrences against magnitude after the mainshock. Graph 9 plots the expected number of aftershocks versus magnitude after the mainshock. All calculations were considered at the beginning and ending time periods of the aftershock sequence as seen in Equations 4 and 6. The probability of the largest aftershock occurrence for magnitude size of 4.2 was calculated as 96.94 % (Graph 8). The magnitude of randomly chosen aftershock was taken as M_L=3.0 and the estimated number aftershocks for this magnitude level is in Graph 9 plotted. The maximum estimated number of aftershocks for magnitude level of 3.0 was computed

approximately 24. For the estimation of *b*-value in G-R relationship maximum likelihood method is preferred because it yields a more robust estimate than least-square regression technique (Aki, 1965). Decay rate parameters in modified OM formula for aftershock data can be estimated correctly by the maximum likelihood method, assuming that aftershock activity follows a non-stationary Poisson process (Ogata, 1983). Some details for the earthquake occurrence of July 3, 2017 are in Table 1 reported. The maximum (Ma_{max}) and minimum (Ma_{min}) magnitudes of aftershock sequence are also given. The number of aftershocks (N), magnitude completeness (Mc), beginning (T_1) and ending (T_2) times for the sequence, b, K, p, and c-values for the aftershock sequence are in Table 2 reported.

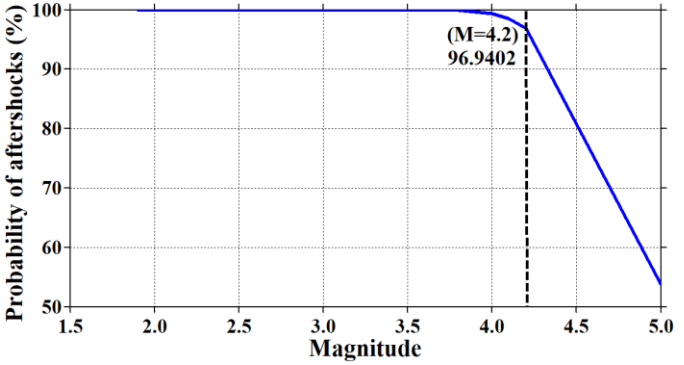

Graph. 8. Probability of aftershocks for one or more events. Estimation is carried out by using the beginning and ending times of the aftershock sequence.

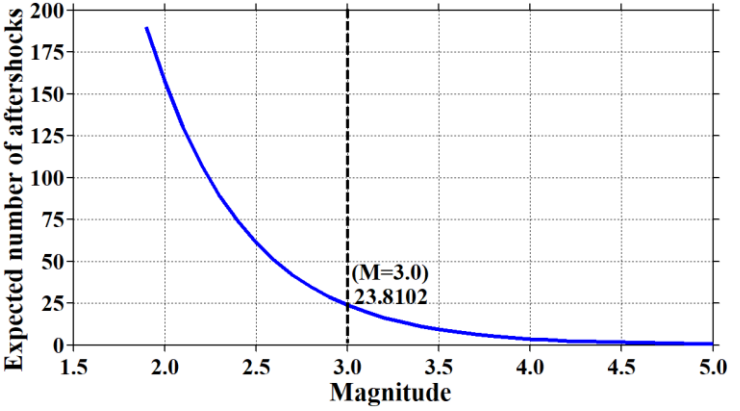

Graph. 9. The expected number of aftershocks for one or more events. Estimation is carried out by using the beginning and ending times of the aftershock sequence.

Table 1. Properties of the Macedonia-Albania border region earthquake

Year	Month	Day	Origin Time (GMT/UTC)	Longitude	Latitude	Depth (km)	(M_L)	Ma_{max}	Ma_{min}
2017	07	03	11:18:20.1	20.96	41.15	5.0	5.0	4.2	1.9

Table 2. Aftershock parameters and statistics used in the probability evaluation

Earthquake	*N*	T_1 (day)	T_2 (day)	*Mc*	*b*-value	*K*-value	*c*-value	*p*-value
July 3, 2017	192	0.0201	53.386	2.0	0.82±0.07	59.87±19.91	0.592±0.285	1.22±0.12

5. CONCLUSIONS

The aftershock probability method has been applied for the statistical evaluation of the aftershock sequence of July 3rd, 2017 border region of Macedonia-Albania earthquake. Aftershock dataset was homogenous for local magnitude, M_L, and covered about 53 day-time period. The catalog included 192 aftershocks with magnitude M_L equal to or larger than 1.9. *Mc*-value is calculated as 2.0 for samples of 10 events/window by using a moving window approach and starting at the origin time of the mainshock. Statistical time-magnitude analyses of the aftershock sequence show that time-magnitude behaviors of aftershock sequence can supply some significant information on the aftershock probability evaluation and aftershock hazard. For this reason, aftershock probability should be accepted as one evaluation method and aftershock hazard must be used as a complementary part of earthquake hazard studies. In this study, a combined model for aftershock probability evaluation based on the combination of Gutenberg-Richter and modified Omori formulas has been used to estimate the number of the large aftershocks following the mainshock and evaluate aftershock possibility that a randomly chosen aftershock is greater than or equal to a certain magnitude of aftershock. *b*-value for aftershock sequence was calculated as 0.82±0.07 by using the events with *Mc*=2.0. This small *b*-value may be resulted from low heterogeneity degree of medium, the higher stress distribution and high strain in this earthquake region after the mainshock time. Aftershock decay parameters

were calculated as p=1.22±0.12, c=0.592±0.285 and K=59.87±19.91 by fitting the data Mc≥2.0. This relatively large p-value shows that aftershock activity from the mainshock time has a fast decay rate. The magnitude of aftershock was randomly chosen, and we selected M_L=3.0 for the estimation of expected number of aftershocks. Also, the largest aftershock M_L=4.2 was used to calculate the probability. Probability for magnitude level of the largest aftershock with M_L=4.2 was estimated as 96.94 % and the expected numbers of aftershocks for magnitude size of 3.0 was computed as 24. Consequently, these types of analyses are necessary for disaster protection studies and a reliable evaluation of earthquake hazard in Macedonia-Albania border region.

REFERENCES

Aki K. 1965. Maximum likelihood estimate of *b* in the formula $\log N = a - bM$ and its confidence limits. *Bulletin of Earthquake Research Institute*., *Tokyo University*. **43**; 237-239.

Aliaj Sh, Sulstarova E, Muço B, Koçiu S. 2001. Seismotectonic map of Albania, scale 1:500.000. *Instituti i Sizmologjisë Tiranë.*

Aliaj Sh, Koçiu S, Muço B, Sulstarova E. 2010. Seismicity, seismotectonic and seismic hazard assessment in Albania. *Published by Academy of Science of Albania.*

Ansari S. 2017. Aftershocks properties of the 2013 Shonbe Mw 6.3 earthquake, central Zagros, Iran. *Journal of Asian Earth Sciences.* **147**; 17–27.

Ávila-Barrientos L, Zúñiga FR, Rodríguez-Perez Q, Guzmán-Speziale M. 2015. Variation of b and p values from aftershocks sequences along the Mexican subduction zone and their relation to plate characteristics. *Journal of South American Earth Sciences.* **63**; 162-171.

Bayrak Y, Öztürk S. 2004. Spatial and temporal variations of the aftershock sequences of the 1999 İzmit and Düzce earthquakes. *Earth Planets and Space.* **56**(**10**); 933-944.

Chung-Han C, Yih-Min W. 2013. Maximum magnitudes in aftershock sequences in Taiwan. *Journal of Asian Earth Sciences.* **73**; 409-418.

Enescu B, Enescu D, Ito K. 2011. Values of b and p: Their variations and relation to physical processes for earthquakes in Japan and Romania. *Romanian Journal of Physics*. **56** (**3-4**); 590–608.

Frohlich C, Davis S. 1993. Teleseismic *b*-values: Or, much ado about 1.0". *Journal of Geophysical Research*. **98**(**B1**); 631-644.

Guo Z, Ogata Y. 1997. Statistical relations between the parameters of aftershocks in time, space, and magnitude. Journal of Geophysical Research, **102**(**B2**); 2857-2873.

Gutenberg R, Richter CF. 1944. Frequency of earthquakes in California. *Bulletin of Seismological Society of America,* **34**; 185-188.

Hirata T. 1969. Aftershock sequence of the earthquake off Shikotan Island on January 29, 1968. Geophys. *Bulletin-Hokkaido University.* **21**; 33-43.

Koçiu S. 2005, Recent seismic activity in Albania and its features. Martinelli, G and Panahi, B. (eds.). Mud Volcanoes, Geodynamics and Seismicity, NATO Sciece Series, series IV: *Earth and Environmental Sciences, Springer, The Netherlands*, 2005, 123-133.

Muço B. 1986. Tërmetet e serisë së Nikaj-Mërturit dhe karakteristikat e tyre (Nikaj-Merturi earthquake series and their characteristics). v. *Studime Sizmologjike (Journal of Seismological studies)*. 137-155.

Muço B. 1993. On the decay of aftershocks in Albania: *The second Congress of Geophysics of Greece.*

Nemati M. 2014. An appraisal of aftershocks behavior for large earthquakes in Persia. *Journal of Asian Earth Sciences.* **79**; 432–440.

Ogata Y. 1983. Estimation of the parameters in the modified Omori formula for aftershock frequencies by the maximum likelihood procedure. *Journal of Physics of the Earth*., **31**; 115-124.

Ogata Y. 2001. Increased probability of large earthquakes near aftershock regions with relative quiescence. *Journal of Geophysical Research*., **106**; 8729-8744.

Ormeni Rr, Öztürk S. 2017. "Aftershock analysis of October 15, 2016, Greece-Albania border region, Rodotopion-Earthquake based on the Gutenberg-Richter and modifird Omori lows" *International Conference on Applied Sciences and Engineering, FIFM, Polytechnic University of Tirana, Albania,* November 16-17,

Ormeni Rr, Öztürk S, Neritan Sh, Daja Sh. 2011. An application of the aftershock probability evaluation methods for recent Albania earthquakes based on Gutenberg-Richter and modıfied Omori models. *International Balkans Conference on Challenges of Civil Engineering*, BCCCE, 19-21 May 2011, EPOKA University, Tirana, Albania.

Öztürk S, Bayrak Y. 2009. Aftershock probability evaluation for recent Turkey earthquakes based on Gutenberg-Richter and Modified Omori Formulae. *5th Congress of Balkan Geophysical Society*, **6505**; 10-16 May, 2009, Belgrade, Serbia.

Öztürk S, Çınar H, Bayrak Y, Karslı H, Daniel G. 2008. Properties of Aftershock Sequence of the 2003 Bingöl, M_D=6.4, (Turkey) Earthquake. *Pure and Applied Geophysics*, **165**(**2**); 349-371.

Reasenberg PA, Jones LM. 1989. Earthquake hazard after a mainshock in California. *Science*, **243**; 1173-1176.

Sulstarova E. 1995. Some aspects of Albania seismicity: *VI Congress of the Carpatho-Balcan Geological Association*, pp 135-140.

Sulstarova E, Lubonja L. 1983. Karakteristikat e pasgoditjeve te termetit te 5 prillit 1979. Termeti i 15 prillit 1979, *Shtepia Botuese 8 Nentori*, pp. 92-120

Utsu T. 1961. A Statistical study on the occurrence of aftershocks. *The Geophysical Magazine*., **30**; 521-603, Tokyo, Japan.

Utsu T. 1971. Aftershock and earthquake statistic (III): Analyses of the distribution of earthquakes in magnitude, time and space with special consideration to clustering characteristics of earthquake occurrence (1). *Journal of the Faculty of Science., Hokkaido University*, Series VII (Geophys.), **3**; 379-441.

Wei-Jin X, Jian W. 2017. Effect of temporal-spatial clustering of aftershocks on the analysis of probabilistic seismic hazard. Chinese Journal of Geophysics-Chinese Edition, **60** (**8**); 3110-3118.

Wiemer S, Katsumata K. 1999. Spatial variability of seismicity parameters in aftershock zones. *Journal of Geophysical Research.*, **104**(**B6**); 13135–13151.

Zhang S, Wang G, Sa W. 2013. Damage evaluation of concrete gravity dams under mainshock–aftershock seismic sequences. Soil Dynamics and Earthquake Engineering, **50**; 16–27.

THE REACTIVATION OF A LARGE DEEP-SEATED OLD LANDSLIDE ALONG OF RRËSHEN-KUKËS MOTORWAY, ALBANIA: CAUSES, CONSEQUENCES, AND SLOPE STABILITY EVALUATION

Ylber MUCEKU
Institute of Geo-sciences, Energy, Water and Environment, Polytechnic University of Tirana, Albania
Ina GJINI, Skënder ÇOTA
Institute of Construction Consulting, Tirana, Albania

ABSTRACT

Morphological and geotechnical properties of soils and rocks and hazard of a reactivated old landslide, occurring in km 43+700- 43+800 of Milot-Kukës motorway have been recently investigated. It is a hilly area in the north-east of Albania consisting of very weak rocks and soils with low geotechnical properties. The causes and consequences of the reactivation of a large deep-seated old landslide are in the present paper investigated. Laboratory investigation and field works involving geological, geomorphological and geotechnical mapping, drillings and physical-mechanical tests of soils and rocks were made to address landslide formation slope stability analysis and the conclusions were drawn based on geotechnical to protect the buildings, motorway and road users.
Keywords: old landslide, landslide reactivation, soils, weak rocks, physical-mechanical properties, causes, consequences, slope stability evaluation, geotechnical conditions

1. INTRODUCTION

Geological and geomorphological data report Albania is considerably affected by mass movements (Muceku *et al*., 2002, Muceku *et al*., 2008, Muceku *et al*., 2014, Muceku *et al*., 2016). The causes and consequences of the reactivation of a large deep-seated old landslide along the Rrëshen-Kukës motorway in Albania is here investigated and the slope stability evaluated. Civil industry has intensely developed in the last two decades even in hilly and mountainous areas with severe consequences in many regions of the

country. The Rrëshen-Kukës motorway locates in northeast of Rrësheni, extending in the section km 43+700- 43+800 of Milot-Kukës motorway. The area is characterised by landslide events. Once inhabited, the Blinishti village does not exist anymore due to landslides. The area has a history of geotechnical investigation Muceku and colleagues (2018) were involved in detailed site investigation, including morphological, geological and geotechnical mapping, drillings and laboratory analysis. However, geotechnical investigation to protect the national road Rrëshen-Pukë and northern part of Blinisht village in 2005-2006, has been previously carried out (Muceku 2007). Geotechnical investigations were carried out for the construction of the Milot-Kukës motorway on 2006-08 on this area. Moreover, regular engineering geological observations addressed the damage of the village's buildings. The results proved that ground movement and structural damage has deteriorated in the last two decades. Finally, as a result of landslide occurrence on March 3, 2018, detailed morphological, geological and geotechnical studies were instigated once again by this partial reactivation of the old deep-seated landslide and were completed on this time, for protection of Milot-Kukës motorway by analysing the causes, consequences of landslides occurrence and slope stability evaluation of the studied area (Muceku *et. al*., 2018). In the end, recommendations for an effective management and the protective engineering measures for hazard mitigation based on landslide characteristics and susceptibility are here drawn.

2. MATERIALS AND METHODS

The area is located in the backslopes of Milot-Morinë highway, at the chainage from 43+6500 to 44+200, in the north of the upslope, from the toe of the highway to the Shpal village. The area as a long history of geotechnical investigation. So, the geotechnical investigation of March – May 2008 involving geological engineering mapping works at scale of 1: 5 000 and detailed field study for this zone including boreholes, test pits and observations on the exposed faces covered a wider area characterised by instability. Three-hole drillings, each 10 m deep, (Muceku 2007) have been made uphill, on the northern of the landslide (Shpal Village), to evaluate the occurring landslide through the same period. Several boreholes with an extension from 43.500 km to 43.80 km were bored at a depth of 10.0-15.0m between 2007 and 2008. Soils and rocks' samples were laboratory analyzed for the mitigation of instability and the risk induced to the highway by potential mass movements on the its north. Latter works in the area also involved geotechnical mapping, excavation works, and laboratory analysis (Muceku and Jaupaj 2018). The results obtained were a means to address the lithological profile and mass movement and rupture surface mapping, and

geotechnical conditions as well. The finite element software of Phase2-FEM (Rocscience, 2011) was used for the slope stability.

3. RESULTS AND DISCUSSIONS

Many field works, and laboratory tests have been carried out (Muceku 2006, Muceku *et al*., 2018) for the geological, morphological, hydrogeological, geotechnical slope stability characteristics. The data obtained are very important for the design specialists and institutions involved as they address the protective engineering measures against any possible hazard that threatens road security.

Geological Setting

Figure 1 depicts the zone investigated geologically rich in Quaternary deposits, mélanges formations-blocks in the matrix (Middle Jurassic-J_2) and volcanic formations (Middle Jurassic-J_2) ().

Quaternary deposits (Q_{p-h})

They are represented by diluvium deposits, which are composed of silts with a mixture of rubble-stones and sands. Generally, they could be met on hills' slopes and are from 1.0-1.8m to 3.0-5.0m thick.

Volcanic formations (Middle Jurassic-J_2)

Figure 1 depicts the volcanic formations located in southern and northern part of the area. These rocks are represented by dacite and rhyolite formations (Middle Jurassic, J_2) in the west and northwest and, andesite and basalts formations (Middle Jurassic, J_2) in the south. These formations are intensively fractured from tectonic phenomena and weathering process. Tectonically, the andesite and basalts formations overthrusts on the "block in matrix" formation. Whereas the dacite and rhyolite formations tectonically underlie to the "block in matrix" (Fig. 1).

Mélange-block in matrix (Middle Jurassic-J2)

This formation lies over the northern and southern slopes of the highway and has a tectonic contact with the surrounding formations. The formation with blocks in the matrix consists of clayey matrix, grey and green in colour. Here, different rock formations (limestone, magmatic, claystone and sandstone) are chaotically suspending. Diffractometer analyses of half quantity reported that the matrix consists of a mixture of clay chlorite - montmorillonite 15% with silt 15-20% and kaolinite 20-30%, in addition to quartz micro depressed 25% up to 35-40% and feldspar 510%. The fragments are mostly represented by arkose sandstone siliceous radiolarite and basalts of

volcano-sedimentary formations dating in the Middle Triassic - Lower Jurassic. Fragments of ophiolitic belt and limestones fragments could be sporadically met. Coarse grained sandstones are the prevailing components of this mélange.

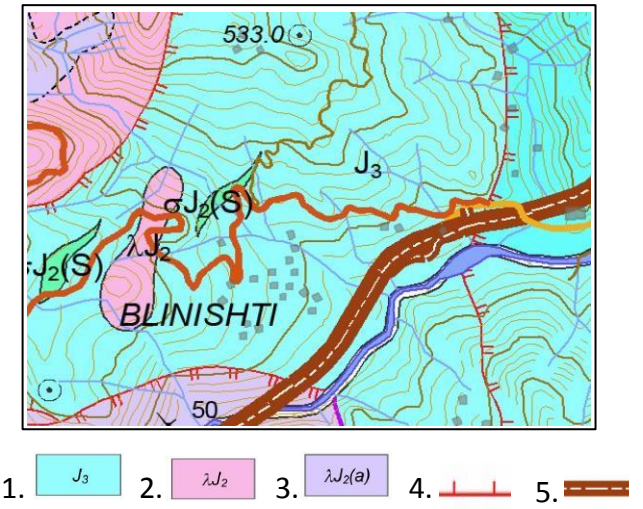

Fig. 1: Geological map of studied area .1. Mélanges formations-blocks in the matrix (Middle Jurassic, J_2), 2. Dacite and rhyolite formations (Middle Jurassic, J_2), 3. Andesite and basalts formations (Middle Jurassic, J_2), 4. Overthrust tectonic, 5. Milot-Kukes motorway.

Geomorphologic characteristics

Geomorphologic investigation was carried out in a hilly zone. The Fani River flows on its left. The altitude increases form southwest to northeast, from 400-700m at Gziqi zone to 600-780m at Shpali zone (Fig. 2). The seasonal waterways crossings have gradually eroded and amplified the fractures in the upper structure of the of the hills' formation. These streams are highly active during intensive rainfalls events (November – March).

The narrow and deep valleys, and the formed terraces show that the vertical elevation is typical of the region.

The region is also characterised by preexisting erosion on different scales due to diluvium layers and soft rocks which are highly susceptible to erosion and the Mediterranean climate stimulates erosion processes. The latter is the source for the conditional jointing of the slopes. In addition, the slope has been subject to mass movement phenomena. Both mass movement and erosion have caused local flat areas which are separated from each other by narrow and deep stream valleys. Generally, the natural hill slope angle ranges from 11° to 22°—becoming locally steeper (Fig. 3).

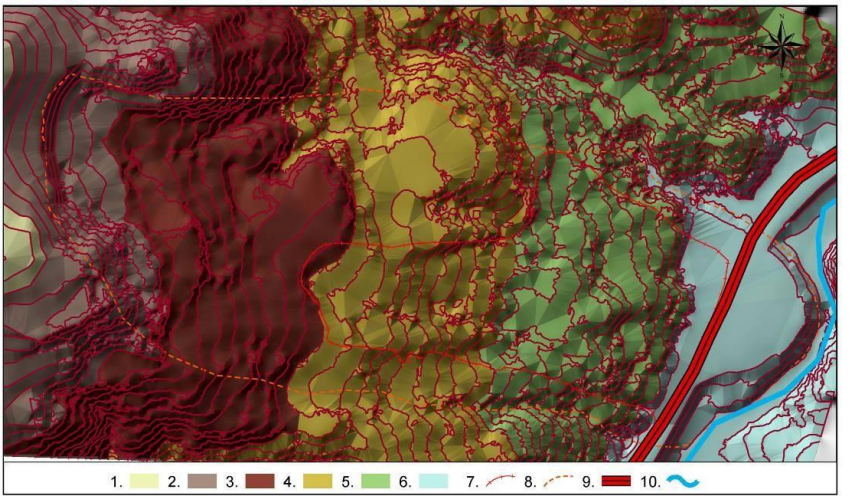

Fig. 2: Geomorphological map of studied area. Hill's morphologic unit with altitude: 1. >450m, 2. 400-450m, 3. 350-400m, 4. 300-350m, 5. 250-300m, 6. 225-250m, 7. Reactivated landslide, 8. Old landslide. 9. Highway, 10. Fani River

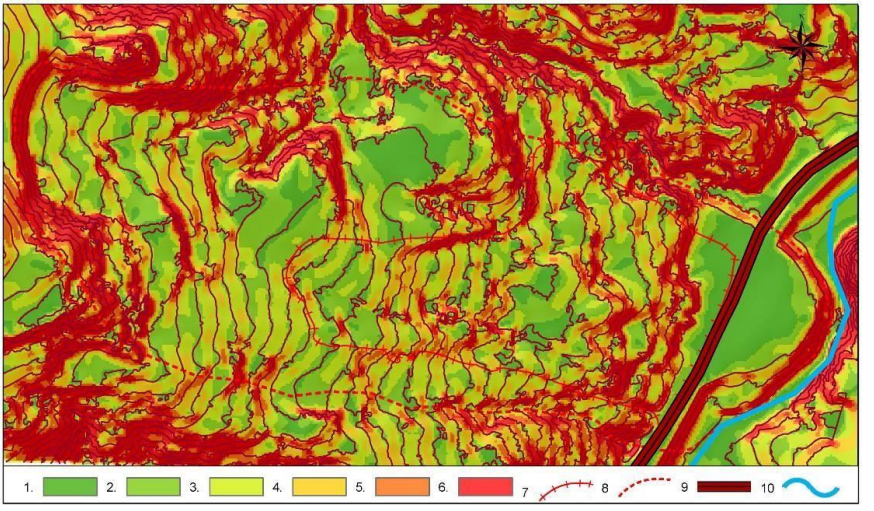

Fig. 3: Slope angle map of studied area. 1. Flat area with 0-5^{o}, 2. Hill slope with angle 6-10^{o}, 3. Hill slope with angle 11-15^{o}, 4. Hill slope with angle 16-20^{o}, 5. Hill slope with angle 21-25^{o}, 6. Hill slope with angle > 25^{o}, 7. Reactivated landslide, 8. Old landslide. 9. Highway, 10. Fani River.

Hydrogeological Characteristics

The slope affected by the landslide, in hydrogeological aspect is composed of intensively fractioned by tectonic activity formations. Consequently, based on tectonic activity, the rock formation "blocks in matrix" is characterized by

a dense broken pattern creating a quite rich aquifer fed by underground water. The latter, impacts significantly the slope modelling (landslide, erosion) and the vegetation of the area. Hydrogeologically, this formation is quite rich in underground water which flow at a depth of 0.50m - 0.7m, close to the ground surface and occasionally emerges in the form of springs. The zone is covered by unconsolidated Quaternary deposits (very low permeability coefficient soils), from 1.8-3.0m to 5.0-7.0m thick (Fig. 4-8). Nevertheless, the underground water is discharged through water springs due to the cracks network. The earlier landslides are the source for the cracks network. These springs flow through the hilly slope to the unconsolidated Quaternary deposits, and through the contact of these formations with the underlying bedrock on the stream valleys. Their discharge fluctuates from 0. 02 -0. 1 l/sec to 0.5 l/sec.

Mass movement

The zone has a long history of landslides events. The geotechnical data of 2005-2007 report that this area represents an old landslide which extends from Shpal village (upper slope) to Blinisht village (the middle of the slope), reaching downslope the Fani River. The landslide is 1280m long, approximately 280m wide and 5.0-7.0m to 12.0-15.0m supposedly thick (Fig. 4, 7, 8). Its surface area (247.43ha) and volume (5 217 047m^3), make it an extremely large landslide (Fell 1994). Muceku *et al*., (2018) said that anthropogenic activity over years and climatic conditions (rainfalls) have intensified a series of mass movement in the form of flows; 50.0-80.0m long, 35.0-60.0m wide and 5.0-8.0 deep, i.e., the slope likely losing its equilibrium at any moment. However, for the moment it is found in a critical stability. If the factors of stability degrade (morphometric degradations of slopes, confinement of underground water, misuse of surficial waters etc.), the slopes become destabilized and start moving downwards. The slopes stability has dramatically dropped due to the interventions on the skirts of the slopes (toe of old landslide) during 2007-2008 for the construction purposes. The largely degraded morphometric characteristics of the slope (inclined slope angle), underground water regime modifications and the surficial water regime disturbance (surficial drainage channels) have reduced slope stability to a critical level. The region is characterised by a highly wet climate (Themelko *et al*., 1996) and the annual precipitation ranges from 1600-1800mm to 2000mm. Intensive precipitations (50-80mm) of short time intervals (24h) are frequent. Given the geotechnical situation and the rainfalls (in large quantities) that increase the weight of the slope's overlaying soils, the reduction of their resistance forces would be unavoidable.

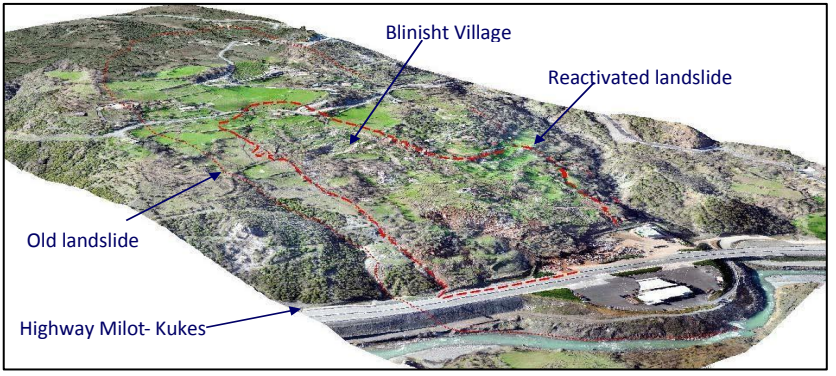

Fig. 4: It shows the reactivation of the old landslide along of Rreshen-Kukës motorway.

Once the resistance forces of soil are reduced, slope mass starts moving downwards. The landslide events of March 3, 2018 in the Blinisht village occurred due to mass movement. Studies (geologic-engineering mapping 1:500) reveal that mass movement is currently 580m long and from 150.0m (upslope) to 260.0m (downslope) wide (Fig. 4, 7, 8). The surface of the landslide is 12.54ha and volume 1128 573 m^3. Consequently, it could be considered a large landslide (Fell 1994). The Figure 4-8 depict the estimated depth of the main surface of rupture varying between 3.0-7.5m (upper and middle part of landslide) and 12.0-15.0m (downslope). The main body of the landslide is saturated from the underground water, which for the moment are confined into the slope due to the lack of drainage, hence significantly degrading the resistance parameters of the slope. This main body is comprised of mix of clayey soils, dust with fragments and blocks of limestone, volcanic rocks, sandstone and claystone, which are in critical stability state. The landslide is of translational type (Cruden *et al*., 1996) with rupture surface with an angle of 11-12^o. In addition to anthropogenic activity and climate, lithological and morphology factors affected mass movement as the area is represented by clayey rock formations (a very weak formation) and the prevailing slope angle is 15^o to 20^o.

Fig. 5: The landslide movement direction to Milot-Morinë highway.

Fig. 6. The picture showing the landslide damages in the Blinisht village.

Geotechnical Characteristics

Geotechnical data report three main geotechnical units with different physical-mechanical properties (Muceku and Lamaj 2005; 2009) as reported on table 1 and depicted in the Figure 7 and 8.

The geotechnical unit no. 1 consists of inorganic clays and silts (CL-ML) brown and grey in colour, medium consistency (ASTM, 2011) with gravels, pebbles and rock block content. It is from 1.5-3.0m to 12.0-15.0m thick. The current landslide body consists of these soils.

The geotechnical unit no. 2 is represented by inorganic clays and silts (CL-ML) brown and grey in colour, (ASTM, 2011) with gravels, pebbles and rock block content. These soils have stiff consistency and are generally from 1.0-2.5m to 7.0-10.0 m thick.

The geotechnical unit no. 3 consists of very weak rocks (Romana, 1996), rich in clayey matrix, grey and green in colour. Here, chaotically suspended different rock blocks (limestone, magmatic, claystone and sandstone) could be met.

Table 1: Physical and mechanical properties of soils and rocks

Unit no	γ (gr/cm^3)	E (kg/cm^2)	(υ)	φ (^{o})	c (kg/cm^2)	Soils/Rock Type
1	1.70-1.75	55.0-75.0	0.38-0.40	10-12	0.07-0.10	CL &ML
2	1.90-1.94	175-200.0	0.33-0.35	16-18	0.25-0.30	CL &ML
3	2.10	1650-1800	0.30	27-29	0.7-1.2	Me-R

γ-unit weight, E-young modulus, υ-Poisson ratio, φ friction angle, c-cohesion

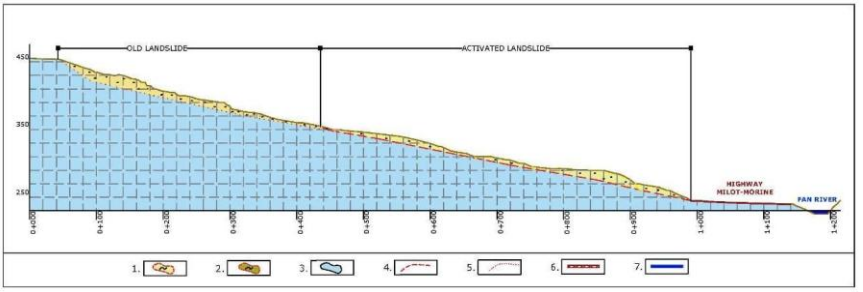

Fig. 7: Lithological profile of mass movement's area 1. Inorganic clays and silts (CL-ML), 2. Landslide body 3. Very weak rocks, block in matrix, 4. Slide surface of current landslide, 5. Slide surface of old landslide, 6. Highway, 7. Fani River.

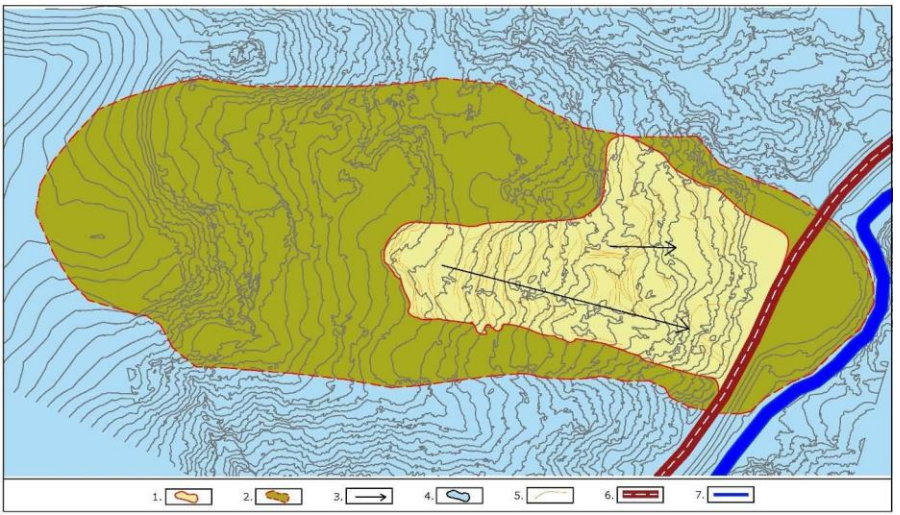

Fig. 8: Geotechnical map of studied area, scale 1: 5000 1. Reactivated landslide, 2. old landslide, 3. landslide movement direction, 4. very weak rocks, block in matrix, 5. cracks. 6. Highway, 7. Fani River.

Slope stability analysis

Field work and laboratory tests have been carried out for slope stability analyses. The finite element software of Phase2-FEM (Rocscience, 2011) was used for slope evaluation. The geotechnical parameters inputted in this model for each layer are γ-unit weight, E-young modulus, υ-Poisson ratio, φ friction angle, c-cohesion, PGA-peak gravity acceleration. As the area is characterised by rainfall events and seismic activity events, earthquakes are likely to occur during or within a few days after rainfalls. So, the slope stability is analysed under different conditions like: i) dry season, ii) heavy rains, ii) seismic activity using PGA = 0.22 hazard values from the Albanian seismicity map (Duni *et al*., 2004), and iii) both rain and seismic activity. Based on Eurocode 7 provisions (BS, 1997-1), $F_S \geq 1.5$ is acceptable for the design of a stable slope the slope stability. If $1 \leq F_S < 1.5$**,** the slope is considered in a state of impending failure critical state. If $F_S < 1$, the slope is considered unstable. The factor safety "FS" of the slope was built by geotechnical units no. 1 and 3 and computed based on different geotechnical data (Table 2 and Figure 9-12).

Under natural condition (dry seasons), the slope is considered in a state of impeding failure critical state, if the factor safety $S_F = 1.03$. Under wet weather (rainfall events), the slope is considered in an unstable state, if the factor safety $S_F = 0.89$. Under seismic activity events, the slope is in unstable state, if the factor safety is $S_F = 0.56$. Under both rainfall events and seismic events, the slope is in unstable state, if the factor safety is $S_F = 0.55$.

Table 2. Slope stability analysis results computed by finite element (Rocscience, 2011)

Factor Safety for the condition			
Dry season	Rain	Seismic	Rain & Seismic
1.03	0.89	0.56	0.55

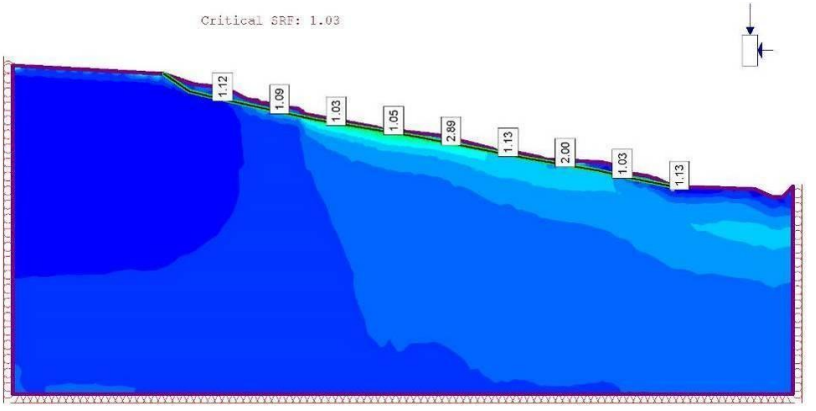

Fig. 9. Model of factor safety computed by finite element in the case of dry season.

.

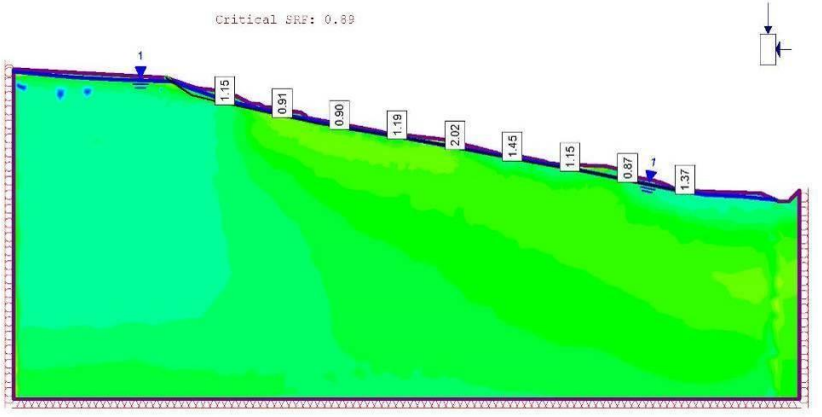

Fig. 10. Model of factor safety computed by finite element in the case of rain season .

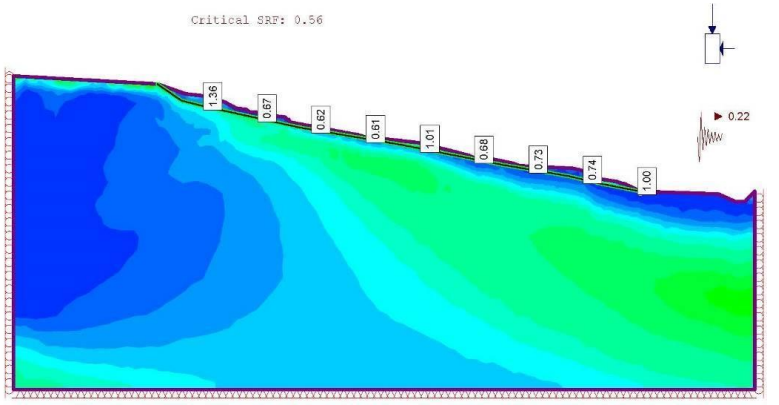

Fig. 11. Model of factor safety computed by finite element in the case of seismicity.

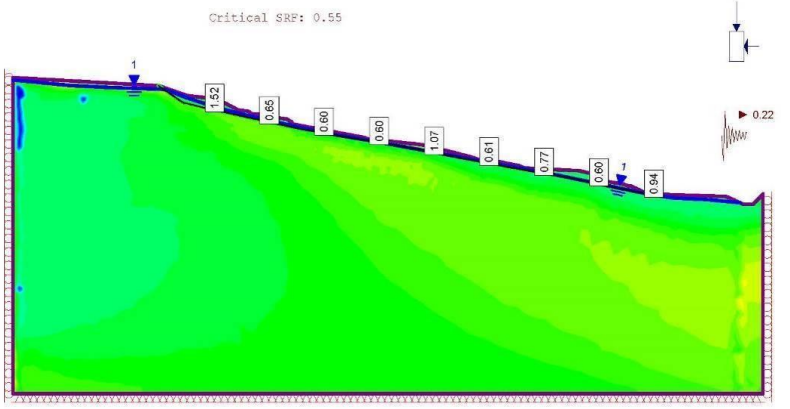

Fig. 12. Model of factor safety computed by finite element in the case of rain and seismicity.

4. Consequences and protective measures

The area is characterised by landslide events. Once inhabited, the Blinishti village does not exist anymore due to landslides occurrence destroying more than 20 dwellings, water supply system and village roads. In addition, agricultural land (topsoil and nutrients in 247.43ha) and trees of commercial value were damaged. The landslide moved into motorway by destroying some objects (gas station and shop's buildings) and blocking it. Moreover, this landslide has caused the change of the river bed (Figs 2-4 and 8). Currently, this sliding represents a potential risk to travellers.

Given the geotechnical conditions, protective measures for landslide disaster mitigation would be of immediate importance. Using plants to stabilize soil to prevent excessive erosion and also to mitigate the effect of landslides and drainages for ground water control are promising methods for road safety.

5. CONCLUSIONS AND RECOMMENDATIONS

This paper reports the morphological, geological and geotechnical data obtained from the reactivation of a large deep-seated old landslide along of Rreshen-Kukës motorway landslides.

Investigation has been carried out to obtain morphological, geological and geotechnical data of the ground surface.

The area consists of quaternary deposits, mélanges formations-blocks in the matrix (Middle Jurassic-J_2) and volcanic formations (Middle Jurassic-J_2). It represents geomorphologically a natural hilly slope with angle ranging from 11-15^o to 22^o.

Geotechnical studies report that the area represents an old landslide which extends from Shpal village (upper slope) to Blinisht village (on the middle of the slope), reaching downslope the Fani River. The landslide is 1280m long, approximately 280m wide and from 5.0-7.0m to 12.0-15.0m thick. Its surface area is 247.43ha and volume 5217 047m^3. Given the dimensions of the landslide, it could be considered an extremely large landslide.

The reactivated landslide is 580m long and from 150.0m (upslope) to 260.0m (down slope) wide. Its surface area is 12.54ha and volume 1128 573 m^3. It could be included into the large landslide group.

The soils and rocks geotechnical conditions, morphology and rainfalls led to a frequent occurrence of landslides in the studied area.

Geotechnical investigation reported three main geotechnical units with different physical-mechanical properties: i) the current landslide body-inorganic clays and silts (CL-ML) brown and grey in colour, medium consistency (ASTM, 2011) with gravels, pebbles and rock block content (1.5-3.0m up to 12.0-15.0m thick), ii) the inorganic clays and silts (CL-ML) brown and grey in colour, (ASTM, 2011) with gravels, pebbles and rock block content (1.0-2.5m up to 7.0-10.0 m thick), and iii) very weak rocks consisting of clayey matrix, grey and green in colour. Here, chaotically suspended different rock blocks (limestone, magmatic, claystone and sandstone) could be met.

The factor safety “FS” of the slope was computed based on geotechnical data. Under natural condition (dry seasons), the slope is considered in a state of impeding failure critical state, if the factor safety S_F = 1.03. Under wet weather (rainfall events), the slope is considered in an unstable state, if the

factor safety S_F = 0.89. Under seismic activity events, the slope is in unstable state, if the factor safety S_F = 0.56. Under both rainfall events and seismic events, the slope is in unstable state, if the factor safety S_F = 0.55.

Using plants to stabilize soil to prevent excessive erosion and also to mitigate the effect of landslides and drainages for ground water control are promising methods for road safety.

REFERENCES

ASTM. 2011. "American Society for Testing and Materials D2487". Standard practice for classification of soils for engineering purposes (Unified Soil Classification System). ASTM International. West Conshohocken, PA. 10. 1520/D2487-11.

Cruden DM, Varnes, DJ. 1996. Landslide types and processes, in: Landslides: Investigations and Mitigation, Transportation Research Board, Special Report 247, edited by: Turner, A. K. and Schuster, R. L., 36–71.

Fell, R. 1994. Landslide risk assessment and acceptable risk. Canadian Geotechnical Journal. 31, 261-272.

Duni Ll, Kuka N. 2004 Seismic hazard assessment and site-dependent response spectra parameters of the current seismic design code in Albania. Acta geodaetica et geophysica hungarica. DOI: 10.1556/AGeod.39.2004.2-3.3

Muceku, Y., & Jaupaj, O. 2018. Landslide Hazard Zonation Along Milot-Kukës Motorway, Albania. Periodica Polytechnica Civil Engineering. https://doi.org/10.3311/PPci.11914

Muceku Y., Gjini I., Papa F, Çota S. 2018. Geotechnical mapping of mass movements occurred in km 43+700- 43+800 of Milot-Kukës motorway. Dolsar Consulting Engineering Company, Tirana, Albania. Rocscience Inc.: Phase 2 Version 8.0-2-D FEM Geotechnical Analysis, www.rocscience.com, Toronto, Ontario, Canada, 2011.

Muceku Y, Korini O, Kuriqi A. 2016. Geotechnical Analysis of Hill's Slopes Areas in Heritage Town of

Berati, Albania. Journal of Periodica Polytechnica of Civil Engineering, Hungary. Volume 60, No. 1, p. 61-73, doi: 10.3311/PPci.7752.

Muceku Y, Korini O. 2014. Landslides and slope stability evaluation in the historical town of Kruja, Albania. Journals of Natural Hazards and Earth System Science, Germany. Publication type: Journals Natural Hazards Earth System Sciences, 14, p. 545–556, doi: 10.5194/nhess-14-545-2014.

Muceku, Y., Reçi, H. 2008. Integrated geotechnical and geophysical approach to investigate Bovilla landslide at Tirana region, Albanian journal of natural & technical sciences-AJNTS, volume. nr 2, p. 6172.

Muceku Y. 2007. Geotechnical investigation of landslide along of road's area from Rubiku town to Shpal village. Illyrian Consulting Engineering Company, Tirana, Albania.

Muceku, Y., Krutja, F. 2002. Mass movement and hazard assessment in south of Kukesi region. Albanian journal of natural & technical sciences-AJNTS, Vol. Nr. 2, p. 81-92.

Romana MR. 1996. A Geomechanical classification for Slopes: Slope Mass Rating. Pergamon Press Ltd, Headington Hill Hall, Oxford, OX3 0BW, England, vol. 3, 15–16.

Sulstarova, E., Koçiu, S., Aliaj, Sh. 1980. Seismic zonation of Albania. Publication of Seismological Centre of Academy of Sciences, Tiranë, 297 p.

Themelko B, Mustaqi V. 1996. Rainfalls in Albania. Water as a national asset, the research and management of water resources of Albania. National Conference, Tirana, Albania, 1-2 October 1996, 129–133.

RESOURCE STARVATION IN ASYMMETRIC DISTRIBUTED LOCK MANAGEMENT IN CLOUD COMPUTING

Artur KOÇI and Betim ÇIÇO
Epoka University, Albania

ABSTRACT

Cloud Storage service maintains and manages its customers' data and makes that data accessible at any time and in any place. Considering the importance of the consumers' data, implementing a reliable system that offers high availability and scalability with a proper solution for maintaining concurrent access on the stored data, a sustainable cloud service would be crucial. Asymmetric distributed lock management in cloud computing provides a solution to the maintenance of the concurrent access to the shared files offering high availability of the cloud storage. The present paper analyzes and evaluates the performance of the lock manager algorithms used to maintain file consistency in cloud storage. We introduce the concept of resource starvation which will act as a tool to address the cloud storage availability. Resource starvation is a defined parameter that avoids servers to get exhausted by dropping all requests over a preset and reset the file permission to initiators state. Consequently, we can analyze the performance of the resources in use and decide the value of the resource starvation parameter in accordance with the amount of the requests that they can process.
Keywords: cloud data storage, file consistency, distributed systems, lock manager algorithm, lock servers, concurrent access etc.

1. INTRODUCTION

Cloud storage services are becoming one of the main options for consumers to store data which are accessible everywhere and from different devices. Most of the biggest companies have been moving their service in cloud services while most of financials transaction worldwide are performed online and not limited by space. Nowadays, there exist clouds storage such as Google, Amazon, Microsoft etc. which provide different solutions and store the user's data up to thousands of terabytes. One of the biggest concerns that distinguish a cloud storage service is the reliability of the users' data, i.e., a

cloud implementing a fault tolerant solution. Dealing with user data, cloud platforms have to provide scalability while sustaining high availability and provide a proper solution to the maintenance of concurrent access on the stored data. Many authors have offered different solutions to this problem, but the optimization of the cloud storages' performance must further. Hadoop (Borthakur 2007; Maurya and Mahajan 2012) is one of the biggest distributed file system designed for the storage of very large data sets reliably and high throughputs. The main components of Hadoop are NameNodes and DataNodes which are used to store the file system metadata and applications' data, respectively. If a client wants to read a data block, he contacts the NameNode to finding the location of data block. Once the location is found, the data block from DataNodes could be read. Another distributing file system is Google File System GFS (Ghemawat *et al*., 2003). The architecture of GFS comprises the single master server and multiple chunk server. Master maintains the file system metadata such as namespace, access control and the current location of the file. The client interacts with the master only for metadata operation and the data-bearing combination goes directly to the chunk server avoiding the overhead of the master server. To avoid single point of failure, master server has its replication server. The file concurrency is avoided by creating snapshots and record appends operation. One of the widely used methods to improve data reliability in distributed systems is the data distribution to several storage devices. While using this method, it is required to associate distributed data with redundant information. Reliability in distributed cloud storage is defined as the tolerance of the node failure, while availability means any time access to the files beside from location and time. Another parameter to be considered in distributed cloud storage is efficiency, defined as the redundant information stored in the system. Many distributed storage systems use the replication technique (Lamport 1998; Lamport 2001; Adya *et al*., 2002; Tewari and Kleinrock 2005) to increase data reliability. Replication is a process where the whole file is replicated a certain number of times in different nodes. If one of the nodes fails, other copies can be available. This is a process that consumes a lot of space and bandwidth causing overhead of the system. To avoid the old form of replication, erasure coding (Sathiamoorthy *et al*., 2013) is introduced. Erasure code is a technique that divides the original file into fragments called chunks. Once encoded, redundant information stores them in different distributed nodes. This is a way to increase the cloud storage capacity. In case of storing many copies of the same file with erasure codes, we store only one copy. In case of failure, the original file can be retrieved using a group from the total number of the stored number of chunks. Maximum distance separable codes (MDS) described in (Dimakis *et al*., 2010; Dimakis *et al.*, 2011) are erasure codes techniques that can generate a node by contacting a subset of the group

used in erasure codes. MDS technique increases the reliability of the cloud storage but compared to replication it requires more bandwidth consumption used while exchanging redundant information. Another aspect that needs to be optimized in cloud storages is file consistency during concurrent access. Therefore, a sustainable lock management should be deployed. Lock managers (Kishida and Yamazaki 2003) are techniques which maintain file consistency and avoid simultaneous access in the same file. They can be implemented for centralized management (Adya *et al*., 2002) and distributed management (Lakshman and Malik 2010). In centralized management, all the clients' requests are directed to it and they can easily get overhead and commit service interruption, while the distributed management lock manager is spread differently in multiple servers and in case of failure of one of them, the access can continue from other servers. One solution for maintaining the file consistency in distributed cloud storages could be found in (Burrows 2006). The offer lock service named Chubby has two main components: a cell that is a set of servers also called replicas, and a library that client applications link against. Client Library maintains all the communications between client application and servers. Another approach called asymmetric distributed lock management in cloud computing - ADLMCC offered by (Koçi and Çiço 2018) consists of a fully distributed lock manger. In this approach the master server concept is completely removed, and every server can act as master for certain requests. The file consistency is maintained locally without communicating with other lock managers servers or in collaboration with other lock managers that depends in the situation of a certain file. When file inconsistency happens, and the servers require granting access to a file which is not the owner, it might require migrating the request to the owner or to a remote server that has already granted access. Following this assumption, any time a server receives a request, it needs to migrate it to a certain server which is going to be overloaded. In this paper we will implement some improvements to the solution provided in (Koçi and Çiço 2018) by introducing the concept of resource starvation. The section 2 describes the improvements and features added to this algorithm. Section 3 analyzes the result received while testing this algorithm after adding the improvements.

2. Resource starvation in asymmetric distributed lock management in cloud computers

The ADLMCC structure has been described in detail in the paper presented by (Koçi and Çiço 2018). In this section we will give a summary of its design and discuss regarding the resource starvation solution that we have offered for controlling the failure of cloud storage services. Referring to (Koçi and Çiço 2018), there are six important key factors in the structure of the lock manager that maintain concurrency control in self-management of the shared

file and in the condition where communication is happening between servers in the cloud. The six key factors in the structure of ADMMCC are: Server Node Table (SNT). File Directory (FD), Requesting Lock Table (RLT), Migrate-out Table (Mout-T), Migrate-in Table (Min-T), Locked File List (LFL). Each lock manager has two different sets of data structure. One maintained locally and not shared with any of the other servers and the second data structure, fully distributed among the other servers. SNT is responsible for memorizing the configurations of all servers in the cloud such as servers ID, servers status and switchover. SNT table is fully synchronized among all other servers. FD is the directory which determines the path of each file stored in nodes and which functions as the server that created the file and has the ownership right for a specific file. We agree that FD is a data structure with pairs of file names and server number and is fully synchronized in the cloud. M-inT and M-outT respectively maintain information about achieved permission for accessing a specific file from another server and the list of files that their lock has been migrated to other servers. RLT stores the list of all locks a server has requested. The information kept in RLT consists of user requester ID, file name requested, lock mode and timestamp. The table is maintained locally and works for managing locks locally in the server. LFL contains all the necessary information for locks that a specific lock manager is managing and is responsible for. The set of attributes LFL consists of: requesters ID, requester server, file name, lock mode and a timestamp, and two lists for queuing lock requests: one for granted and the other for blocked locks. The lock manager algorithm maintains the file consistency and concurrent access in four different steps i) self-management of shared locks in servers, ii) finding a lock manager owner, iii) checking a request migration and, d) lock acquisition.

Step I: Self-management of shared locks in servers

In the improved algorithm, the two first steps remain unchanged the same as they were before.

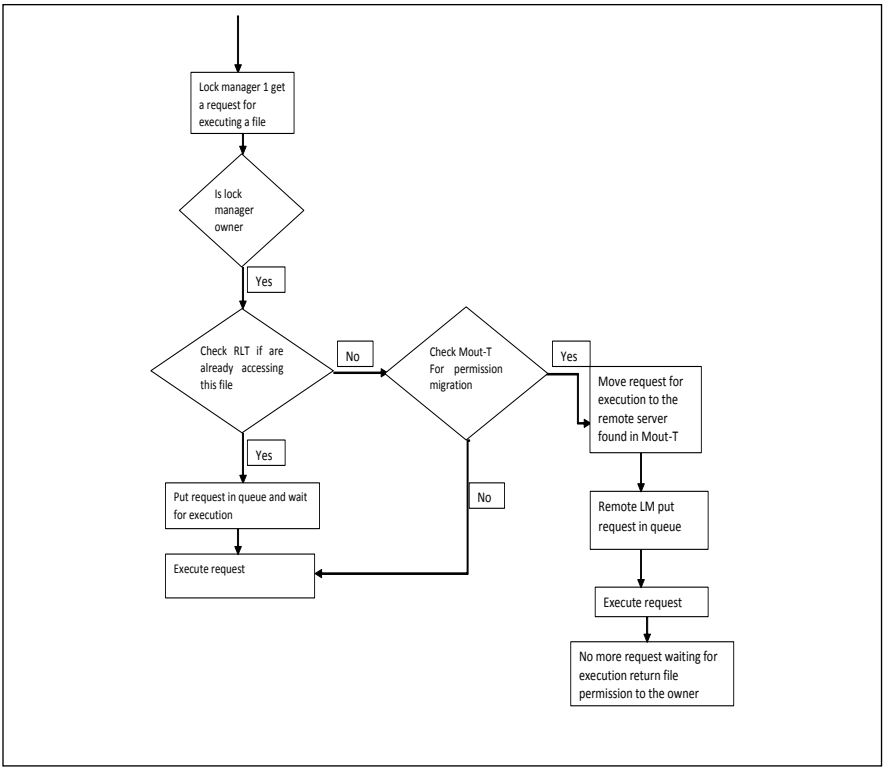

Fig. 1: Self-management of shared locks in servers

As in these two steps no major interaction with other servers occurs, it could be assumed that everything happens in a flat way and no failure occurs.

The figure 1 describes the working principles of the self-management mode. When one of the servers receives a request for executing a certain file, the lock manager firstly checks in FD to find the owner of the file. In case that this server is the owner, lock manager immediately checks one after the other in RLT and Mout-T if the file is under execution or the permission has been migrated to another server. If the file is not found in RLT and Mout-T, it could be concluded that the file is free from locks and the request can immediately be executed. In case that the file is found in RLT, request for file is added in queue waiting the turn for execution.

Step 2: Finding a lock manager

In cases when the server receiving the request which we will call as initiator server, is not the owner, collaboration with other servers for

maintaining the consistency of the file is required. The figure 2 shows the lock managers performing two consecutive checks in FD and SNT to find the owner lock manager of the file. The initiator lock manager sends a lock request message to the owner lock manager for acquitting execution right permissions.

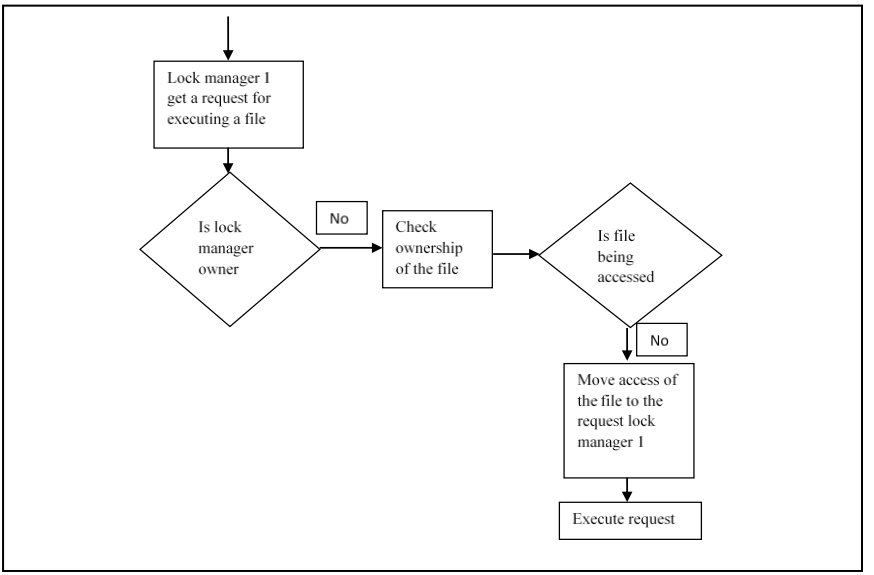

Fig. 2: initiator Server gets execution permissions from Owner Server

The owner lock manager, after performing the checks in the RLT table and on M-out T and if any lock is applied to the file or the lock management is not migrated to a lock manager on another server, places the file in M-out T and migrates the lock management to the server initiator.

Step 3: Checking a request migration

If the owner lock manager realized that the request could be found either in its RLT or in Mout-T, server initiator could not grant any more the right for accessing the file. At this point, it must collaborate for migrating the request execution to the owner or a third lock manager. There exist two possibilities for the file; either the file is under execution from owner or its right permissions have been migrated to a third server.

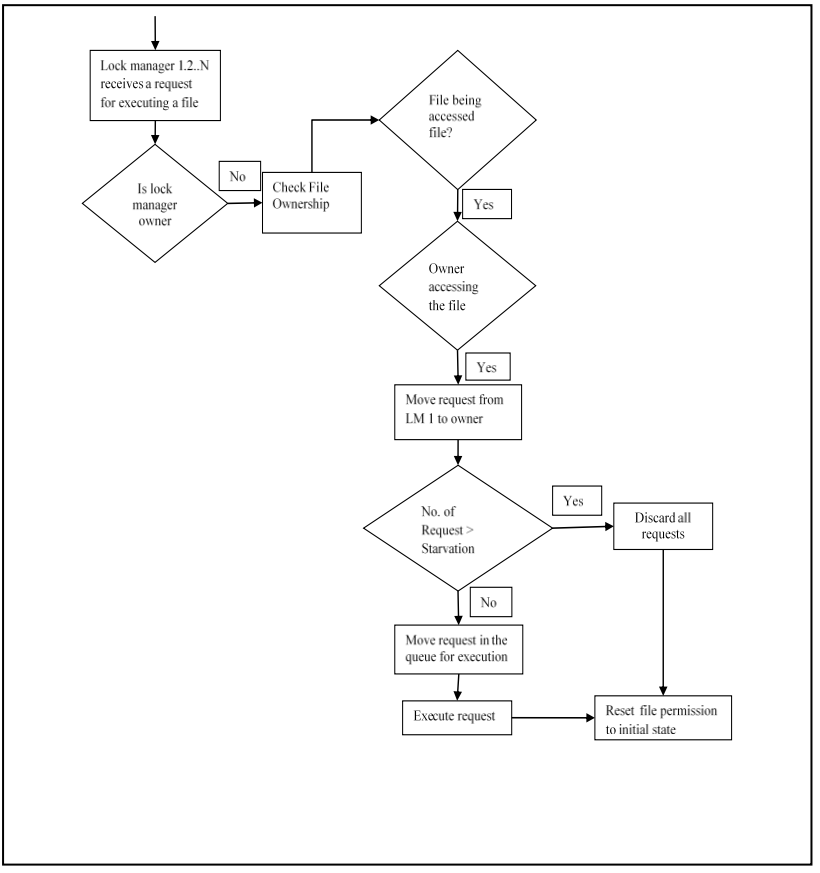

Fig. 3: Server initiator migrates execution permissions to server owner.

Referring to the diagram in the figure 3, N lock managers have the right to request the execution permission of a file but only the one who was the first one requesting will grant it in a moment of time. If the file is under owner execution, any time that one of the lock managers will request to execute the file needs to migrate the request for execution to the owner. This can happen to an endless time and owner lock manager will get exhausted without any resource for serving to later coming requests. In the literature of cloud computing this is called resource starvation and requires developer's attention for finding an appropriate equilibrium to supply to users the agreed service performance. Coming back to our algorithm, to provide the required availability we define a parameter called Resources Starvation that is responsible for maintaining cloud services running. When the requests in queue reach to a certain number same as starvation number, owner lock

manger discards all requests and resets file permissions. In this mode all the requests need to be reinitiated for getting the permission of the file.

Step 4: Lock acquisition

For the same analysis, when the file in the request is found in Mout-T of the owner and, when a new request has been delivered from any of other servers, it is needed to migrate it to the remote server which has already granted permission from the owner. Figure 4 shows the consistent requests from N-2 lock managers plus owner requesting to execute file. Within this state, we will have two main aspects that will affect the cloud service, one is the delay for one request to be migrated from the initiator to the executor server and the resource starvation happing to the same logic as described before. The new state of the system is in the Figure 4 reported.

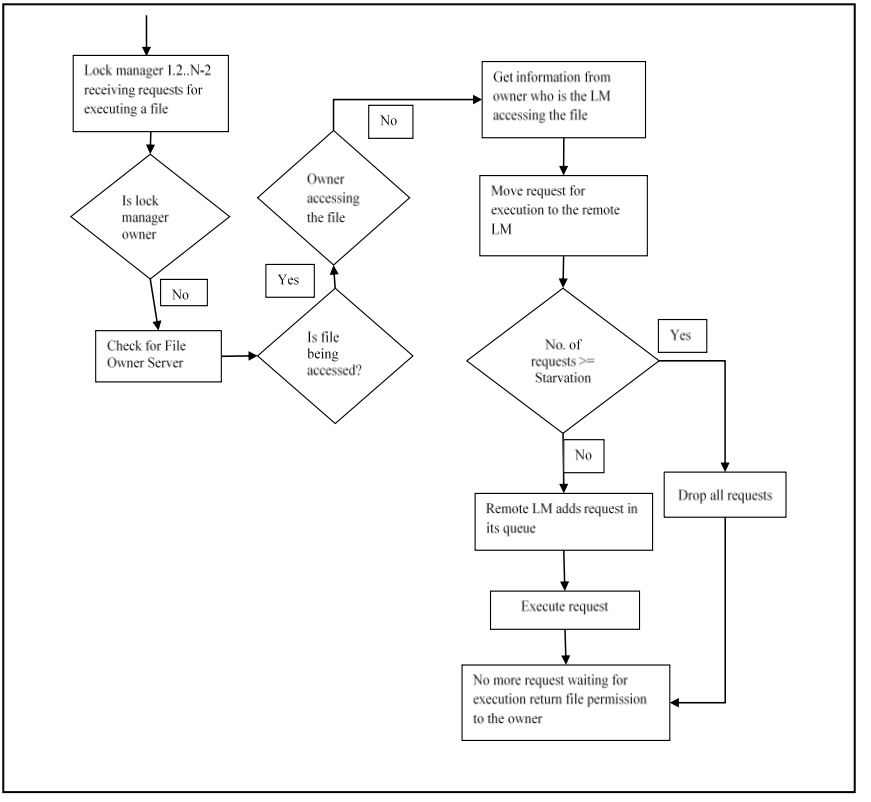

Fig. 4: Server initiator migrates execution permissions to remote server.

Following the same explanation in every lock manger, we denote the starvation parameter and any time that the number of requests is equal to the starvation parameter all the requests in queue, despite from the one that is under execution, will be dropped. After finishing the execution of the last requests, the file permissions are reset to default and the ownership of the file is given back to the owner. The rest of the functionalities of the lock manager remain unchanged, same as before.

3. EXPERIMENTAL RESULTS AND DISCUSSION

In the section 2, we have been explaining the basics of the lock manger algorithm and its functionalities. We have redesigned it by introducing the new concept of resource starvation. With the new design, the execution behavior will change, and a new equilibrium is required for maintaining the overall cloud performance. The algorithm is implemented in programming language Java with a simple graphical user interface that allows us to build different cluster infrastructure and populate the node with files.

In this section we are going to analyze the data collected from test held with our algorithm simulating the situation that the request is executed from remote lock manager. This simulation refers to the algorithm status that is required for the initiator servers to migrate the request to a remote server that has been already granted the execution permission right form owner lock manager. The simulations will be held for the same environment conditions when we apply resource starvation parameter to the lock manager and for the condition that no resource starvation parameter is applied. The platform is composed by 10 servers, 10 node storages, 300 files, 50 clients and for both simulations the number of requests remains unchanged to 200 requests. For performing the tests, we have defined in presets that all the requests are delivered to server 10 and they ask the same file that is under ownership of server 4. Server 4 has already migrated file permission right to server 9. The same test with the same presets is two times issued. In the first time it is issued without defining resource starvation parameter. In the second time we have adjusted the algorithms settings in accordance with the new improvements adding the starvation parameter.

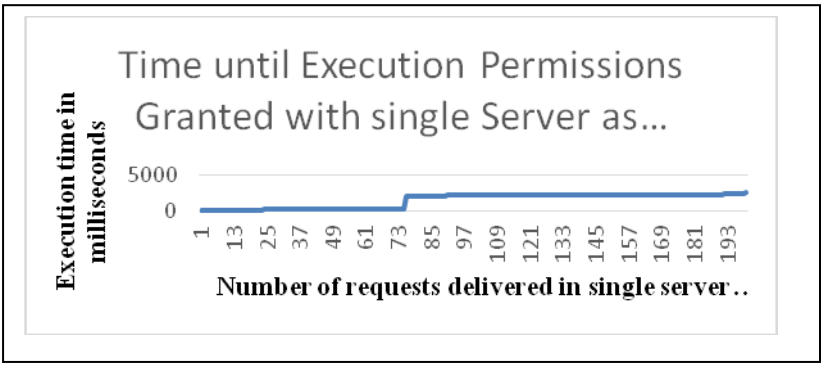

Graph. 1: Execution time in milliseconds for 200 requests in single server mode without starvation.

The graph 1 plots time until execution permission granted with single server as executor without starvation. According to the curve of the graph, we can denote three parts that require a special attention. The first part of the graph plots a very low execution time. The second part plots the vertical increase of the time. The third part plots the stability of the execution process. All this is based on the type of the executed requests. In the first part we must deal with read requests that are parallelly executed. Since read-write, write-write, write-read cannot be executed simultaneously, the vertical increase represents the moment when write request is waiting for read requests to finish and then start their execution. Again, we have a stability of the graph that represents the moment when the same type of requests is executed one after another. The maximum time until granted for 200 requests reached the value of 2500 milliseconds which is quite a significant value that needs to be taken in consideration. Following the same assumption, if the number of requests continues to be increased, then server 9 will undergo in exhausted mode and no more requests will be processed.

In the second simulation performed (Figure 6) we denoted a starvation parameter that has prohibited server 9 to enter in exhausted mode.

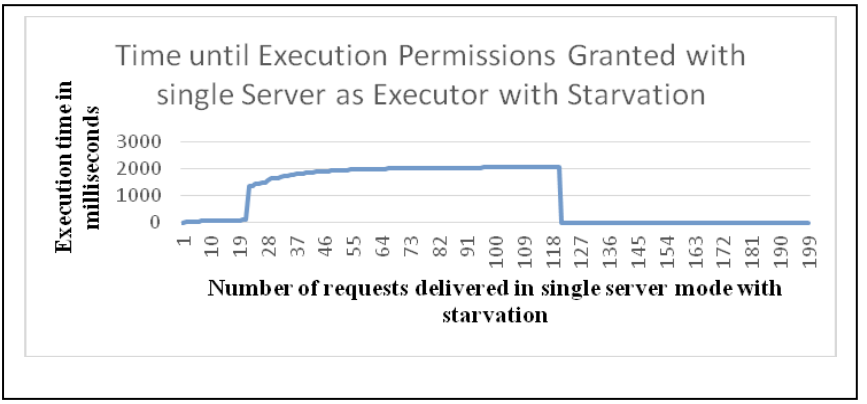

Graph. 2: Execution time in milliseconds for 200 requests in single server mode with Starvation.

Once the server receives a certain number of requests, the requests are automatically discarded (Graph 2). For the simplicity of our work, the discarded request is presented in the graph with value 0. The other part of the graph remains unchanged as in Graph.1. However, the difference lies in the changes of the moment once the requests are delivered. The resource starvation parameter can be adjusted from provider to provider and will be mostly dependent on the hardware parameters of the servers in use and according to the sensitivity of the running services.

4. CONCLUSIONS

The lock manager algorithm here presented offers a sustainable solution to the main features for reliable cloud storage such as availability and scalability. On the other hand, it maintains the stored data free from errors.

We have defined a parameter called resource starvation which is responsible for maintaining the availability of the resources.

Based on test results and analysis, the definition of such parameter is very essential. If no proper attention is payed, the server might become exhausted and commit server failure.

The algorithms proposed is applicable to any cloud storage. However, the client needs must be met as because some requests might get lost and need to be reissued when starvation point is reached.

The resource starvation parameter is here reported, and its effect is here analyzed. As a future work, we propose to use switchover server as load balancer for mitigating the resource starvation effect.

REFERENCES

Adya A, Bolosky WJ, Castro M, Cermak G, Chaiken R, Douceur JR, Howell J, Lorch JR, Theimer M, Wattenhofer RP. 2002. "FARSITE: Federated, available, and reliable storage for an incompletely trusted environment." *ACM SIGOPS Operating Systems Review 36(SI): 1-14.*

Borthakur D. 2007. "The hadoop distributed file system: Architecture and design." *Hadoop Project Website 11(2007): 21.*

Burrows M. 2006. The Chubby lock service for loosely-coupled distributed systems. *Proceedings of the 7th symposium on Operating systems design and implementation, USENIX Association.*

Dimakis AG, Godfrey PB, Wu Y, Wainwright MJ, Ramchandran K. 2010. "Network coding for distributed storage systems." *IEEE transactions on information theory 56(9): 4539-4551.*

Dimakis AG, Ramchandran K, Wu Y, Suh C. 2011. "A survey on network codes for distributed storage." *Proceedings of the IEEE 99(3): 476-489.*

GhemawatS, Gobioff H, Leung S-T. 2003. "The Google file system." *SIGOPS Oper. Syst. Rev. 37(5): 29-43.*

Kishida H, Yamazaki H. 2003. SSDLM: architecture of a distributed lock manager with high degree of locality for clustered file systems. *Communications, Computers and signal Processing, 2003. PACRIM. 2003 IEEE Pacific Rim Conference on, IEEE.*

Koçi A, Çiço B 2018. "ADLMCC–Asymmetric distributed lock management in cloud computing." *International Journal on Information Technologies and Security 10(3): 37-52.*

Lakshman A, Malik P. 2010. "Cassandra: a decentralized structured storage system." *ACM SIGOPS Operating Systems Review 44(2): 35-40.*

Lamport L. 1998. "The part-time parliament." *ACM Transactions on Computer Systems (TOCS) 16(2): 133-169.*

Lamport L. 2001. "Paxos made simple." *ACM Sigact News 32(4): 18-25.*

Maurya M, Mahajan S. 2012. Performance analysis of MapReduce programs on Hadoop cluster. *Information and Communication Technologies (WICT), 2012 World Congress on, IEEE.*

Sathiamoorthy M, Asteris M, Papailiopoulos D, Dimakis AG, Vadali R, Chen S, Borthakur D. 2013. Xoring elephants: Novel erasure codes for big data. *Proceedings of the VLDB Endowment, VLDB Endowment.*

Tewari S, Kleinrock L 2005. Analysis of search and replication in unstructured peer-to-peer networks. *ACM SIGMETRICS Performance Evaluation Review, ACM.*

REGULATION OF AGRICULTURAL LAND AS A FACTOR FOR AGRICULTURAL DEVELOPMENT

Rexhep I. NIKÇI
Vermessungsbüro, Federal Republic of Germany

ABSTRACT

The present paper reports about the current agricultural situation in Kosovo. The splitting of agricultural parcels and recession of agriculture have been damaging for agriculture restricting its development. Given the situation and the country's integration process to European Union a solution the situation for a proper sustainable development and competitiveness in the EU market would be unavoidable. Land consolidation, joining fragmented parcels preserving the environment and landscape would be some of the measures. Here, geodesy activities in procedures of land consolidation, such as the design of the road and duct networks would ameliorate the situation.
Keywords: agriculture, regulation of agricultural land, development, land consolidation

1. INTRODUCTION

The growth of the world's population leads to the need for greater food production. United Nations Food and Agriculture Organization (FAO) has once again confirmed the right of everyone to have access to safe and qualitative food. The food is the fundamental biological factor in human life which is directly related to agricultural products.

On one hand, the worldwide growth in knowledge has led us to an efficient use of natural assets. On the other hand, the new technology has revolutionized modern farming, increased production and incomes. Such development has provided in one part, the non-purification and destruction of the human environment. Due to environmental and landscaping preservation,

some countries with developed agriculture have stopped complementary regulation, particularly at those of highly regulated agricultural lands.

Agricultural development has slowed down and found in a bad situation since 1997 and could be compared to the transition countries. One of the reasons is the splitting of cadastral parcels on agricultural land, which is one of the main factors for the development of agricultural production. Landscapingand grouping of parcels is an indispensable step for the development of agricultural products. Considering the experiences of other countries in the planning of such requests on space, environmental and landscape preservation, should be considered. The European Union envisions the development of rural areas and appropriate agrarian policy, as the main factor for the development of all European states. This direction has three strategic points: The increasing of European agriculture competitiveness, the integral development of rural areas and assistancethrough ecological programs [4]. I believe these directions can greatly affect both the transition countries and particularly to the development of geodesy andother nearby expertise fields.

2. STRUCTURE OF AGRICULTURAL LAND POSSESSION

Kosovo has 10988 ha of agricultural land. Most of the agricultural land is private and a publicpart has begun to be privatized. The state co-operatives have had the best agricultural land as well as a large part ofmeadows. The number of farmers is 400,000, while agricultural parcels are very largedivided, where one can say, "braked apart", with the result that it represents the basic obstacle for a rational utilization of productive agricultural potentials (Figure 1.) This can be better distinguished from the existing data, where there are 2,000,000 parcels with the average area of 0.28ha [1]. The population and its structure are also important factors for agricultural production as well. The present situation of ownership and cadastral parcels is as a result of historical development conditions dating back to feudal times. Even with the capitalism the changes are more drastic due trade growing, which has led to a more splitting of existing parcels.

Family inheritance, road construction and channels and other facilities has increased the splitting of parcels as well. Between the two World wars, the former Yugoslavia has been one of thecountries with the smallest number of parcels, not just in Europe but in the whole world. Shortly before the second world war, the average size of parcels per family was 5.44ha. After the second world war, the properties were still divided. During Agrarian Reform of 1945, it was regulated that maximum working parcel for each owner to be 20 to 35ha. All properties with greater area were split according to this law. Properties for non-farmers are reduced to 3 to 5ha.

The agrarian reform of 1953 reduced the maximum area of labored land on parcels to 10ha. According to the data, since 1960, the average size of the cadastral ofworking parcels was 0.31ha, withan average number of them of 14.0 pereach property. By 1980, the above mentioned values have been still reduced with an average area of parcels 0.27ha and number of parcels per property of 11. Between 1945 and 1981, the number of rural populationdecreased from 75% to 20%.

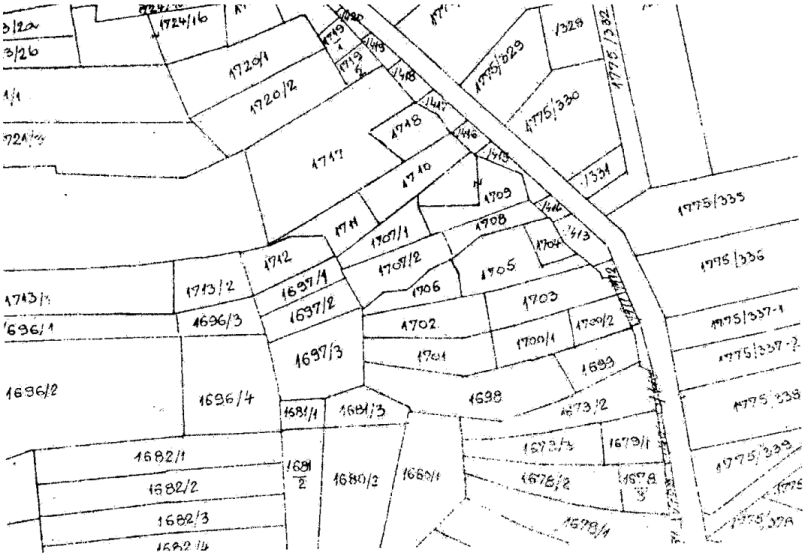

Figure 1: Example of division of cadastral parcels

3. AGRICULTURE AND HUMAN ENVIRONMENT

The main effecting factors of agriculture are climate, soils, plants, domestic animals and humans.

The agricultural-ecological system can only be understood through unification of agricultureand its application to the agricultural community life. Its stability depends on how many manufacturing sectors are in harmonywith the ecological factor of environmental. Nowadays, the most importance, on how to put down again an equilibrium to the scattered situation and how to find optimal steps for the development of humans and its environment, is given to ecology. Figure 2 describes better thehuman weaknesses towards nature and it surrounding.

Figure 2: Ecological awareness

There is a connection of agronomy and ecology,where agro-ecology is used to study theoretical ecology, design, leadership and evaluation of agricultural systems that areproductive, but on the other hand, preserve and protect natural resources. The purpose ofagro-ecology is the maintenance of a productive agriculture.

4. AGRICULTURAL LAND REGULATION

Productive agricultural areas are regulated through agrarian operations. Agrarian operations include agrarian reform, nationalization, expropriation, parceling, "**arrondim" and "comasacion".**

The development of these operations had time criteria in such approved governing systems, but geodetic operations that are used mostly are *"arrondim"* and *"comasation"*. With arrondimone can treat the regulation of small parcelswithin large properties, taking into account that for the properties of small parcel a compensation was given.

The main aim of the arrondim, was the unification of scatteredparcels on socially public properties for a better rational working and economic exploitation of agricultural areas.

The socially landowners (Agricultural Cooperatives) have participateddirectly on the arrondim, whereas individual farmers have been indirect participants. The Landscaping of small parcels at public properties, has led to positive results, by joining the large number of scattered parcelsin large complexes, and has enabled better tools for a rational exploitation. Despite this, the arrondim has chosen only the scattering properties of the public sector, whereas the properties of private sectors was more scattered.

Comasacion (regulation) is the most complete agrarian operation, which as a main goal always has the unifying of the scattered parcels (Figure 3), where nowadays is seen as a tool for improving the agrarian structures and for the

regulation and development of the village as well as. Starting from the purpose of the comasation, one can divide it into radical and partial. According to its application the partial comasation is similar to arrondim, but the only difference is that it unifies the proprieties of all users. The radical comasacion involves the cadaster of entire territory of the municipality, including settlements and forest complexes. Along with the joining of parcels these are also done:

- Inclusion of the entire cadastral of the municipality
- Regulation of settlements for current and future needs
- Regulation of the meadows of forest complexes
- The construction of irrigation systemsand if necessary, land drainage
- Providing of a functional network of countryside roads
- Providingland for the eventual network of roads to be built in the future
- Designing plans for the areas to be planted with multi-annual plants (trees, vines, etc.), and with forests as well.
- Construction of wood fences for protection from the wind
- Taking measures for protection against erosion on steep hilly terrain
- Regulating the water regime of the territory (regulation of river beds, stream, etc.) having as a scope flood protection and
- Providingland areas for all present and future needs.

The importance of comasacion is also the regulation of the legal-property status and the comparison ofcadastral records and property book during years with the current situation on the site.

In Kosovo land consolidation has started since 1983 and has been applied according to1976 law. According to the archives of the Cadastral Agency, land regulation applying the consolidationfrom 1983 to 1986 has included parts of the areas of 78 cadastral zones, while the land consolidation has finished at at 26927ha. Regulation of agricultural land with land consolidation in Kosovo is mainly applied to the territories of the municipalities that are under the irrigation system of "IberLepenc"and “Radoniq". In the commune of Vitiare included areas outsideirrigation system, meaning that is realized the land adjustment but not irrigation system.

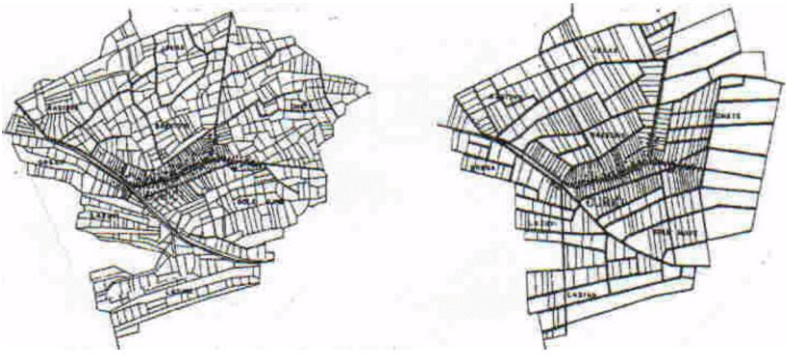

Figure 3: The condition before and after Land consolidation

Even nowadays where there is an unrestricted right of the owner on the properties such as the renting, but also to the normal need to regulate the land, the land regulation is still important.Land ownership is impossible without physical regulation and cadastral records.

5. PRESERVATION AND PROTECTION OF HUMAN ENVIRONMENT

Agriculture, in addition to economic role, has a particularly important role in protecting andpreserving the human environment. Agriculture is also a key element in village regulation, where the protectionof the environment even before the village is regulated is important. Farm spaces are created during many generations of farmers. Along the time, lands had become even richer in the viewpoint of various plant and creatures. Where particular value have the fields, meadows, vineyards, similar trees and biotopes which are the spaces in which grow and live creatures, plant species in case they are not endangered and damaged over exploitation of agricultural areas. Special value also includes areas that are lessproductive on the production,but are part of it. In planning the adjustment of agricultural areas,taking into account the connection that exist between agricultural areas and the ecosystem, it is necessary to find a compromise between the interests of agricultural producers and environment protection. In the preservation andthe revitalization of creatures, plants and biotopes of agricultural lands the main measures to be taken are:

- Division of areas for nature conservation (1- 3% of total areas), whichshould be divided in the same way across the agricultural territory.
- Biotopes that are new, should be protected by law, but also by an agreement between agricultural producers, who besides producing, should also consider the need for restand recreation in rural areas.

- For land use, biotopes covering the surrounding area of roads, streams and different boundaries should have a link between themselves. It should alsocover the slopes and similar structures of agricultural land. As has been said above comasacion is the main agricultural operation. The main purpose of comasacion is preserving the surrounding area during land regulation (Figure 4).

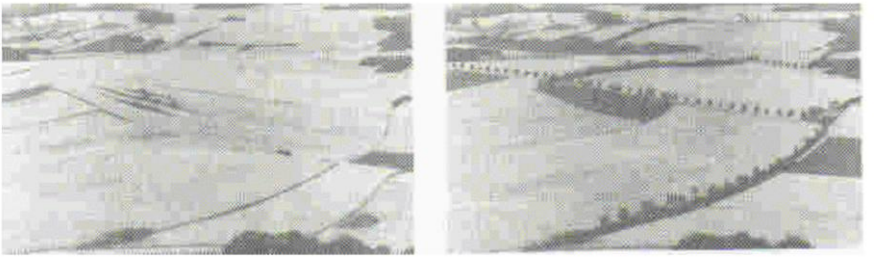

Figure 4: Preservation and protection of surrounding with comasacion, on new conditions, before and after

The purpose of preserving the human environment is firstly preserving the natural environment which includes:

- preservation of the beauties and characteristics of nature,
- taking responsible measures to protect the plant's and animal species according to Europeanlegislation for the protection of our continent,
- bycomasacion to preserve the natural resources,first waters and lands, from the influence oferosion, wind and water, with main purpose the mitigation of the risks on the loss of fertile land.

6. CONCLUSION

The question arises as to what possibility andhow is generally possible, in a relatively short time "to rebuild" Kosovo's agriculture to reach competition at European and world level. One of the main perspectives of agriculture is production ofan healthy ecological food, in an healthy ecological space. The decision makers should haveregulated such production by law.

The offer of ahealthy food isalso one of the agricultural perspectives. Increasing the average size of scattered agricultural economies, is one of the agro-technical measures to be taken but for their efficient use, comasacion should be done as complete and integral procedure for regulating agricultural areas. Also comasacionhelps to be regulatedthe cadaster and cadastral books, whichis a big problem in Kosovo. Before land regulation, most of the experiences of European countries should be taken into account. Particular importanceshould be devoted to preserving and protecting the human

environment, where important is the preservation of a natural and ecological equilibrium. The science of geodesy in theseprocesses have a very large and important role. In the developed European countries, geodetic experts play role especially in spatial planning and regulation, and not just in the calculation ofspatial database and implementation of fieldwork projects. There is not such experience inKosovo yet, but this is necessary and feasible step to be followed. Geodesy is strongly connected with ecology and space. The geodesist during his field work is in direct contact with nature and human environment, and because of that their participation in planningand spatial regulation is necessary. In reality the geodesists are identified with this and they deserve to be engaged on those activities.

7. LITERATURE

[1] Meha M., Kuleta A., Gashi F., 2003: Kadastri digjital në zonat e komasacionit. Seminar GIS dhe të dhënat hapsinore në Kosovë, Prishtinë, 26 Maj 2003.

[2] Ligji për Komasacion (Fletorezyrtare KSAK nr. 31/87).

[3] Bundesministerium für Gesundheit und Umweltschutz(1986) Flurbereinigung und Landschaftspflege, Wien.

[4] Schlagheck, H (1999): EntwicklungländlicherRäume-Zukunft gemeinsam gestalten, Bundesministerium für Ernährung, Landwirtschaft und Forsten, Bonn.

THE THIRD INTERNATIONAL WORKSHOP ON RECENT LHC RESULTS AND RELATED TOPICS IN TIRANA TACKLING THE FUTURE OF PHYSICS AND EDUCATION IN THE AREA

Artan BORIÇI and Blerina SHKRETA

> The important thing is not to stop questioning. Curiosity has its own reason for existence. One cannot help but be in awe when he contemplates the mysteries of eternity, of life, of the marvellous structure of reality.
>
> **Albert Einstein**

The Third International Workshop on Recent LHC Results and related topics was held from 10–12 October 2018 at the Albanian Academy of Sciences. This event was the third of its kind to be held in Tirana and its history lies in October 8, 2012, when Professor Ludwik Dorbrzynski and Professor Daniel Denegri, two eminent personalities in the field of physics came in Tirana and held a meeting with the Albanian scientists involved in the area at the Rectorate of the University of Tirana, Albania and decided to organise the first workshop in LHC results. The meeting was concluded with the the signing of the agreement between the Albanian government and CERN. So the first workshop run in Shkodra in 2014 and the second one in 2016. Given the importance of physics and its implication to other life sciences, the situation of this scientific field in Albania, and the increasing demand of the specialsts in the country, prof. Ludwik Dobrzysnki, the chairman of the Scientific Committee and Organising Committee proposed the third event to be held at the Albanian Academy of Sciences, in Tirana. Professor Vasil Tole, General Secretary of the Albanian Academy of Sciences and one of tis members, Acad. Salvator Bushati the Chairman of the Section of Natural and Technical Sciences and Acad. Floran Vila, Physicist, member of the Department of Physics at the University of Tirana and of the Albanian Academy of Sciences were very enthusiastic about the idea and a closer collaboration between the Academy and the Department of Physics of the Faculty of Natural and Technical, University of Tirana.

The workshop was organized by the Albanian Academy of Sciences and the University of Tirana and supported by the Embassy of France, the Embassy of Italy, the Embassy of Switzerland in Albania and the Italian Institute of Culture.

A list of guests included the ambassadors of Italy, France and the representative of the Swiss Embassy in Albania, the Dean of the Faculty of Natural and Technical Sciences, Deputy Minister of Education, Sports and Youth, from private universities in Albania, General Secretary of the Albanian Academy of Sciences and other representatives from the higher education institutions.

Greetings were made on behalf of the Ministry of Education, Sports and Youth by the Deputy Minister, Mrs. Besa Shahini and on behalf of the Academy by Professor Bushati, on behalf of the Faculty of Natural Sciences by the Dean of the Faculty, Prof. Spiro Drushku. In their talk they emphasised the importance of scientific research for Albania, the potential of the young generation of researchers, the funding opportunities when studying abroad. In his talk, Acad. Bushati, the Chairman of the Section of Natural and Technical Sciences mentioned the beauty of physics and its implication with other science areas such as medicine, environment, earth sciences etc. He talked about the importance of the young reseachers to the Section of Natural and Technical Sciences and the Academy and also the use of science to solve many problems of our everyday life, the science diplomacy.

H.E. Alberto Cutillo, Ambassador of Italy in Albania, H.E. Christina Vasak, Ambassador of France in Albania and Mrs. Debora Kern, representative of the Embassy of Switzerland in Albania also greeted the event. In their talks, the ambassadors reported about the importance of scientific research to the economy of any country, our everyday life and future, how it answers our questions like the end of the world, whether alliens exist or not etc. They emphasised once again, on behalf of their respective governments as members of the EU, the support of the Union to the Albanian researchers, the projects the EU finances like HORIZON 2020, IPA projects, TAIEX etc.

The second part of the workshop in each day were the oral presentations made by students of every academic level to support their academic performace. In addition, a special attention was paid by prof. Denegri and Dobrzysnki to the students from the ‚Asim Vokshi, Foreing Languages High School, the Lyceum of the French Language, International Highschool and the ‘Harry Fultz’ Technical High School as a means to address the future of physics in Albania and foster intelectual pursuits. The students showed their wonder and interest to the scientific enterprise of CERN.

The scientific novelty of this workshop was the participation of the researchers in the field of particle physics and astrophysics such as Nicola de

Filippis and Francesco Laparco from Bari, close partners with the University of Tirana. From theorists we can mention Philippe de Forcrand from ETH Zurich-Switzerland and CERN, Leonardo Giusti from Milan, Italy, and Christof Gattringer from Graz, Austria. Eva Barabara Holzer from CERN was also a new contributor to the workshop. This event brought together the Albanian diaspora involved in the fundamental physics like Bianka Meçaj from the Johannes Gutenberg University, Mainz (JGU), Germany.

The closing remarks on the 4th day of the workshop were dedicated to the future physics in the country, weak and the strong points of the workshop, collaboration with other institutions involved in the area such as Institute of Nuclear Physics, Polytechnic University of Tirana and other state universities.

By holding such a prestigious event where experiment meets lattice, as an indispensable tool for complementing experimental discovery with non-perturbative inputs and experimentalists, theorists and lattice field theorists as and astrophysicists come together, it is hoped to find solution to the main questions about physics and enhance this scientific area in the country.

1ST TIRANA MATHEMATICAL AND COMPUTATIONAL BIOLOGY WORKSHOP GIVES A MAJOR BOOST TO MATHS, BIOLOGY, INFORMATICS AND ALL THE LIFE SCIENCES IN ALBANIA[3]

Blerina SHKRETA, Erida GJINI

The 1st **Mathematical and Computational Biology Workshop (www.tiranamathbio2018.com)** was held in Tirana, Albania for the first time from 22 to 25 October 2018, uniting students and researchers across disciplines. This event was held in the framework of 2018 as the Year of Mathematical Biology, announced by the European Mathematical Society, to promote the importance of mathematics in biology and medicine. The meeting was organized by Erida Gjini, Principal Investigator at the Gulbenkian Institute of Science in Portugal, in collaboration with the Albanian Academy of Sciences, and was generously sponsored by the Company of Biologists (UK) and the Society for Mathematical Biology (USA). By holding such a prestigious interdisciplinary and international event, with lectures from highly reputed international researchers, it is hoped that the integration between mathematics, biology, computer science and informatics will be enhanced in the country.

The workshop in Tirana was the first scientific event of its kind to be held in Albania and welcomed more than 80 participants across 4 days, including a majority of Master and PhD students and lecturers from the Department of Mathematics and Physics, Faculty of Natural Sciences, University of Tirana, Albania and the remainder coming from the University of Medicine, the Department of Biology, the Institute of Public Health, Institute for the Food Safety and Veterinary Sciences and the Polytechnic University of Tirana.

[3] The report was written by Blerina Shkreta, Albanian Academy of Sciences, Tirana and Erida Gjini, Gulbenkian Institute of Science, Portugal

The opening of the workshop was made by Erida Gjini, the main organizer of the workshop who is a researcher in mathematical biology for 7 years. With a Bachelor and master's degree in applied mathematics from the University of Utrecht in the Netherlands, a PhD in Mathematics from the University of Glasgow and international research experience in Portugal and USA; she is member of the Albanian Young Academy under the Albanian Academy of Sciences since 2017. In her opening speech, Erida outlined the programme for the 4 days and introduced the international invited lecturers from France, Portugal and the UK: Dr. Jean Clairambault, Dr. Samuel Alizon, Prof. Adélia Sequeira, Dr. Paula Silva and Dr. Christina Cobbold. In a second welcome speech, Academician Prof. Salvatore Bushati emphasised the importance of multi-disciplinary approaches in the sciences, and how mathematics can help studies and research in all the life sciences. The list of guests the first day included the Rector of the University of Tirana, Prof. Dr. Mynyr Koni, the Director of the Institute for Nuclear Research, Prof. Elida Bylyku etc. Academicians Prof. Bashkim Resuli, Ilirjan Malollari, Dhimitër Haxhimihali, Neki Frasheri, members of the Albanian Academy of Sciences and many representatives of higher education and research institutions were also present. All the participants appreciated the importance of mathematical and computational biology for Albania's scientific development and applications in medicine and environmental studies.

The Workshop comprised an intense three-day program, alternating lectures and advanced research seminars in mathematical epidemiology, ecology, and medicine of cancer and cardiovascular diseases. The second day included also oral poster presentations from Albanian students and professionals.

The closing remarks on the 4th day of the workshop were dedicated to the future of biomathematics in Albania. The participants emphasized once again the importance of multidisciplinary studies between mathematics and biology and cross-disciplinary collaboration, but also highlighted challenges in relation to funding in state institutions, quality of collaboration, opportunities for young researchers and facilities for interdisciplinary research structures. New ideas and possible projects rose among the attendees representing different science institutions in the round table as a first step to develop mathematical biology.

Despite the difficulties unfolded in the discussion, Acad. Bushati, the Chairman of the Section of Natural and Technical Sciences, repeated the commitment and support of the Academy, the Section of Natural and Technical Sciences as a science entity, ready to fulfil a range of responsibilities such as fostering intellectual pursuit among the young generation of researchers through internships, exchanges and open access to the e-library, collaborating with research and education institutes of scientific excellence and introducing new initiatives in the area of research and education to support current needs of the country. The Academy of Sciences is committed to help find solutions to many crucial issues concerning the development of the country by providing high state institutions with appropriate advice and expertise; running of congresses and science conferences on a wide range of topics related to science, both at a national and international level; creating *ad-hoc* commissions of highly regarded science priorities om research and development; running of competitions and awards in the form of medals and prizes for outstanding achievement in the area of

research and science etc., analysing criteria fulfilment from the candidates running for Academy's membership.

The successful completion of the *1st Tirana Mathematical and Computational Biology workshop* in 2018, as a collaboration between an Albanian researcher outside of Albania, international researchers and Albanian institutions should be an inspiration for Albanian science of the future, to join efforts across disciplines, sectors and all barriers, to promote development and innovation.

29.10.2018

For further information, please visit the website: www.tiranamathbio2018.com

STANISŁAW ZUBER (1893-1947)

Get out of the press the book of prof. Arqile Teta "Prof. Stanisław Zuber Życie I Dzieło".[4]

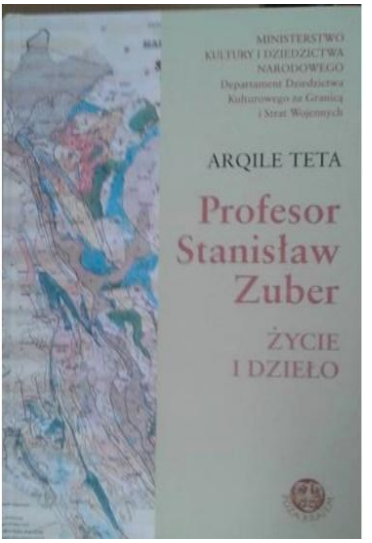

The book about Stanisław Zuber (1893-1947) – an eminent Polish personality in the field of geology. He remains one of the most important scientists who authored many books and manuscripts and compiled many maps at different scales, referred to by the Albanian geologists. Banned and forgotten throughout the times of communism, he is now brought back to the history of geoscience, but also to Albanians, the nation painfully affected by totalitarianism, as well as to the memory of his fellow countrymen.

Arqile Teta presents the history of geological studies in the Balkans from the earliest 30s of the 19th century, when mostly French, Italian, Austrian and English, and after World War -Soviet and Yugoslav naturalists were interested in this area. From the 60s of the 20th century Albanian geologists were active in this regard, many of them educated in Poland. The author presents the circles from which Zuber came- his immediate family including his father were geologists. Stanisław Zuber started his professional work by looking for oil in the Eastern Caucasus and devoted his life to this area of activities. He was a pioneer in the use of aerial photography in geological study. Since 1927 he was linked to Albania through the cooperation with Azienda Italiana Petroli Alabania (AIPA) Albania, an Italian oil company, latter belonging to Azienda Generale Italiana Petroli (AGIP). He was trying to keep ties with Poland, among others, with Jagiellonian University and Academy of Mining and Metallurgy in Krakow. In the days of Hoxha's regime, he was accused of espionage and sabotage,

[4] In the loving memory to the Polish geologist Prof. Stanisław Zuber- eminent personality who worked and died in Albania. He was persecuted and imprisoned by the regime.

and was later tortured and died in prison in Tirana. Teta quotes touching memories of his students and Albanian colleagues, as well as documents and letters, creating a vivid picture of tragic times in this part of the Europe. The book ends with a detailed list of publications and manuscript, materials of Zuber.

The political changes allowed the circles of Albanian geologist to rehabilitate the polish geologist. Stanisław Zuber was awarded post-mortem with the order of Mother Theresa. In Kuçovë a monument was unveiled, and one of the streets was named after him. This book is slightly amended for translation (supplemented with polish excerpts) of an Albanian publication from 2010: *Profesor Stanislav Zuber, jeta dhe vepra.*

Warsaw, 2017

Jacek Miler
Director, Department of Cultural Heritage Abroad and Wartime Losses
Ministry of Culture and National Heritage, Poland